

Cite this: *Chem. Soc. Rev.*, 2012, **41**, 7108–7146

www.rsc.org/csr

CRITICAL REVIEW**Deep eutectic solvents: syntheses, properties and applications****Qinghua Zhang, Karine De Oliveira Vigier, Sébastien Royer and François Jérôme****Received 11th May 2012*

DOI: 10.1039/c2cs35178a

Within the framework of green chemistry, solvents occupy a strategic place. To be qualified as a green medium, these solvents have to meet different criteria such as availability, non-toxicity, biodegradability, recyclability, flammability, and low price among others. Up to now, the number of available green solvents are rather limited. Here we wish to discuss a new family of ionic fluids, so-called Deep Eutectic Solvents (DES), that are now rapidly emerging in the current literature. A DES is a fluid generally composed of two or three cheap and safe components that are capable of self-association, often through hydrogen bond interactions, to form a eutectic mixture with a melting point lower than that of each individual component. DESs are generally liquid at temperatures lower than 100 °C. These DESs exhibit similar physico-chemical properties to the traditionally used ionic liquids, while being much cheaper and environmentally friendlier. Owing to these remarkable advantages, DESs are now of growing interest in many fields of research. In this review, we report the major contributions of DESs in catalysis, organic synthesis, dissolution and extraction processes, electrochemistry and material chemistry. All works discussed in this review aim at demonstrating that DESs not only allow the design of eco-efficient processes but also open a straightforward access to new chemicals and materials.

1. Introduction

In the past 20 years, room temperature ionic liquids (RTILs) have attracted considerable attention especially in the fields of

Université de Poitiers/CNRS, UMR 7285, Institut de Chimie des Milieux et Matériaux de Poitiers, ENSIP, 1 rue Marcel Doré, 86022 Poitiers, France. E-mail: francois.jerome@univ-poitiers.fr; Fax: + 33 (0)5 49 45 33 49

**Qinghua Zhang**

major research interests focus on the development of new green solvents (ionic liquids, deep eutectic solvents, etc.) for the biomass pretreatment, as well as their applications in biomass conversion.

catalysis, electrochemistry, material chemistry, and more recently for the pre-treatment of biomass.^{1–3} At the early stages of these research studies, scientists mainly focused on the formation of ionic liquids by mixing metal salts, mostly zinc, aluminium, tin and iron chlorides, with quaternary ammonium salts. Although both salts have very high melting points, their proper mixing leads to the formation of a liquid phase, the so-called eutectic mixture. These eutectic mixtures are generally characterized by

**Karine De Oliveira Vigier**

carbohydrates chemistry (from cellulose to platform molecules) and the valorization of fats and oils. She pays a particular attention to the catalysis and the development of new reaction media for the conversion of biomass.

Published on 17 July 2012. Downloaded by Centro Federal de Educacão Tecnologica do Rio de Janeiro on 12/10/2018 12:18:23 PM.

a very large depression of freezing point, generally higher than 150 °C. With the introduction of the concept of green chemistry in the early 1990's, the search for metal-free ionic liquids (ILs) has become of growing interest.⁴ In this context, a lot of works were dedicated to the design of ILs by combining an organic cation (usually imidazolium-based cations) with a large variety of anions, the most common ones being Cl⁻, BF₄⁻, PF₆⁻, NTf₂⁻. From that time, ILs have emerged as a new class of promising solvents. The possibility to chemically modify the cationic moiety almost infinitely in combination with a very large choice of anions offers chemists a broad range of ILs exhibiting different physical properties such as melting point, solubility, viscosity, density, conductivity, and refractivity, among others. For instance, in 2009, Seddon and co-workers have reported that 10¹⁸ different ILs can be theoretically produced, 250 of them being already commercialized.⁵ Owing to their low vapour pressure and high boiling point, which facilitates their recycling, ILs were qualified as green solvents. However, the "green affiliation" of these neoteric solvents is now largely contested in the current literature.⁶ Indeed, many reports pointed out the hazardous toxicity and the very poor biodegradability of most ILs.⁷ ILs with high purity are also required since impurities, even in trace amounts, affect their physical properties. Additionally, their synthesis is far to be environmentally friendly since it generally requires a large amount of salts and solvents in order to completely exchange the anions. These drawbacks together with the high price of common ILs unfortunately hamper their industrial emergence and new concepts are now strongly needed in order to utilize these systems in a more rational way.

To overcome the high price and toxicity of ILs, a new generation of solvent, named Deep Eutectic Solvents (DES), has emerged at the beginning of this century. Formation of these DESs can be obtained by simply mixing together two safe components (cheap, renewable and biodegradable), which are

capable of forming a eutectic mixture. One of the most widespread components used for the formation of these DESs is choline chloride (ChCl). ChCl is a very cheap, biodegradable and non-toxic quaternary ammonium salt which can be either extracted from biomass or readily synthesized from fossil reserves (million metric tons) through a very high atom economy process. In combination with safe hydrogen bond donors such as urea, renewable carboxylic acids (*e.g.* oxalic, citric, succinic or amino acids) or renewable polyols (*e.g.* glycerol, carbohydrates), ChCl is capable of rapidly forming a DES. Although most of DESs are made from ChCl as an ionic species, DESs cannot be considered as ILs because (1) DESs are not entirely composed of ionic species and (2) can also be obtained from non-ionic species.

As compared to the traditional ILs, DESs derived from ChCl gather many advantages such as (1) low price, (2) chemical inertness with water (*i.e.* easy storage), (3) easy to prepare since DESs are obtained by simply mixing two components, thus by-passing all problems of purification and waste disposal generally encountered with ILs and (4) most of them are biodegradable,⁸ biocompatible⁹ and non-toxic,¹⁰ reinforcing the greenness of these media.¹¹ Physico-chemical properties of DESs (density, viscosity, refractive index, conductivity, surface tension, chemical inertness, *etc.*) are very close to those of common ILs. For this reason, DESs derived from ChCl are also familiarly named "biocompatible" or "biorenewable" ionic liquids in a few studies. Thanks to their low ecological footprint and attractive price, DESs have now become of growing interest both at academic and industrial levels and the number of publications dedicated to the use of DESs is now rapidly increasing in the current literature, further demonstrating the attractiveness of these media.

2. Definition of DESs

A DES is generally composed of two or three cheap and safe components which are capable of associating with each other,



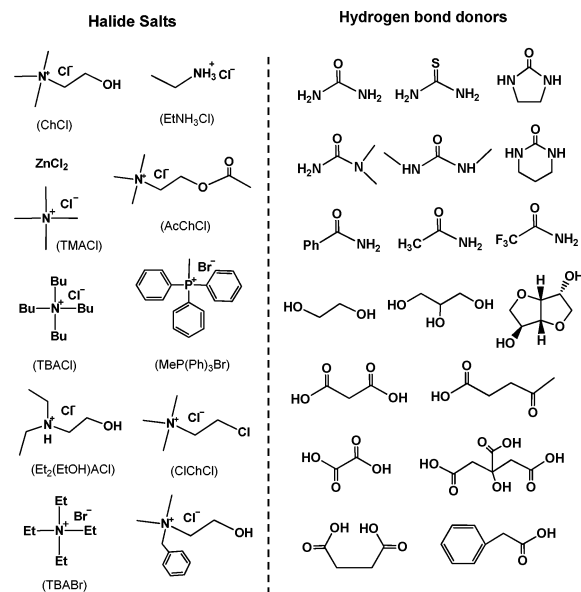
Sébastien Royer

Sébastien Royer received his PhD in Chemical Engineering in 2004 from the Laval University, Quebec. His research focuses on the catalytic properties of nanocrystalline perovskites for oxidation reactions. In 2006, he got a position of Associated Professor at LACCO Poitiers. His actual research focuses on the design of size- and shaped-controlled active oxides for applications in environment and energy.



François Jérôme

François Jérôme received his PhD degree in chemistry from the University of Burgundy (France) in 2000. Then, he moved to the University of California of Davis (USA) as a postdoctoral researcher. Then, he returned to France for a second postdoctoral position at the University of Rennes 1 with Pr P. H. Dixneuf, where he worked on homogeneous catalysis. In 2002, he joined the CNRS as a permanent researcher in the Laboratoire de Catalyse en Chimie Organique at the University of Poitiers. Recently he was promoted as a CNRS research director at the Institut de Chimie des Milieux et Matériaux de Poitiers. His scientific research studies are focussing on the conversion of biomass with a particular attention to catalysis and non-conventional media. In 2010, his research studies have been awarded by the french division of catalysis (SCF-DIVCAT).



Scheme 1 Typical structures of the halide salts and hydrogen bond donors used for DES syntheses.

through hydrogen bond interactions, to form a eutectic mixture. The resulting DES is characterized by a melting point lower than that of each individual component. Generally, DESs are characterized by a very large depression of freezing point and are liquid at temperatures lower than 150 °C. Note that most of them are liquid between room temperature and 70 °C. In most cases, a DES is obtained by mixing a quaternary ammonium salt with metal salts or a hydrogen bond donor (HBD) that has the ability to form a complex with the halide anion of the quaternary ammonium salt. Scheme 1 summarizes the different quaternary ammonium salts that are widely used in combination with various HBDs in the formation of DESs.

In 2007, Abbott and co-workers defined DESs using the general formula $R_1R_2R_3R_4N^+X^- \cdot Y^-$.¹²

Type I DES $Y = MCl_x$, $M = Zn, Sn, Fe, Al, Ga$

Type II DES $Y = MCl_x \cdot yH_2O$, $M = Cr, Co, Cu, Ni, Fe$

Type III DES $Y = R_5Z$ with $Z = -CONH_2, -COOH, -OH$

Note that the same group also defined a fourth type of DES which is composed of metal chlorides (*e.g.* $ZnCl_2$) mixed with different HBDs such as urea, ethylene glycol, acetamide or hexanediol (type IV DES).

Owing to its low cost, biodegradability and low toxicity, $ChCl$ was widely used as an organic salt to produce eutectic mixtures generally with cheap and safe HBDs such as urea, glycerol, carbohydrate-derived polyols or renewably sourced carboxylic acids. These DESs are attractive since they exhibit similar physico-chemical properties to traditional imidazolium-based ILs and thus can advantageously replace them in many applications. As compared to traditional organic solvents, DESs are not considered as volatile organic solvents and not flammable, making their storage convenient. From the view point of green chemistry, these DESs are even more attractive since some of them have been proven to be biodegradable and compatible with enzymes further increasing their interest. Additionally, synthesis of DESs is 100% atom economic, easy

to handle and no purification is required, thus making their large-scale use feasible.

In the following sections, we wish to present an overview of the recent advances made in the field of DESs. Through selected examples, we will show that DESs are particularly promising for the design of innovative catalytic processes, the preparation of new materials and novel structures, the dissolution of valuable substrates and also in the field of electrochemistry. In all these DES-based processes, we will try to demonstrate that use of DESs not only allows the design of safer processes but also provides a straightforward access to new chemicals and materials.

3. Physicochemical properties of DESs

Similar to ILs,¹³ DESs are chemically tailorable solvents since they can be designed by properly combining various quaternary ammonium salts (*e.g.* $ChCl$) with different hydrogen bond donors (HBD). Hence, task-specific DESs with different physicochemical properties such as freezing point, viscosity, conductivity, and pH, among others, can be prepared. Owing to their promising applications, many efforts have been devoted to the physicochemical characterization of DESs. In this section, the main physicochemical properties of DESs will be described and discussed.

3.1 Freezing point (T_f)

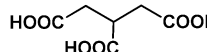
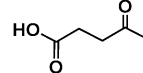
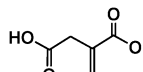
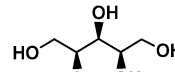
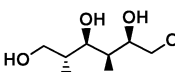
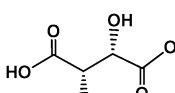
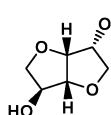
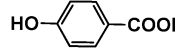
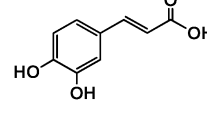
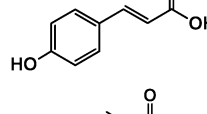
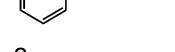
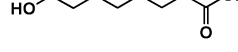
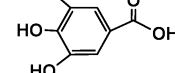
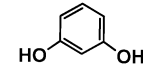
As mentioned above, DESs are formed by mixing two solids capable of generating a new liquid phase by self-association *via* hydrogen bonds. This new phase is generally characterized by a lower freezing point than that of individual constituents. For instance, when $ChCl$ and urea are mixed together in a molar ratio of 1 : 2, the freezing point of the eutectic is 12 °C, which is considerably lower than that of $ChCl$ and urea (melting point of $ChCl$ and urea are 302 and 133 °C, respectively). The significant depression of the freezing point stems from an interaction between the halide anion and the hydrogen bond donor component, here urea. For all reported DESs, their freezing points are below 150 °C. Generally, DESs with a freezing point lower than 50 °C are more attractive since they can be used as inexpensive and safe solvents in many fields.

Tables 1 and 2 list the freezing points of various DESs described in the literature. Although a broad range of amides have been employed in combination with $ChCl$ to produce DESs with a freezing point lower than 100 °C, it should be pointed out that the number of DESs which are liquid at room temperature is still very limited. Among them, urea and 2,2,2-trifluoroacetamide are capable of forming a liquid DES with $ChCl$ at room temperature, presumably due to their stronger ability to form hydrogen bond interactions with $ChCl$. It means that in the case of $ChCl$, the choice of HBDs is a critical point in the formation of a DES with a low freezing point. When carboxylic acids (*e.g.* levulinic acid, malonic acid, phenylpropionic acid, *etc.*) or sugar-derived polyols (*e.g.* xylitol, D-isosorbide, and D-sorbitol) are used as HBDs, room temperature liquid DESs can also be obtained. Similar to the HBDs, the nature of the organic salts (*e.g.* ammonium or phosphonium salts) also affects the freezing points of the corresponding DESs. For example, when urea is selected as

Table 1 Freezing point (T_f) of the reported DESs. (T_m^*): melting point of pure HBD; RT = room temperature

Hydrogen bond donor (HBD)		ChCl : HBD (molar ratio)	$T_m^*/^\circ\text{C}$	$T_f/^\circ\text{C}$	Ref.
	Urea	1 : 2	134	12	15
	Thiourea	1 : 2	175	69	15
	1-Methyl urea	1 : 2	93	29	15
	1,3-Dimethyl urea	1 : 2	102	70	15
	1,1-Dimethyl urea	1 : 2	180	149	15
	Acetamide	1 : 2	80	51	15
	Benzamide	1 : 2	129	92	15
	Ethylene glycol	1 : 2	-12.9	-66	16
	Glycerol	1 : 2	17.8	-40	17,27
	2,2,2-Trifluoroacetamide	1 : 2.5	72	-45	16
	Imidazole	3 : 7	89	56	18
	Adipic acid	1 : 1	153	85	14
	Benzoic acid	1 : 1	122	95	14
	Citric acid	1 : 1	149	69	14
	Malonic acid	1 : 1	135	10	14
	Oxalic acid	1 : 1	190	34	14
	Phenylacetic acid	1 : 1	77	25	14
	Phenylpropionic acid	1 : 1	48	20	14
	Succinic acid	1 : 1	185	71	14

Table 1 (continued)

Hydrogen bond donor (HBD)		ChCl : HBD (molar ratio)	$T_m^*/^\circ\text{C}$	$T_f/^\circ\text{C}$	Ref.
	Tricarballylic acid	1 : 1	159	90	14
	Levulinic acid	1 : 2	32	Liquid at RT	19
	Itaconic acid	1 : 1	166	57 ± 3	19
	Xylitol	1 : 1	96	Liquid at RT	19
	D-Sorbitol	1 : 1	99	Liquid at RT	19
	L-(+)-Tartaric acid	1 : 0.5	171	47 ± 3	19
	D-Isosorbide	1 : 2	62	Liquid at RT	19
	4-Hydroxybenzoic acid	1 : 0.5	215	87 ± 3	19
	Caffeic acid	1 : 0.5	212	67 ± 3	19
	p-Coumaric acid	1 : 0.5	214	67 ± 3	19
	trans-Cinnamic acid	1 : 1	133	93 ± 3	19
	Suberic acid	1 : 1	142	93 ± 3	19
	Gallic acid	1 : 0.5	251	77 ± 3	19
	Resorcinol	1 : 4	110	87	20

the HBD and mixed with different ammonium salts in a molar ratio of 2 : 1 (urea : salt), the obtained DESs exhibit very different freezing points ranging from $-38\ ^\circ\text{C}$ to $113\ ^\circ\text{C}$ (Table 2). The anion of choline-derived salts also impacts the freezing point of DESs. For instance, in combination with urea, the freezing point of a choline salt-derived DES decreases

in the order $\text{F}^- > \text{NO}_3^- > \text{Cl}^- > \text{BF}_4^-$, suggesting a correlation with the hydrogen bond strength. The organic salt/HBD molar ratio has also a significant impact on the freezing point of DESs. For example, when ChCl was mixed with urea in a molar ratio of 1 : 1 and 1 : 2, the resulting DESs exhibited a freezing point $> 50\ ^\circ\text{C}$ and $12\ ^\circ\text{C}$, respectively.

Table 2 Freezing point (T_f) of other DESs

Organic salts	Hydrogen bond	Salt :			
Cation	Anion donor (X ⁻)	(HBD)	HBD	(molar	
			(ratio)	$T_f/^\circ\text{C}$	Ref.
	F	Urea	1 : 2	1	15
	BF ₄	Urea	1 : 2	67	15
	NO ₃	Urea	1 : 2	4	15
	Cl	Urea	1 : 2	-38	15
	Br	Urea	1 : 2	113	15
	Cl	Urea	1 : 2	-14	15
	Cl	Urea	1 : 2	-33	15
	Cl	Urea	1 : 2	15	15
	Br	Urea	1 : 2	55	15
	Br	Glycerol	1 : 2	3-4	21
	Br	Glycerol	1 : 3	-5.5	21
	Br	Glycerol	1 : 4	15.6	21
	Cl	Glycerol	1 : 5	50	21
	Br	Ethylene glycol	1 : 3	-46	21

Table 2 (continued)

Organic salts	Hydrogen bond	Salt :			
Cation	Anion donor (X ⁻)	(HBD)	HBD	(molar	
			(ratio)	$T_f/^\circ\text{C}$	Ref.
	Br	Ethylene glycol	1 : 4	-50	21,27
	Br	Ethylene glycol	1 : 5	-48	21
	Cl	Ethylene glycol	1 : 3	47.9	22
	Br	Triethylene glycol	1 : 3	-8	21
	Br	Triethylene glycol	1 : 4	-19	21
	Br	Triethylene glycol	1 : 5	-21	21
	Cl	2,2,2-Trifluoracetamide	1 : 2	91	22
	Br	2,2,2-Trifluoracetamide	1 : 8	-69	22
	Cl	Glycerol	1 : 2	-1	26
	Cl	Glycerol	1 : 3	1.7	26
	Cl	Glycerol	1 : 4	2	26
	Cl	Ethylene glycol	1 : 2	-31	26

Table 2 (continued)

Organic salts	Hydrogen bond	Salt : HBD	(molar ratio)	$T_f/^\circ\text{C}$	Ref.
Cation	Anion donor (X^-) (HBD)				
	Cl	Ethylene glycol	1 : 3	-22	26
	Cl	Ethylene glycol	1 : 4	-21	26

Fig. 1 shows the phase diagram for mixtures of ChCl with five carboxylic acids as a function of the molar composition. For phenylpropionic acid and phenylacetic acid-based DESs, the lowest freezing point was formed at a composition of 67 mol% of acid, which was similar to the case of the ChCl–urea system (Fig. 1a). This also means that two carboxylic acid molecules are required to complex each chloride anion of choline in order to form the eutectic mixture. In the case of diacids such as oxalic, malonic and succinic acid, the eutectic is formed at 50 mol% of diacid, suggesting a 1 : 1 complex between the HBD and chloride. This is in accordance with the interaction of two carboxylic acid functions per chloride of ChCl (Fig. 1b). Although these systems are also characterized by a significant decrease of the freezing point, no clear correlation between the freezing point of DESs and the melting points of the pure components (HBDs or ChCl) has been established (Tables 1 and 2). When using acids as HBDs, it seems that the acid with the lowest molecular weight shows the largest depression of freezing point. Abbott *et al.*¹⁴ proposed

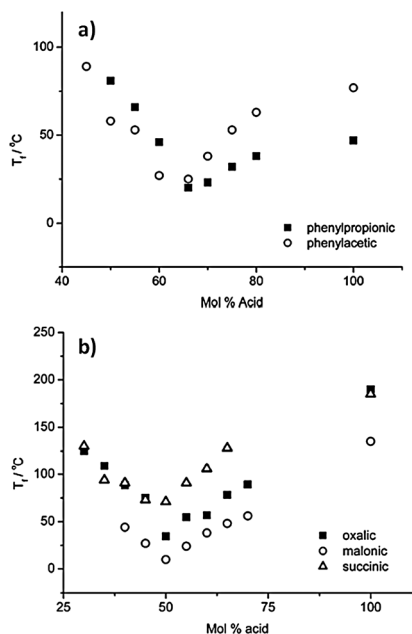


Fig. 1 Freezing points of choline chloride with five carboxylic acids as a function of composition.¹⁴ (Reproduced with permission from ref. 14. Copyright (2004) American Chemical Society.)

that the freezing point of HBD-salt eutectic mixtures should be dependent on (1) the lattice energies of DESs, (2) the way how the couple anion–HBD interacts, and (3) the entropy changes arising from the formation of a liquid phase. In a first approximation, the depression of freezing point might be a measure of the entropy change.

3.2 Density

The density is one of the most important physical properties for a solvent. Generally, densities of DESs are determined by means of a specific gravity meter. Table 3 lists the density data of common DESs. Most of DESs exhibit higher densities than water. For instance, type IV ZnCl_2 –HBD eutectic mixtures have densities higher than 1.3 g cm^{-3} . Among them, density of ZnCl_2 –urea (1 : 3.5) and ZnCl_2 –acetamide (1 : 4) are different (1.63 and 1.36 g cm^{-3} , respectively). This notable difference of density might be attributed to a different molecular organization or packing of the DES. Note that densities of both DESs are higher than those of pure HDBs (acetamide: 1.16 and urea: 1.32 g cm^{-3}). This phenomenon may be explained by the hole theory. Similar to imidazolium-based ILs, DESs are composed of holes or empty vacancies. When ZnCl_2 was mixed with urea for instance, the average hole radius was decreased, resulting in a slight increase of the DES density as compared to that of neat urea.¹²

The organic salt/HBD molar ratio also has an obvious effect on the densities of DES. Fig. 2 shows the density of a glycerol/ChCl DES as a function of the molar composition.

Table 3 Densities of common DESs at 25°C

Salts	HBD	Salt : HBD (mol : mol)	Density (ρ , g cm^{-3})	Ref.
EtNH_3Cl	CF_3CONH_2	1 : 1.5	1.273	23
EtNH_3Cl	Acetamide	1 : 1.5	1.041	23
EtNH_3Cl	Urea	1 : 1.5	1.140	23
ChCl	CF_3CONH_2	1 : 2	1.342	23
AcChCl	Urea	1 : 2	1.206	23
ChCl	Urea	1 : 2	1.25	23,24
ZnCl_2	Urea	1 : 3.5	1.63	12
ZnCl_2	Acetamide	1 : 4	1.36	12
ZnCl_2	EG	1 : 4	1.45	12
ZnCl_2	Hexanediol	1 : 3	1.38	12
ChCl	Glycerol	1 : 2	1.18	25,27
ChCl	Glycerol	1 : 3	1.20	25
ChCl	Glycerol	1 : 1	1.16	26
ChCl	Glycerol	1 : 3	1.20	26
ChCl	EG ^b	1 : 2	1.12	25,26
ChCl	EG	1 : 3	1.12	25,26
ChCl	Malonic acid	1 : 2	1.25	24
$\text{Et}_2(\text{EtOH})\text{NCl}^a$	Glycerol	1 : 2	1.17	26
$\text{Et}_2(\text{EtOH})\text{NCl}^a$	Glycerol	1 : 3	1.21	26
$\text{Et}_2(\text{EtOH})\text{NCl}^a$	Glycerol	1 : 4	1.22	26
$\text{Et}_2(\text{EtOH})\text{NCl}^a$	EG	1 : 2	1.10	26
$\text{Et}_2(\text{EtOH})\text{NCl}^a$	EG	1 : 3	1.10	26
$\text{Et}_2(\text{EtOH})\text{NCl}^a$	EG	1 : 4	1.10	26
$\text{Me}(\text{Ph})_3\text{PBr}^c$	Glycerol	1 : 2	1.31	26
$\text{Me}(\text{Ph})_3\text{PBr}^c$	Glycerol	1 : 3	1.30	26
$\text{Me}(\text{Ph})_3\text{PBr}^c$	Glycerol	1 : 4	1.30	26
$\text{Me}(\text{Ph})_3\text{PBr}^c$	EG	1 : 3	1.25	26
$\text{Me}(\text{Ph})_3\text{PBr}^c$	EG	1 : 4	1.23	26
$\text{Me}(\text{Ph})_3\text{PBr}^c$	EG	1 : 6	1.22	26

^a $\text{Et}_2(\text{EtOH})\text{NCl}$: *N,N*-diethylenethanol ammonium chloride. ^b EG is ethylene glycol. ^c $\text{Me}(\text{Ph})_3\text{PBr}$: methyltriphenylphosphonium bromide.

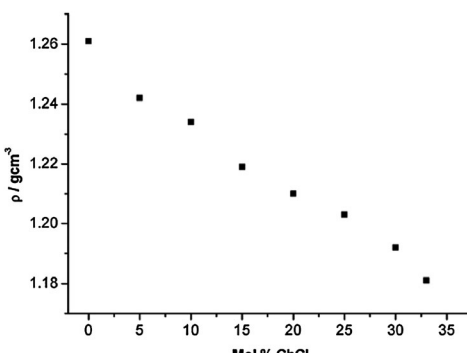


Fig. 2 Densities of the glycerol/ChCl DES as a function of the molar composition.²⁷ (Reproduced with permission from ref. 27. Copyright (2011) Royal Society of Chemistry.)

Addition of ChCl to glycerol results in a decrease of the DES density, which may be explained in terms of free volume.²⁶

Experimental measurements of DES densities as a function of the temperature are sometimes difficult to be achieved. Hence, particular attention was given to the development of new methods capable of providing these data with a maximum of accuracy. The Rackett equation modified by Spencer and Danner was employed to predict the density of DES with an error of $\pm 1.9\%$.²⁸

3.3 Viscosity

Like most of the ILs, viscosity of DESs is an important issue that needs to be addressed. Except for ChCl–ethylene glycol (EG) eutectic mixture, most of the DESs exhibit relatively high viscosities (> 100 cP) at room temperature. The high viscosity of DESs is often attributed to the presence of an extensive hydrogen bond network between each component, which results in a lower mobility of free species within the DES. The large ion size and very small void volume of most DESs but also other forces such as electrostatic or van der Waals interactions may contribute to the high viscosity of DES. Owing to their potential applications as green media, the development of DESs with low viscosities is highly desirable. In general, viscosities of eutectic mixtures are mainly affected by the chemical nature of the DES components (type of the ammonium salts and HBDs, organic salt/HBD molar ratio, etc.), the temperature, and the water content. As discussed above, viscosity of DES is also dependent on the free volume. Hence, the hole theory can also be used to design DESs with low viscosities. For instance, use of small cations or fluorinated hydrogen-bond donors can lead to the formation of DES with low viscosity.²³

Viscosity of binary eutectic mixtures is essentially governed by hydrogen bonds, van der Waals and electrostatic interactions. Table 4 lists the viscosity data of common DESs at different temperatures. It can be seen that the viscosity of ChCl-based DESs is closely dependent on the nature of the HBD. For instance, ChCl/EG (1 : 4) DES exhibits the lowest viscosity (19 cP at 20 °C). In contrast, use of derived sugars (e.g. xylitol, sorbitol) or carboxylic acids (e.g., malonic acid) as HBDs led to DESs exhibiting high viscosities (e.g., 12 730 cP at 20 °C for ChCl/sorbitol) due to the presence of a more robust 3D intermolecular hydrogen-bond network.

Table 4 Viscosities of selected DESs at different temperatures

Organic Salts	HBD	Salt : HBD molar ratio	Viscosities (cP)	Ref.
ChCl	Urea	1 : 2	750 (25 °C)	24
ChCl	Urea	1 : 2	169 (40 °C)	23
ChCl	EG	1 : 2	36 (20 °C)	25
ChCl	EG	1 : 2	37 (25 °C)	24
ChCl	EG	1 : 3	19 (20 °C)	25
ChCl	EG	1 : 4	19 (20 °C)	25
ChCl	Glucose	1 : 1	34 400 (50 °C)	19
ChCl	Glycerol	1 : 2	376 (20 °C)	25
ChCl	Glycerol	1 : 2	259 (25 °C)	24
ChCl	Glycerol	1 : 3	450 (20 °C)	25
ChCl	Glycerol	1 : 4	503 (20 °C)	25
ChCl	1,4-Butanediol	1 : 3	140 (20 °C)	25
ChCl	1,4-Butanediol	1 : 4	88 (20 °C)	25
ChCl	CF ₃ CONH ₂	1 : 2	77 (40 °C)	23
ChCl	Imidazole	3 : 7	15 (70 °C)	18
ChCl	ZnCl ₂	1 : 2	85 000 (25 °C)	29
ChCl	Xylitol	1 : 1	5230 (30 °C)	19
ChCl	Sorbitol	1 : 1	12 730 (30 °C)	19
ChCl	Malonic acid	1 : 2	1124 (25 °C)	24
ZnCl ₂	Urea	1 : 3.5	11 340 (25 °C)	25
Bu ₄ NBr	Imidazole	3 : 7	810 (20 °C)	18
EtNH ₃ Cl	CF ₃ CONH ₂	1 : 1.5	256 (40 °C)	23
EtNH ₃ Cl	Acetamide	1 : 1.5	64 (40 °C)	23
EtNH ₃ Cl	Urea	1 : 1.5	128 (40 °C)	23
AcChCl	Urea	1 : 2	2214 (40 °C)	23
Bu ₄ NBr	Imidazole	3 : 7	810 (20 °C)	18

Interestingly, in the case of a ChCl/glycerol DES, an increase of the ChCl/glycerol molar ratio results in a decrease of the DES viscosity (Fig. 3). For example, at 20 °C, viscosities of ChCl–glycerol mixtures with a molar ratio of 1 : 4, 1 : 3, 1 : 2 were 503, 450, and 376 cP, respectively. Glycerol has a strong cohesive energy due to the presence of an important intermolecular hydrogen bond network. This drastic decrease of the glycerol viscosity upon addition of ChCl was attributed to the partial rupture of this hydrogen bond network.²⁷

Viscosity (η) of most eutectic mixtures obviously changes significantly as a function of the temperature. Like ILs, the viscosity–temperature profiles also follow an Arrhenius-like behaviour. As the temperature increases, the viscosity decreases.

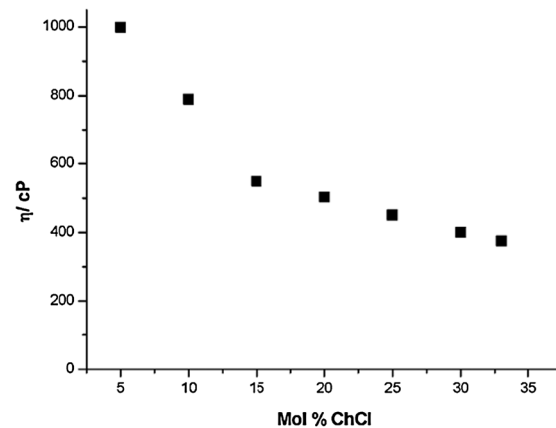


Fig. 3 Effect of ChCl on the viscosity, η , of glycerol as a function of composition at 298 K.²⁷ (Reproduced with permission from ref. 27. Copyright (2011) Royal Society of Chemistry.)

3.4 Polarity

Generally, polarity of a solvent can be evaluated by its polarity scale, E_T (30), which is the electronic transition energy of a probe dye (*e.g.* Reichardt's Dye 30) in a solvent. By means of UV-vis technology and using Reichardt's Dye 30, $E_T(30)$ can be calculated according to eqn (1).

$$\begin{aligned} E_T(30)(\text{kcal mol}^{-1}) &= h_{\text{CU max}} N_A \\ &= (2.8591 \times 10^{-3}) U_{\text{max}}(\text{cm}^{-1}) = 28591/\lambda_{\text{max}} \quad (1) \end{aligned}$$

In Table 5, the polarity data of various ChCl-glycerol eutectic mixtures using the Reichardt's Dye method are summarized.²⁷ These results show that ChCl/glycerol DESs exhibit similar polarity to those of $\text{RNH}_3^+ \text{X}^-$ and $\text{R}_2\text{NH}_2^+ \text{X}^-$ ILs bearing discrete anions.³⁰ Clearly, an increase in the ChCl/glycerol molar ratio results in an increase of the $E_T(30)$ of the DES. Additionally, a roughly linear increase of $E_T(30)$ with the ChCl concentration was observed.²⁹

3.5 Ionic conductivity

Owing to their relatively high viscosities, most of DESs exhibit poor ionic conductivities (lower than 2 mS cm^{-1} at room temperature). Table 6 lists the ionic conductivities of various DESs at different temperatures. Conductivities of DESs generally increase significantly as the temperature increases due to a decrease of the DES viscosity. Hence, Arrhenius-like equation can also be used to predict the conductivity behavior of a DES.

Considering that changes of the organic salt/HBD molar ratio significantly impact the viscosities of DES, it is clear that this parameter also dramatically influences the conductivities of DESs.¹⁴ The conductivity of DES increases with increasing the ChCl content.²⁵ When the molar fraction of ChCl is

Table 5 Solvent polarity parameters of various ChCl-glycerol mixtures

Solvents	Molar ratio of ChCl: Glycerol	$E_T(30)/\text{kcal mol}^{-1}$
Glycerol	—	57.17
ChCl: Glycerol	1 : 3	57.96
ChCl: Glycerol	1 : 2	58.28
ChCl: Glycerol	1 : 1.5	58.21
ChCl: Glycerol	1 : 1	58.49

Table 6 Ionic conductivities of part DESs at different temperatures

Salts	HBD	Salt : HBD (mol : mol)	Conductivity ($\kappa, \text{mS cm}^{-1}$)	Ref.
ChCl	Urea	1 : 2	0.199 (40 °C)	23
ChCl	EG	1 : 2	7.61 (20 °C)	25
ChCl	Glycerol	1 : 2	1.05 (20 °C)	25
ChCl	1,4-Butanediol	1 : 3	1.64 (20 °C)	25
ChCl	CF ₃ CONH ₂	1 : 2	0.286 (40 °C)	23
ChCl	Imidazole	3 : 7	12 (60 °C)	18
ChCl	ZnCl ₂	1 : 2	0.06 (42 °C)	29
ZnCl ₂	Urea	1 : 3.5	0.18 (42 °C)	29
Bu ₄ NBr	Imidazole	3 : 7	0.24 (60 °C)	18
EtNH ₃ Cl	CF ₃ CONH ₂	1 : 1.5	0.39 (40 °C)	23
EtNH ₃ Cl	Acetamide	1 : 1.5	0.688 (40 °C)	23
EtNH ₃ Cl	Urea	1 : 1.5	0.348 (40 °C)	23
AcChCl	Urea	1 : 2	0.017 (40 °C)	23
Bu ₄ NBr	Imidazole	3 : 7	0.24 (20 °C)	18

increased to 25 mol%, the conductivity of the ChCl-glycerol DES is 0.85 mS cm^{-1} . At higher salt concentrations, these ChCl/glycerol-based DESs exhibit a viscosity (<400 cP) and conductivity (> 1 mS cm^{-1}) comparable to those of an IL.

3.6 Acidity or alkalinity

The Hammett function has been widely used to evaluate the acidity and basicity of nonaqueous solvents by determining the ionization ratio of indicators in a system. For a basic solution, the Hammett function measures the tendency of the solution to capture protons. When weak acids are chosen as indicators, the Hammett function H_- is defined by the following equation.

$$H_- = pK(\text{HI}) + \log([\text{I}^-]/[\text{HI}]) \quad (2)$$

where $pK(\text{HI})$ is the thermodynamic ionization constant of the indicator in water, $[\text{I}^-]$ and $[\text{HI}]$ represent the molar concentrations of anionic and neutral forms of the indicator, respectively. A medium with large H_- value has strong basicity. When 4-nitrobenzylcyanide was used as indicator, the H_- value of the ChCl/urea (1 : 2) DES was 10.86, suggesting that this DES is weakly basic.³¹ Note that when the system contains 1–3 wt% of water, the H_- values decrease slightly (from 10.77 to 10.65) due to a partial solvation of basic sites.

Owing to the weak alkalinity of the ChCl-urea eutectic mixture, this DES is capable of absorbing a small amount of acid gas such as CO₂. In the presence of 1 atm of CO₂, the H_- value of ChCl/urea decreases from 10.86 to 6.25. After bubbling of N₂, the initial H_- value was recovered, suggesting that the acidity or basicity of this DES can be switched reversibly by bubbling CO₂ and N₂ through the solution alternately.

Obviously, the chemical nature of the HBDs has a strong effect on the acid or basic strength of the corresponding DESs. Fig. 4 shows the pH of several phosphonium-based DESs as a function of the temperature.²² From these curves, it is clear that the Me(Ph)₃PBr/glycerol (1 : 1.75) DES has a neutral pH, which did not vary significantly with the temperature. Conversely, the pH of the Me(Ph)₃PBr-CF₃CONH₂ (1 : 8) eutectic mixture was very low (2.5 at 20 °C) and increased when the temperature was raised. Note that when sugar-derived

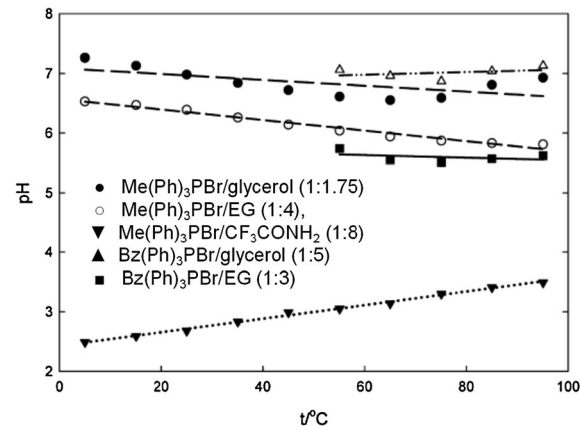


Fig. 4 pH values for selected phosphonium-based DESs as a function of temperature t in the range of 5 to 95 °C. (Reproduced with permission from ref. 22. Copyright (2010) American Chemical Society.)

polyols are used as HBDs in combination with ChCl, the obtained DES always exhibits a neutral pH.¹⁹

3.7 Surface tension

Up to now, studies related to the surface tension of DESs have been very scarce. Abbott *et al.* reported some data about the surface tension of ChCl-based and ZnCl₂-based DESs. Surface tensions of ChCl/malonic acid (1 : 1) and ChCl/phenylacetic acid (1 : 2) DESs were about 65.68 and 41.86 mN m⁻¹, respectively.¹⁴ Additionally, surface tensions of ChCl–ethylene glycol (1 : 3), ChCl–glycerol (1 : 3) and ChCl–1,4-butanediol (1 : 3) eutectic mixtures were 45.4, 50.8, and 47.6 mN m⁻¹ at 20 °C, respectively.²⁵ Surface tension of ZnCl₂/urea (1 : 3.5) DES was 72 mN m⁻¹, while the ZnCl₂/acetamide (1 : 4) DES has a smaller surface tension (53 mN m⁻¹ at 25 °C). The ZnCl₂/ethylene glycol (1 : 4) and ZnCl₂/1,6-hexanediol (1 : 3) DESs have surface tensions of 56.9 and 49 mN m⁻¹ at 25 °C, respectively. All these values were larger than the surface tensions of most of molecular solvents and comparable to those of imidazolium-based ILs and high temperature molten salts, *e.g.* 1-butyl-3-methylimidazolium tetrafluoroborate ([BMIM]BF₄, 38.4 mN m⁻¹ at 63 °C) and KBr (77.3 mN m⁻¹ at 900 °C).

Surface tension is also expected to follow a similar trend to viscosity since it strictly depends on the strength of intermolecular interaction that governs the formation of DESs. In particular, the surface tensions of various ChCl/glycerol DESs showed a linear correlation with temperature.²⁷ Additionally, surface tension of the ChCl/glycerol DES decreases as the ChCl concentration increases, supporting that addition of ChCl to glycerol disrupts the extensive hydrogen bond network of glycerol, as previously discussed for viscosity.

4. Dissolution and separation in DESs

4.1 CO₂ solubility

It is now well established that many ILs have strong ability to dissolve CO₂. Similar to ILs, DESs consist predominantly of ionic species, and thus also have interesting solvent properties for high CO₂ dissolution. Considering that combination of CO₂ with green DES systems has a great potential for a variety of chemical processes (separation and purification of gas, chemical fixation of CO₂, catalysis, *etc.*), studies on the CO₂ solubility in DESs are of prime importance. Recently, Han and co-workers determined the solubility of CO₂ in a ChCl/urea DES at different temperatures, pressures and with different ChCl/urea molar ratio.³²

The solubility of CO₂ (x_1) in ChCl/urea DES depends on three factors: (1) x_1 values increased with increase in the CO₂ pressure (solubility of CO₂ is more sensitive to the pressure in the low-pressure range); (2) x_1 values decreased with increase in the temperature whatever the pressure and (3) the ChCl/urea molar ratio also has a significant effect on x_1 values (*e.g.* at the same temperature and pressure, the ChCl/urea (1 : 2) eutectic mixture exhibits higher x_1 values than DES with a ChCl/urea molar ratio of 1 : 1.5 and 1 : 2.5).

Similar to the case of ILs, the gaseous phase can be assumed to be pure CO₂ due to the very low vapor pressure of DESs at low temperatures (≤ 60 °C). Thus, Henry's constants (k_H) of

CO₂ in different DESs can be obtained. At 333.15 K, the ChCl/urea (molar ratio 1 : 2.5) DES exhibited a k_H value of 29.0 MPa. Because ChCl is hygroscopic, most of the ChCl-based DESs always contain a small amount of water. Water acts as an antisolvent that drives CO₂ out from rich solutions, thereby affecting the solubility of CO₂. Recently, Wong and co-workers studied the solubility of CO₂ in ChCl/urea/H₂O DES at different temperatures (303, 308, and 313 K) and Henry's constants and at a CO₂ pressure of 0.1 MPa.³³ Results showed that the solubility of CO₂ in the ChCl/urea (molar ratio 1 : 2) DES decreased with increase in the water content. Determination of the enthalpy of CO₂ absorption demonstrated that at a DES/water molar fraction higher than 0.231, the absorption of CO₂ was endothermic. Below this molar ratio, the CO₂ absorption was exothermic. These data were very helpful for the evaluation and development of a concentration swing absorption–stripping process for capturing CO₂.

4.2 Dissolution of metal oxides

DESs are capable of donating or accepting electrons or protons to form hydrogen bonds which confers them excellent dissolution properties.³⁴ For example, in a ChCl/urea (1 : 2) DES at 50 °C, a large number of compounds can be dissolved, including water-soluble inorganic salts (*e.g.* LiCl > 2.5 mol L⁻¹), salts that are sparingly soluble in water (*e.g.* AgCl solubility = 0.66 mol L⁻¹), aromatic acids (*e.g.* benzoic acid solubility = 0.82 mol L⁻¹) and amino acids (*e.g.* D-alanine solubility = 0.38 mol L⁻¹).¹⁵ More interestingly, DESs are also capable of dissolving various metal oxides, thereby opening a “green” strategy for the separation and recycling of metals, a key point in electrochemistry technology (see Section 7). The dissolution and solubility of metal oxides in DESs still remain poorly explored due to the lack of data in comparable systems. In 2003, Abbott *et al.* first demonstrated the possibility of using DESs for the dissolution of metal oxides.¹⁴ For instance, at 50 °C, the solubility of CuO in a ChCl–urea eutectic mixture was 0.12 mol L⁻¹. Shortly after, Abbott *et al.* investigated the solubility of three metal oxides (ZnO, CuO, and Fe₃O₄) in different DESs. The employed DESs were formed by mixing ChCl with different carboxylic acids such as malonic, propionic and phenylpropionic acid. As shown in Table 7, ZnO, CuO, and Fe₃O₄ are soluble to a large extent in these DESs (0.071–0.554 mol L⁻¹ at 50 °C). However, notable differences in solubilities were observed according to the nature of DESs. For instance, Fe₃O₄ is highly soluble in the ChCl–oxalic acid (1 : 1) eutectic mixture, whereas it is nearly 20 times less soluble in the ChCl–phenylpropionic acid (1 : 2) DES. In contrast, CuO shows the opposite behavior, *i.e.* it is more soluble in ChCl–phenylpropionic acid (1 : 2) than in the ChCl–oxalic acid (1 : 1) eutectic mixture.

Table 7 Solubility of ZnO, CuO, and Fe₃O₄ in three DESs at 50 °C

DESs	Solubility (mol L ⁻¹)		
	CuO	Fe ₃ O ₄	ZnO
ChCl/malonic acid	0.246	0.071	0.554
ChCl/oxalic acid	0.071	0.341	0.491
ChCl/phenylpropionic acid	0.473	0.014	>0.491

Table 8 Solubility of metal oxides in a ChCl/urea (1 : 2) at 60 °C

Metal oxides	mp/°C	Solubility ^a /ppm
Al ₂ O ₃	2045	<1
CaO	2580	6
CuO	1326	470
Cu ₂ O	1235	8725
Fe ₂ O ₃	1565	49
Fe ₃ O ₄	1538	40
MnO ₂	535	493
NiO	1990	325
PbO ₂	888	9157
ZnO	1975	8466

^a The metal solubility was determined using ICP-AES.

Oxides such as aluminates or silicates are, however, insoluble in tested DESs. This difference of solubility of metal oxides in DESs can be used for the selective recovery of metals. Note that metals such as copper can be recovered electrochemically from the DES with high current efficiencies using bulk electrolysis.

The solubility of metal oxides in a ChCl/urea (1 : 2) DES was also explored. Solubility data at 60 °C were collected and summarized in Table 8. Dissolution of metal oxides in ChCl/urea DES is mainly governed by the complexation abilities of urea and the chloride anion. The electrospray mass spectrometry (MS) showed that a group of signals at *m/z* 174, 176, and 178, with an isotope pattern consistent with the formation of the [ZnClO-urea]⁻ anion, were observed when ZnO was dissolved in a ChCl-urea system, pushing forwards the coordination role of urea in the dissolution process. Such phenomenon was also observed by UV-vis spectrometry analysis in the case of CuO and CuCl₂.

Abbott *et al.* also systematically studied solubilities of ZnO, CuO, and Al₂O₃ in a DES formed between ChCl and thiourea. Although ZnO and CuO were soluble in such DES, Al₂O₃ remained insoluble.³⁵

This difference of solubility of metal oxides in DES has been successfully applied for the selective recovery of Zn and Pb from a waste material produced by an electric arc furnace (EAF). In particular, the ChCl-urea eutectic mixture was capable of selectively extracting zinc oxide (solubility = 4288 ppm at 60 °C) and lead oxides *versus* iron and aluminium oxides from waste of EAF. A similar result was reported using less viscous (56 cP at 298 K) DES such as ChCl/ethylene glycol/urea (molar ratio = 1 : 1.5 : 0.5).

A systematic study related to the solubility of transition metal oxides of Period 4 of the periodic table in three different DESs was reported by Abbott *et al.*³⁶ In ChCl-malonic acid (1 : 1), ChCl-urea (1 : 2), and ChCl-ethylene glycol (1 : 2) eutectic mixtures, metal oxides with a high ionic nature such as ZnO were highly soluble. Conversely, metal oxides with a more pronounced covalent nature such as TiO₂ were poorly soluble in these DESs. As expected, the solubility of metal oxides in DESs is strongly dependent on the temperature, especially Cu₂O and ZnO. FAB-MS spectrometry was also used to identify the metal-containing species in the DES after dissolution. In the cases of ChCl/malonic acid (1 : 1), CuO, Cu₂O, MnO, and ZnO gave predominantly chlorometallate species of the form MCl_x⁻.

Owing to their ability to dissolve metal oxides, DESs have become of great interest for surface cleaning, metallurgy, *etc.* It has been discussed above that the dissolution process of metal oxides in a ChCl-urea eutectic mixture involves the formation of a metal complex with urea. Very recently, density function theory (DFT) was employed to determine the extent of molecular ionic character of urea in a DES and how urea in its neutral and anion states binds with the surface of metal oxides or metals.³⁷ Quantum chemical calculations are proven very efficient to determine the binding energy of neutral and anionic urea with copper oxide and metallic copper, the main complexes believed to participate in surface cleaning with ChCl/urea (molar ratio 1 : 2) DES. These calculations suggested that the hydrogen bond interactions between urea and the chloride anion of choline maintain an open cluster structure. Proton transfer can then occur with an increase of the temperature or with metallic complex formation, leading to more aggressive solvent action.

4.3 Drug solubilization

To date, explorations of the solubility properties of DESs were mainly focusing on the dissolution of metal oxides. Studies on the dissolution of organic macromolecules in DESs are very scarce. Morrison *et al.* investigated the dissolution of several poorly soluble drugs including benzoic acid, griseofulvin, danazol, itraconazole and *N*-[4-[[6-[4-(trifluoromethyl)phenyl]-4-pyrimidinyl]oxy]-2-benzothiazolyl]acetamide (AMG517) in ChCl/urea and ChCl/malonic acid DESs.³⁸ Solubility was measured in pure DESs, mixtures of DESs with water (75 : 25 and 50 : 50 by weight), and pure water. Tested drugs are 5–22 000 folds more soluble in pure DESs (*i.e.*, ChCl/urea and ChCl/malonic acid) than in pure water. For example, the solubility of AMG517 in pure water was lower than 0.0001 mg mL⁻¹ vs. 0.01 mg mL⁻¹ and 0.4727 mg mL⁻¹ in pure ChCl/urea and ChCl/malonic acid, respectively. In the case of aqueous solution of DES, solubility of drugs was also enhanced as compared to neat water. Note that a separate use of aqueous solution of urea or ChCl or malonic acid did not result in an increase of the solubility of drugs, highlighting the particular behavior of eutectic mixtures for the dissolution of drugs. Owing to their low toxicity, DESs are now emerging as promising vehicles for oral dosing of rats during the early development of pharmacokinetic investigations. Indeed, toxicity (oral lethal dose for rats) for urea, choline chloride and malonic acid is 8471 mg kg⁻¹, 3400 mg kg⁻¹ and 1310 mg kg⁻¹, respectively, while the toxicity profile for mice for urea, choline chloride and malonic acid is 11 000 mg kg⁻¹, 3900 mg kg⁻¹ and 4000 mg kg⁻¹, respectively.

Moreover, it is noteworthy that recently the DESs have also been proven to be promising anhydrous solvents for nucleic acids. Hud and coworkers³⁹ showed that the nucleic acids can form several secondary structures that are reversibly denatured upon heating in DESs. In our opinion, this work definitely provides a new concept to widen the scope of DESs for life science.

4.4 Purification of biodiesel

Owing to their high polarity, DESs have also been used to separate residual glycerol from raw biodiesel. Biodiesel is

Published on 17 July 2012. Downloaded by Centro Federal de Educacão Tecnologica do Rio de Janeiro on 12/10/2018 12:18:23 PM.

produced through a transesterification reaction of vegetable oils either with methanol or ethanol. In this reaction, glycerol is released as a side product. Conversely to biodiesel, glycerol is highly polar. Hence, glycerol is commonly separated from biodiesel by liquid–liquid phase decantation. However, a non-negligible amount of glycerol remains in the biodiesel phase, thus requiring extra-treatments in order to reach the ASTM specifications prior to its use in vehicles. In this context, Abbott *et al.*⁴⁰ took benefit of the ability of various quaternary ammonium salts to form eutectic mixtures in the presence of glycerol in order to extract residual glycerol from raw biodiesel. Five quaternary ammonium salts including Pr_4NBr , EtNH_3Cl , $\text{ClEtMe}_3\text{NCl}$, ChCl , and AcChCl (acetylcholine chloride) were employed and all of them were capable of forming eutectic mixtures with glycerol. These DESs were miscible with water and immiscible with biodiesel. Soy bean oil was chosen as tested raw material because separation from glycerol is known to be difficult in this case. Initially, pure quaternary ammonium salts were directly added to raw biodiesel in order to evaluate if a DES could be spontaneously formed with residual glycerol contained in biodiesel. Unfortunately, this approach failed.

Next, the authors decided to extract residual glycerol from raw biodiesel with a quaternary ammonium salt–glycerol (1 : 1) eutectic mixture. In this case, the DES/biodiesel ratio was adjusted in order to obtain, after extraction of residual glycerol, an ammonium salt/glycerol molar ratio of 1 : 2 (sum of glycerol in the starting eutectic mixture with residual glycerol contained in the biodiesel phase). By means of ^1H NMR analysis of the biodiesel recovered after treatment with the ammonium salt/glycerol (1 : 1) DES, the authors observed a significant decrease of the content of glycerol in biodiesel, showing that DES can be used for the purification of biodiesel.

Fig. 5 presents the evolution of the glycerol mole fraction in an AcChCl (acetylcholine chloride)–glycerol eutectic mixture when mixed with raw biodiesel as a function of time.

Results showed that the eutectic mixture was saturated with glycerol after 10 min of contact time, which corresponded to the formation of an AcChCl –glycerol eutectic mixture in a molar ratio of 1 : 2. At this stage, 99% of glycerol was removed from biodiesel. According to the nature of the

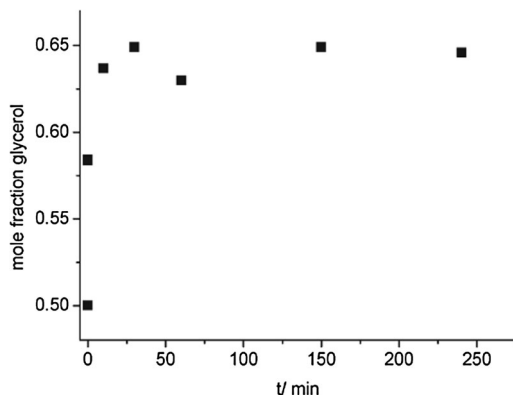


Fig. 5 Glycerol mole fraction in an AcChCl –glycerol mixture in contact with biodiesel containing glycerol as a function of time. (Reproduced with permission from ref. 40. Copyright (2007) Royal Society of Chemistry.)

quaternary ammonium salts, the extraction efficiency was changed to some extent. For example, formation of glycerol-based DES with ammonium bromide such as Pr_4NBr was found to be less efficient than with ammonium chloride. The higher extraction efficiency observed with ammonium chloride-based DES may be attributed to the higher electronegativity of the chloride anion. After extraction, quaternary ammonium salts were partly separated from the saturated DESs by recrystallisation from 1-butanol, although this process was not very efficient. Similarly, Hayyan *et al.* showed that ChCl /glycerol based DESs can also be used as a solvent for extracting glycerol from palm oil-derived biodiesel in a continuous mode.¹⁷ In such a process, a ChCl /glycerol molar ratio of 1 : 1 was found to be the best composition for an efficient extraction of residual glycerol.

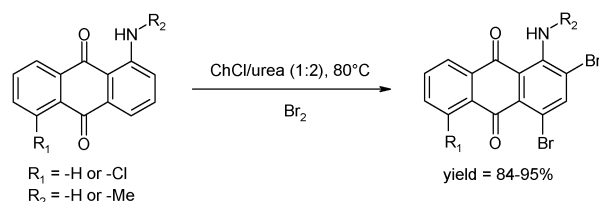
Recently, other ChCl -based DESs have also been used for the extraction of residual glycerol from biodiesel. For example, ChCl /ethylene glycol and ChCl /2,2,2-trifluracetamide DESs were also found to be efficient.¹⁶ Best extraction efficiency was obtained using a ChCl –ethylene glycol (1 : 2.5) or ChCl –2,2,2-trifluracetamide (1 : 1.75) eutectic mixture together with a DES/biodiesel ratio of 2.5 : 1 and 3/1, respectively. Phosphonium bromide based DESs were also used for the purification of palm oil-derived biodiesel.²¹ DESs were obtained by mixing methyl triphenyl phosphonium bromide with three different HDBs such as glycerol, ethylene glycol, or triethylene glycol. This study revealed that ethylene glycol and triethylene glycol-based DESs were very efficient for removing residual glycerol from palm oil-derived biodiesel. Note that, in these cases, a DES/biodiesel ratio of 0.75 : 1 was found to be optimum. Interestingly, all tested DESs were also capable of reducing the content of monoglycerides (MGs) and diglycerides (DGs) contained in raw biodiesel, thus affording biodiesel with the required ASTM specifications.

5. Catalysis in DESs

In the field of catalysis, the choice of the solvent is crucial. The solvent not only allows a better contact between reactants and catalysts but also determines the choice of work-up procedures and recycling (including the catalyst) or disposal strategies. In this context, the search of cheap and safe media for catalysis has become a very important topic. Recently, ILs have received considerable attention, especially for the stabilization of nanoparticles, the immobilization of homogeneous catalysts, the catalytic conversion of renewable raw materials (*i.e.* biomass, CO_2), among others. Comprehensive reviews covering this topic can be found in the current literature.⁴¹ Although fascinating results have been reported, ecological and economical footprint of these ILs-based processes still remains at an unacceptable level for an industrial application. As mentioned earlier, DESs exhibit similar properties to ILs. Hence, much effort is devoted to the use of DESs as cheap and safe solvents for catalysis. In this section, advances reported in the utilization of DESs for catalysis will be discussed.

5.1 Base-catalyzed reactions

In 2010, Shankarling and co-workers reported the electrophilic substitution of 1-aminoanthra-9,10-quinone derivatives in the

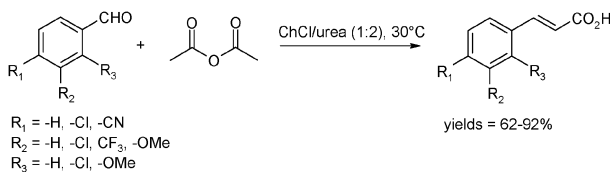


Scheme 2 Electrophilic substitution of 1-aminoanthra-9,10-quinone derivatives in ChCl/urea (1 : 2). (Adapted from ref. 42.)

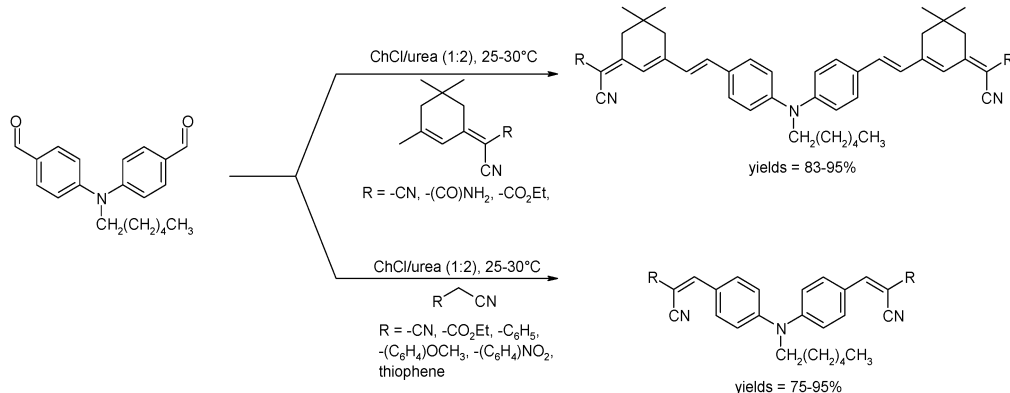
safe and cheap ChCl–urea (1 : 2) system.⁴² In particular, in the presence of 2.5 eq. of bromine, dibrominated products were obtained with a yield ranging from 84% to 95% at 80 °C (Scheme 2). As compared to traditionally-used organic solvents such as methanol or chloroform, the reaction rate was greatly improved in the ChCl–urea eutectic mixture. Although no explanation was provided by the authors, one may suspect that this rate enhancement might be attributed to the basic nature of the DES and/or to the ability of urea to stabilize transition states as previously observed for catalysis in water.⁴³

At the end of the reaction, products were selectively separated from the ChCl–urea (1 : 2) eutectic mixture by precipitation upon addition of water. Then, water was removed under vacuum, thus allowing the ChCl–urea (1 : 2) system to be recycled at least five times without appreciable decrease of reaction yields.

Later, the same group has reported the use of ChCl/urea (1 : 2)-based DES for the synthesis of cinnamic acid *via* the base-catalyzed Perkin reaction (Scheme 3).⁴⁴ Owing to its basic properties, the ChCl–urea (1 : 2) eutectic mixture was found to be a solvent of choice for promoting this reaction. From an equimolar mixture of benzaldehyde derivatives and acetic anhydride heated at 30 °C in a ChCl/urea (1 : 2)-based



Scheme 3 Base-catalyzed synthesis of cinnamic acid derivatives in ChCl/urea (1 : 2)-based DES. (Adapted from ref. 44.)



Scheme 4 Base-catalyzed Knovenagel in the ChCl–urea (1 : 2) system. (Adapted from ref. 45.)

DES, a large library of cinnamic acids were obtained with good to excellent yields (62–92%).

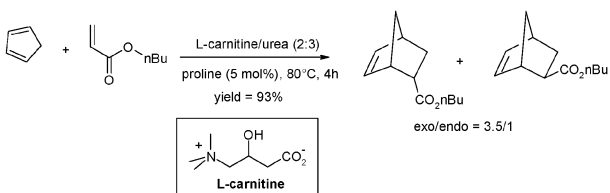
As compared to the conventional route (benzaldehyde/acetic anhydride/sodium acetate trihydrate in a molar ratio of 1 : 2 : 3), the reaction proceeded at much lower temperature (30 °C vs. 140 °C) allowing saving 62% of energy (estimated to 14.15 kJ g⁻¹ by calculation).

The basic nature of ChCl–urea (1 : 2) eutectic mixture can also be used for catalyzing other reactions such as a Knoevenagel reaction (Scheme 4). In this context, Sonawane *et al.* have reported the synthesis of diphenylamine-based chromophores in ChCl/urea (1 : 2) DES.⁴⁵ In particular, they have shown that a large library of valuable chromophores can be synthesized with high yields (75–95%) in ChCl/urea (1 : 2), offering an attractive alternative route to lipases or imidazolium-based ILs (Scheme 4). As mentioned earlier, this DES was successfully recycled five times thanks to the easy isolation of the products of the reaction from the DES phase.

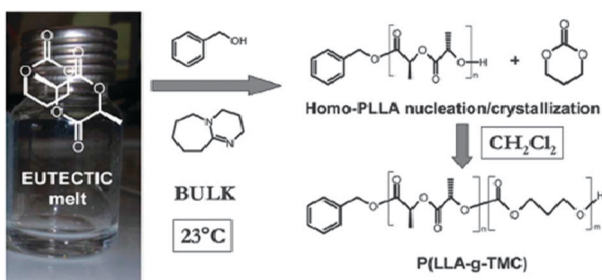
In 2009, B. König and co-workers reported that base-catalyzed Diels–Alder reaction can be performed in L-carnitine (obtained by fermentation from renewable bulk product)/urea (2 : 3) melt in the presence of 5 mol% of proline as a basic catalyst.⁴⁶ After 4 hours of reaction at 80 °C, the Diels–Alder adduct was obtained with 93% yield, offering an alternative to Sc(OTf)₃ traditionally used as a Lewis acid catalyst or imidazolium-based ILs, supercritical CO₂ and water used as solvent (Scheme 5).

Very recently, Coulembier and co-workers reported the copolymerization of lactide (LA) and 1,3-dioxan-2-one (TMC) in the presence of 1,8-diazabicyclo[5.4.0]undec-7-ene (DBU) as a basic catalyst.⁴⁷ Although use of lactide is attractive for the fabrication of safer and biodegradable polymers, assistance of potentially toxic organic solvents required for the solubilization of lactide dramatically decreases the environmental benefit of using this monomer. Within this context, the authors have found that LA and TMC were capable of forming a DES at 21.3 °C when mixed in a ratio of 1 : 1. At room temperature and in the presence of benzyl alcohol as initiator and DBU as catalyst, the resulting poly(lactide) (PLLA) chain started to nucleate in the eutectic and to crystallize out of the melt, limiting the growing of PLLA (15 500 g mol⁻¹).

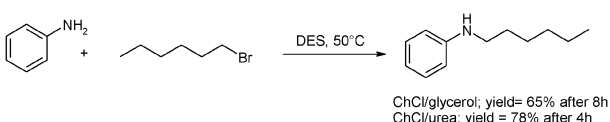
Interestingly, when the medium was slightly heated (up to 60 °C) or rapidly solubilized in dichloromethane when the



Scheme 5 Base-catalyzed Diels–Alder reaction in the L-carnitine/urea melt. (Adapted from ref. 46.)



Scheme 6 Co-polymerization of the LA–TMC eutectic mixture in the presence of DBU as catalyst. (Reproduced with permission from ref. 47. Copyright (2007) Royal Society of Chemistry.)



Scheme 7 Mono-*N*-alkylation of aniline with hexyl bromide in ChCl-derived DES. (Adapted from ref. 48.)

PLLA chain started to crystallize out of the melt, incorporation of TMC occurred (Scheme 6).

In 2011, Shankarling and co-workers reported that ChCl/urea and ChCl/glycerol DESs can be used as both catalyst and solvent for the mono-*N*-alkylation of aromatic amines.⁴⁸ In particular, the ChCl–urea eutectic mixture was more efficient than the ChCl–glycerol DES, presumably due to its higher basicity (Scheme 7). This methodology was tolerant to a wide range of substrates since various aromatic amines and alkyl bromides were successfully reacted affording, at 50 °C, the corresponding mono-*N*-alkylated amines with 70–89% yield. At the end of the reaction, products were selectively extracted from the ChCl–urea eutectic mixture by liquid–liquid phase extraction using ethylacetate. Hence, the authors successfully recycled the DES at least 5 times without noticeable decrease of yield, thereby offering an alternative route to lipase-catalyzed reaction for which a deactivation of the enzyme was observed cycle after cycle.

5.2 Acid-catalyzed reactions

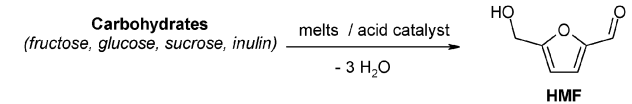
Acid-catalyzed dehydration of hexoses to 5-hydroxymethylfurfural (HMF) has gained considerable attention in recent years since HMF is a valuable molecule platform, especially for the fabrication of safer polymers and fuel additives.⁴⁹ In most of the works, acid-catalyzed dehydration of hexoses to HMF is achieved in imidazolium-based ILs for three reasons: (1) imidazolium-based ILs can dissolve large amounts of

hexoses, (2) imidazolium-based ILs can dilute released water, thus limiting the side rehydration of HMF to levulinic and formic acids and (3) HMF can be conveniently separated from imidazolium-based ILs by liquid–liquid phase extraction. However, as mentioned earlier, the price and toxicity of imidazolium-based ILs is a strong limitation for the commercialization of this process. To date, much effort has been paid to dehydrate hexoses in a more rational way using cheap and safe DESs.

In 2009, König and co-workers reported the acid-catalyzed dehydration of fructose to HMF in choline chloride/urea (1 : 2)-based DES.¹⁰ In this work, a high concentration of carbohydrates (40 wt%) was used. In the presence of an acid catalyst (10 mol% CrCl₂, CrCl₃, FeCl₃, AlCl₃ or Amberlyst 15), HMF was unfortunately obtained with low yields (<30%) due to side reaction between fructose and urea. When tetramethylurea was used instead of urea, side reactions were suppressed and HMF was obtained with 89% yield in the presence of 10 mol% of FeCl₃. However, the toxicity and problem of separation arising from the use of TMU represent two serious limitations. These results are in accordance with a previous work of Han and co-workers who have reported that basic DES (ChCl/urea) and Lewis acid (ZnCl₂, CrCl₃) in ChCl/metal chlorides-based DES were poorly efficient in the dehydration of fructose to HMF.⁵⁰ In order to overcome these problems, B. König and co-workers have next investigated the production of HMF in a eutectic mixture composed of carbohydrates and choline chloride. These high concentrated melts exhibit a low melting point (<80 °C), a low viscosity and a low toxicity.

In Table 9 are summarized the yields of HMF obtained from various melts. Except in the presence of ZnCl₂, HMF was obtained with 40–60% yields from melts composed of ChCl and fructose or inulin. Solid catalysts were also capable of promoting the dehydration of fructose to HMF (40–49% yield). From inulin, one should mention that montmorillonite is however less efficient than homogeneous catalysts. Conversion of glucose to HMF is more challenging and requires first an isomerization step to fructose before dehydration to HMF. As previously observed by Zhao *et al.* in imidazolium-based ILs,⁵¹

Table 9 Acid-catalyzed dehydration of carbohydrates to HMF in various melts



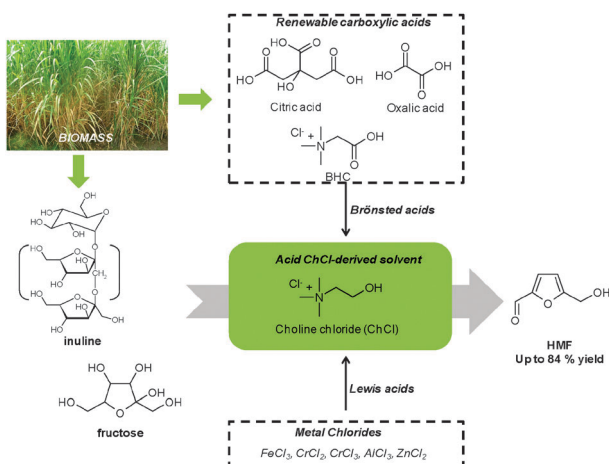
Catalyst	Yield of HMF (%) obtained from			
	Fructose/ChCl (2 : 3), 70 °C	Inulin/ChCl (2 : 3) nd	Glucose/ChCl (1 : 1), 80 °C	Sucrose/ChCl (1 : 1), 80 °C
FeCl ₃	59	55	15	27
ZnCl ₂	8	3	6	6
CrCl ₂	40	36	45	62
CrCl ₃	60	46	31	43
pTsOH	67	57	15	25
Sc(OTf) ₃	55	44	9	28
A15	40	54	9	27
Montmorillonite	49	7	7	35

^a 10 mol% of homogeneous catalyst or 5 wt% for solid catalyst, 100 °C.

chromium-based catalysts were found to be the most efficient in concentrated carbohydrate-derived DESs affording HMF with 31–45% yield and 43–62% yield from glucose and sucrose, respectively.

Han and co-workers have reported that HMF can also be produced in ChCl-derived DES without assistance of metal chloride-based catalysts, thus offering an even more attractive strategy from the view point of green chemistry.⁵⁰ In particular, the authors have shown that more than 76% yield of HMF (at 80 °C, 1 h, ratio DES/fructose = 5) can be obtained by dehydration of fructose in Brønsted DES composed of ChCl and citric acid, a cheap and renewable carboxylic acid readily obtained in large scale by fermentation of agricultural wastes. Note that other renewably sourced carboxylic acids such as oxalic and malonic acids were also eligible. Owing to the low solubility of HMF in ChCl/citric acid, the process can be performed in a continuous mode (biphasic system) using ethylacetate as an extraction solvent affording HMF with 91% yield. It should be noted that a slight decrease of the HMF yield was observed upon performing recycling experiments. The authors ascribed this drop of yield to the accumulation of water in the reaction media that affected the selectivity of the process (presumably due to the dominant acid catalyzed rehydration of HMF to levulinic and formic acid). After drying the ChCl–citric acid eutectic mixture, the initial yield of HMF was recovered, further demonstrating the stability of ChCl/citric acid-derived DES in such conditions.

Later, the same authors extended the scope of this process to the tandem depolymerization/dehydration of inulin, a bio-polymer of fructose, to HMF.⁵² In particular, in ChCl–oxalic acid and ChCl/citric acid, HMF was produced with 56% and 51% yield, respectively (80 °C, 2 h, 16 mol% of fructose in DES) (Scheme 8). In these systems, water plays a pivotal role by governing the depolymerization of inulin to fructose. For this reason, DESs were formed using hydrated oxalic and citric acids. Note that yields of HMF can be slightly improved by addition of water to the system. The authors defined *R* as the molar ratio of the additional water to fructose units in inulin. The HMF yield was optimal (nearly 60%) with *R* = 20 and 25 from ChCl/oxalic acid and ChCl/citric acid, respectively.



Scheme 8 Acid-catalyzed dehydration of inulin and fructose in ChCl-derived DES.

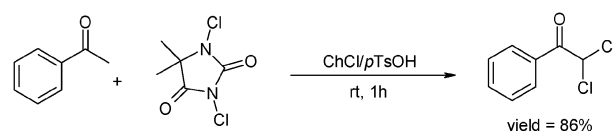
As described above, in a biphasic system (ChCl–oxalic acid–ethylacetate), the yield of HMF can be slightly improved up to 64%. After separation of the ethylacetate phase containing HMF, the ChCl/oxalic acid was recycled at least 6 times without appreciable loss of HMF yield.

In a similar way, De Oliveira Vigier *et al.* reported that betaine hydrochloride (BHC), a side product of the sugar beet industry, can be used as a renewably sourced Brønsted acid in combination with ChCl and water for the production of HMF from fructose and inulin.⁵³ In a ternary mixture ChCl–BHC–water (10/0.5/2), HMF was produced with 63% yield (at 130 °C from 40 wt% of fructose). As observed by Han and co-workers, when the reaction was performed in a biphasic system using methylisobutylketone (MIBK) as an extraction solvent, HMF was recovered with a purity higher than 95% and an isolated yield of 84% (from 10 wt% of fructose), further demonstrating that these systems similarly behave like traditional imidazolium-derived ILs (Scheme 8). Here also, the ChCl–BHC–water system was successfully recycled 7 times. In the same work, the authors have shown that the dehydration of fructose to HMF can also conveniently take place in a BHC–glycerol (1 : 1) mixture. Although 51% yield of HMF was obtained at 110 °C (from 10 wt% of fructose), extraction of HMF from the BHC/glycerol medium remained very difficult due to the very high solubility of HMF in this mixture.

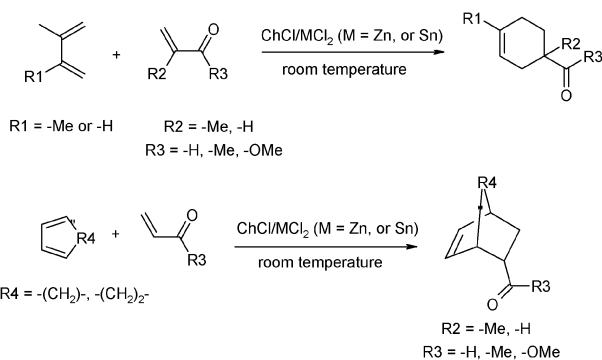
One should comment that the recent progress reported in the field of ChCl-derived DESs now offers suitable ways for the catalytic conversion of valuable renewable raw materials such as starch, lignin and cellulose.⁵⁴ It makes no doubt that DESs will definitely contribute to the catalytic conversion of lignocellulosic biomass in a more rational way and thus to the emergence of new bio-based chemicals in a close future.⁵⁵

Acid-catalyzed reactions in DESs have been also explored to access higher value added chemicals. In 2009, Zou and co-workers reported the α,α -dichlorination of acetophenone derivatives in an acidic DES composed of ChCl and *p*-toluene sulfonic acid (*p*-TsOH) mixed in a ratio of 1 : 1.⁵⁶ When the ratio DES/acetophenone was 2 : 1, the α,α -dichlorinated adduct was obtained with 86% yield at room temperature and in the presence of 1,3-dichloro-5,5-dimethylhydantoin as a chlorinating agent (Scheme 9). At the end of the reaction, the α,α -dichlorinated adduct was easily and selectively extracted from the ChCl/*p*TsOH DES using methyltertiobutylether as an extraction solvent, thereby allowing the authors to successfully recycle such DES at least 5 times.

In 2002, Davies and co-workers have reported the possible Diels–Alder reaction in ChCl/MCl₂ (M = Zn or Sn).⁵⁷ The Lewis acid nature of these eutectic mixtures significantly enhanced the reaction rate. Various dienes and dienophiles were reacted in ChCl/MCl₂, affording the Diels–Alder adduct



Scheme 9 α,α -dichlorination of acetophenone in ChCl/*p*TsOH. (Adapted from ref. 56.)



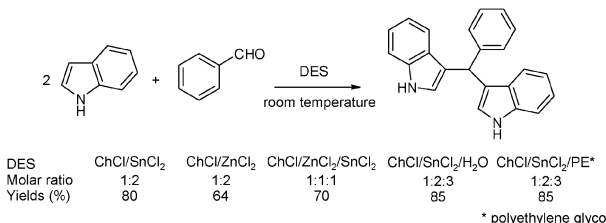
Scheme 10 Diels–Alder reaction in Lewis acid ChCl/MCl₂ (M = Zn or Sn). (Adapted from ref. 57.)

with 85–91% yield along with an *endo/exo* selectivity in the range of 83 : 17 to 97 : 3 (Scheme 10).

As compared to imidazolium-based ILs, ChCl/MCl₂ was not sensitive to the presence of water. For instance, the same reaction can be successfully performed in a mixture ZnCl₂–ChCl–H₂O (2 : 1 : 2), resulting in a decrease of the medium viscosity. Products of the reaction were not soluble in the ChCl–MCl₂ eutectic mixture. Hence, products can be conveniently isolated by simple decantation allowing, the recycling of the ChCl/MCl₂ DES.

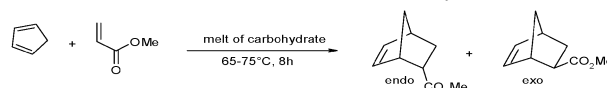
Very recently, Azizi and co-workers reported the acid-catalyzed synthesis of bis(indolylmethane) in a ChCl/SnCl₂ (1 : 2) DES (Scheme 11).⁵⁸ In such media a broad range of indole and aldehydes derivatives were successfully converted to the desired bis(indolyl)methane with moderate to excellent yields. Note that other ChCl-derived DESs were also eligible for this reaction.

In 2005, Imperato *et al.* investigated the Diels–Alder reaction in various melts composed of renewably sourced carbohydrates (or derived polyols) such as fructose, maltose, lactose, mannitol, glucose and sorbitol in combination with either urea or *N,N*-dimethylurea (DMU).⁵⁹ In a fructose/DMU (7 : 3) melt, the reaction proceeded well and the Diels–Alder adduct was obtained with a quantitative yield after 8 h of reaction at 71 °C. As shown in Table 10, other carbohydrate-derived melts were found to be very efficient for promoting the Diels–Alder reaction. In all cases, 72–100% yields were obtained while the *endo/exo* selectivity (2.7 : 1 to 5 : 1) was comparable to what was previously reported for other green solvents such as supercritical solvent, water, or imidazolium-based ILs. Addition of 10 mol% of a Lewis acid such as Sc(OTf)₃ to the sorbitol/DMU/NH₄Cl melt increases the *endo/exo* selectivity.



Scheme 11 Synthesis of bis(indolyl)methane in acid derived ChCl DESs. (Adapted from ref. 58.)

Table 10 Diels–Alder reaction in various carbohydrate-derived melts



Melt	T/°C	Yield (%)	Endo/exo ratio
Fructose/DMU (7 : 3)	71	Quant.	2.9 : 1
Maltose/DMU/NH ₄ Cl (5 : 4 : 1)	83	79	3.3 : 1
Lactose/DMU/NH ₄ Cl (6 : 3 : 1)	88	83	3.6 : 1
Mannitol/DMU/NH ₄ Cl (5 : 4 : 1)	89	74	2.7 : 1
Glucose/urea/CaCl ₂ (5 : 4 : 1)	75	76	3.2 : 1
Sorbitol/DMU/NH ₄ Cl (7 : 2 : 1)	67	Quant.	5.0 : 1
Sorbitol/DMU/NH ₄ Cl ^a (7 : 2 : 1)	67	Quant.	6.0 : 1

^a In the presence of 10 mol% of Sc(OTf)₃.

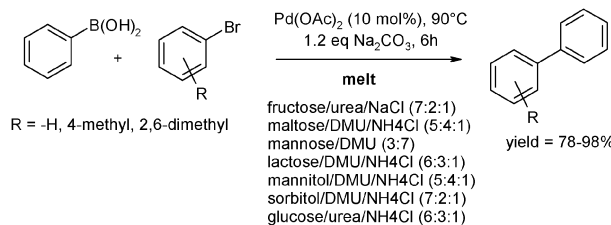
Efficiency of these carbohydrate-derived DESs was also successfully demonstrated using butyl acrylate as another dienophile.⁵⁹ At the end of the reaction, products of the reaction can be separated by decantation (upon addition of water) or distillation, offering the possibility to reuse these carbohydrate-derived DESs.

In 2011, del Monte and co-workers reported a frontal polymerization reaction using acid DES as a medium but also as a reservoir of monomer.⁶⁰ In particular, acrylic acid and methacrylic acid form a DES when mixed with ChCl in a ratio of 1 : 6 and 2 : 1, respectively. These DESs exhibit high viscosities (115 cP and 193 cP), which are helpful to stabilize the polymerization front. Upon addition of benzoyl chloride (thermal initiator) and ethyleneglycol (crosslinker), the frontal polymerization takes place. Under these conditions, conversion of acrylic and methacrylic are 75% and 85%, respectively. After dilution in water, the resulting poly(acrylic acid) was easily recovered and the ChCl was recycled. Proceeding on the same line, Serrano *et al.* have attempted the synthesis of poly(octanediol-*co*-citrate) elastomers loaded with lidocaine, an attractive anti-inflammatory compound.⁶¹ In this work, 1,8-octanediol and lidocaine were used as components of the DES. Here, the DES played multiple roles (1) as a reservoir of monomer (1,8-octanediol), (2) as a reservoir of active pharmaceutical ingredient (lidocaine) and (3) as a solvent for the dissolution of citric acid used as an initiator in this polymerization reaction.

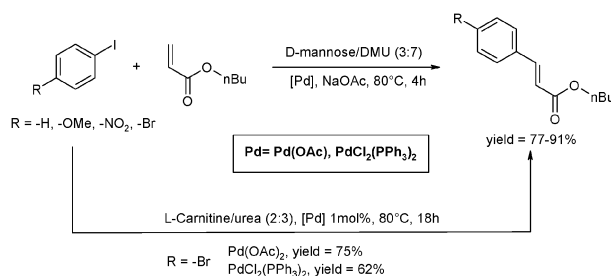
5.3 Transition-metal-catalyzed reactions

5.3.1 Catalytic C–C bond coupling. In 2006, König and co-workers investigated the palladium-catalyzed Suzuki coupling of phenyl boronic acid with aryl bromides in different carbohydrates–urea–inorganic salts eutectic mixtures.⁶² In all tested melts, quantitative conversion was observed and biarylated products were isolated with 78–98% yields (Scheme 12). At the end of the reaction, products were isolated by liquid–liquid phase extraction with pentane (after dilution in water).

Next, the same group highlighted that palladium-catalyzed Heck coupling can be successfully performed in low melt composed of *D*-mannose and *N,N*-dimethylurea (DMU) in a ratio of 3 : 7.⁴⁶ In the presence of homogeneous catalysts such as Pd(OAc)₂ or PdCl₂(PPh₃)₂, the cross-coupling was achieved with good to excellent yields (77–91%, Scheme 13). As compared



Scheme 12 Palladium-catalyzed Suzuki coupling in various carbohydrate–urea–inorganic salts eutectic mixtures. (Adapted from ref. 62.)



Scheme 13 Palladium-catalyzed Heck coupling in D-mannose/DMU melts. (Adapted from ref. 46.)

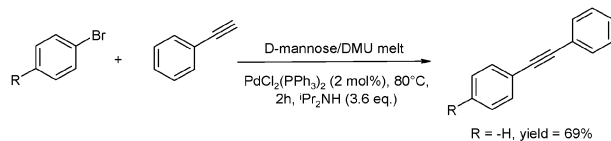
to the traditionally used imidazolium-based ILs ($[BMIM]PF_6$), lower reaction temperature ($80\text{ }^\circ\text{C}$ vs. $120\text{ }^\circ\text{C}$) and higher reaction rate were observed. In the presence of a heterogeneous catalyst such as Pd/C, the reaction rate was dramatically lowered, which was attributed to an increase in the reaction viscosity.

In such a case, the authors found that assistance of ultrasound allowed enhancing the reaction rate by a factor of 4.3.

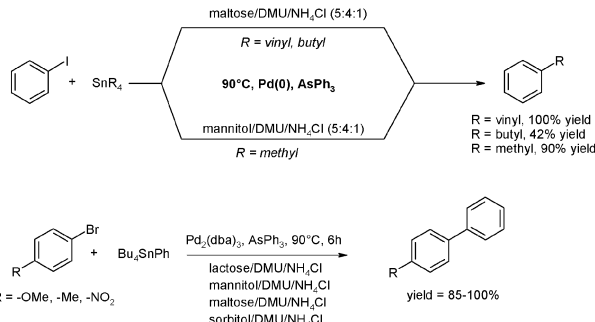
Catalytic Heck coupling can also be conveniently performed in low melting melt composed of L-carnitine and urea mixed in a ratio of 2 : 3.⁴⁶ The viscosity of such a melt, however, is slightly higher than that of other melts based on renewable feedstocks, which unfortunately lowers the reaction rate.

Sonogashira cross coupling is catalyzed by palladium but assistance of copper is generally required. Interestingly, in the presence of the $PdCl_2(PPh_3)_2$ in a D-mannose/DMU melt, the Sonogashira coupling takes place without assistance of copper, affording the Sonogashira adduct with 61–79% yield (Scheme 14).

Imperato *et al.* have investigated the Stille cross-coupling in various sugar–urea–salt melts.⁶³ In a typical procedure, iodobenzene was first coupled at $90\text{ }^\circ\text{C}$ with tetravinyltin, tetramethyltin and tetrabutyltin in the presence of the tris(dibenzylideneacetone)dipalladium(0) chloroform complex as palladium source and $AsPPh_3$ as ligand. Maltose/DMU/NH₄Cl was found to be the most promising eutectic mixture for the catalytic transfer of butyl and vinyl groups from tin to



Scheme 14 Sonogashira coupling in D-mannose/DMU melts. (Adapted from ref. 46.)



Scheme 15 Palladium-catalyzed Stille coupling of aryl bromide and iodide with alkyl and aryl stannane in polyol/DMU/NH₄Cl melts. (Adapted from ref. 63.)

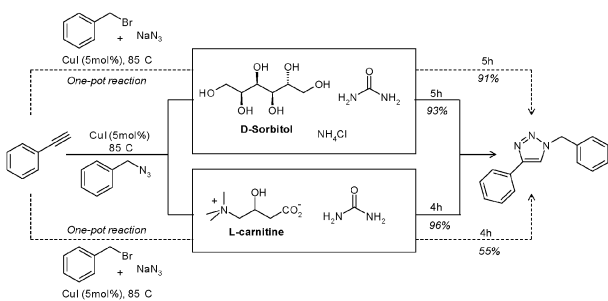
iodobenzene, affording the targeted alkylaryl with 42% and 100% yield, respectively. From tetramethyltin, the highest yield (90%) was obtained in the mannitol/DMU/NH₄Cl melt (Scheme 15). The authors highlighted that DMU can be replaced by urea without significant decrease of yields, thereby offering an even cheaper and greener route. As compared to imidazolium-based ILs, no biphenyl was produced in the melt. However, formation of benzene was noticed.

Synthesis of biaryl by Stille coupling also smoothly proceeds in polyol/DMU/NH₄Cl (with polyol = lactose, maltose, mannitol and sorbitol) from aryl bromide and tributylphenylstannate. After 6 h of reaction at $90\text{ }^\circ\text{C}$ in the presence of 1 mol% of tris(dibenzylideneacetone)dipalladium(0) and 4 mol% of $AsPPh_3$ as ligand, desired biaryl derivatives were produced with 85–100% yield. The amount of catalyst can be lowered up to 0.001 mol% without significant alteration of the reaction efficiency (TON = 87 000). More importantly, the recycling of the palladium-based catalyst is possible because products can be conveniently and selectively isolated from the catalytic phase by precipitation after addition of water, thereby offering an environmentally friendly route as compared to dimethylformamide or dioxane traditionally used as extraction solvents in such a coupling reaction.

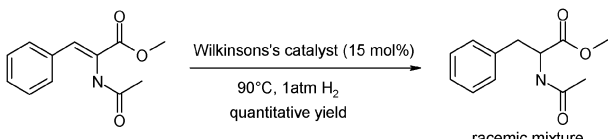
5.3.2 Copper-catalyzed azide alkyne 1,3-dipolar cycloaddition.

The Cu^I -catalyzed Huisgen 1,3-dipolar cycloaddition is a very useful synthetic tool in organic synthesis. In this context, D-sorbitol (hydrogenated form of glucose)/urea/NH₄Cl melt (7 : 2 : 1) has been used as a solvent owing to its high stability in the presence of a strong nucleophile such as sodium azide.⁴⁶ After 5 h of reaction at $85\text{ }^\circ\text{C}$ in the presence of 5 mol% of CuI, the 1,4-substituted 1,2,3-triazoles were obtained with 93% yield (Scheme 16). More importantly, the azide formation and cycloaddition can be performed in a one-pot process (from alkyne, benzyl bromide and sodium azide) in D-sorbitol/urea/NH₄Cl without affecting the reaction yield and allowing reduction of the number of synthetic steps (Scheme 16).

As described above for Diels–Alder reaction, click chemistry can also be successfully performed in L-carnitine–urea eutectic mixture.⁴⁶ Under similar conditions, the reaction rate was slightly enhanced in L-carnitine/urea (96% after 4 h of reaction vs. 93% after 5 h of reaction in D-Sorbitol/urea/NH₄Cl) presumably due to the stabilization of Cu^I by L-Carnitine as previously suggested by Ma and co-workers with proline.⁶⁴



Scheme 16 Cu-catalyzed azide-alkyne 1,3-dipolar cycloaddition in D-sorbitol/urea/NH₄Cl or L-carnitine/urea melts. (Adapted from ref. 46.)



Scheme 17 Catalytic hydrogenation of methyl α -cinnamate in citric acid/DMU (2 : 3). (Adapted from ref. 62.)

However, the one-pot reaction is more efficient in D-sorbitol/urea/NH₄Cl than in L-carnitine/urea due to the higher reactivity of the latter melt (55% yield vs. 91% in D-sorbitol/urea/NH₄Cl).

5.3.3 Hydrogenation reaction. In 2006, König and co-workers have reported the hydrogenation of methyl α -cinnamate in various carbohydrate/urea melts in the presence of Wilkinson's catalyst.⁶² Among all tested melts, the citric acid/DMU (2 : 3) was the most efficient eutectic mixture affording the hydrogenated product in a quantitative yield at 90 °C and under 1 atm of H₂ (Scheme 17). Although some of tested eutectic mixtures were chiral (sorbitol/DMU/NH₄Cl (7 : 2 : 1) or mannitol/DMU/NH₄Cl (5 : 4 : 1)), no asymmetric induction was observed.

5.4 Biocatalysis in DESs

Utilization of DES for biotransformations has not been extensively investigated because strong hydrogen bond donors such as urea are known to denature proteins.⁶⁵ In 2008, Kazlauskas and co-workers reported the first example of biocatalysis in various DESs.⁶⁶ In this work, the authors have investigated the activity of enzymes in the transesterification of ethyl valerate with butanol. Although poorly stable in an aqueous solution of ChCl (5 mol L⁻¹) and urea (10 mol L⁻¹), enzymes were found to be stable in a ChCl/urea DES. This remarkable stability was ascribed by the authors to the hydrogen bond network of DES that lowered the chemical reactivity of the DES components towards enzymes. As shown in Table 11, activity of enzymes in selected DES was similar to that observed in toluene. In particular, use of ChCl/glycerol or ChCl/urea DESs in the presence of lyophilized *Candida antarctica* lipase B (CLAB) or its immobilized form on acrylic resin (*i*CLAB) was the most efficient combination leading to more than 90% conversion of ethyl valerate to butyl valerate. Note that activity of *i*CLAB in ChCl/urea (20 $\mu\text{mol h}^{-1} \text{mg}^{-1}$) or in ChCl/glycerol (50 $\mu\text{mol h}^{-1} \text{mg}^{-1}$) was also found to be comparable and even higher than those collected in imidazolium-based ILs such as [BMIM]NTf₂ (24 $\mu\text{mol h}^{-1} \text{mg}^{-1}$) or

Table 11 Yield of butylvalerate obtained by transesterification of ethyl valerate by butanol at 60 °C in the presence of various enzymes

		DES, 60 °C enzyme	
Solvent	<i>i</i> CALB ^a	CALB ^b	CALA ^c
ChCl/acetamide	23	96	0.5
ChCl/glycerol	96	96	70
ChCl/malonic acid	30	58	0.7
ChCl/urea	93	99	1.6
Toluene	92	92	76
			PCL ^d
			5.0

^a Novozym 435 (*Candida antarctica* lipase B immobilized on acrylic resin).

^b Roche chirazyme L-2 (lyophilized *Candida antarctica* lipase B).

^c Roche chirazyme L-5 (lyophilized *Candida antarctica* lipase A).

^d Amano PS (lyophilized *burkholderia* (formerly *pseudomonas*) *cepacia* lipase).

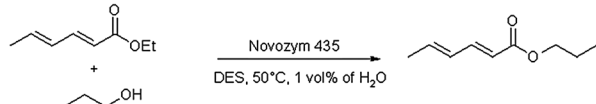
[BMIM]BF₄ (7 $\mu\text{mol h}^{-1} \text{mg}^{-1}$), further demonstrating the potential of DESs for biotransformations.

Interestingly, in ChCl/glycerol DES, side transesterification reaction between ethyl valerate and glycerol occurred to a very low extent (<0.5% of glyceryl esters), further demonstrating the lower reactivity of glycerol when involved in the formation of a DES. Next, use of ChCl/urea and ChCl/glycerol was successfully extended to the biocatalytic aminolysis of ethyl valerate with butylamine and to the ring opening of styrene oxide. Finally, the authors pointed out that ChCl/urea and ChCl/glycerol DESs were also suitable co-solvents with water for hydrolase-catalyzed reactions. In this case, DESs enhanced the reaction rate up to 20 times.

Positive effect of a DES as a co-solvent on the hydrolase-catalyzed reaction rate was later confirmed by Widersten and co-workers in the hydrolysis of 1S, 2S-2-methylstyrene epoxide.⁶⁷ Among all tested DESs, the ChCl-glycerol eutectic mixture was the most efficient medium. In this case, 50% of the relative activity of a potato epoxide hydrolase was indeed retained in the presence of 60% of ChCl/glycerol in an aqueous solution of sodium phosphate (0.1 M). At higher concentration of ChCl/glycerol DES, a loss of activity was observed. In the presence of ChCl-glycerol eutectic mixture, the regioselectivity was improved and the ring opening at the benzylic position became dominant. More importantly, the ChCl-glycerol eutectic mixture was capable of dissolving 1.5 times more epoxide than the phosphate buffer without affecting the optimal conversion rate, further demonstrating the potential offered by such DES for biocatalysis.

In 2011, Zhao and co-workers reported the use of DES based on choline acetate (ChOAc) and glycerol as a renewable hydrogen-bond donor for lipase-catalyzed transesterification reaction.⁶⁸ The main advantage of glycerol/choline-derived DES stems from their reduced viscosity as compared to the ChCl-urea system (80 mPa s vs. 120 mPa s at 50 °C). Additionally, the ChOAc-glycerol eutectic mixture is much less hygroscopic than ChCl-urea. One should also comment that viscosity and hygroscopicity of the ChOAc-glycerol eutectic mixture are, however, still higher than that of a hydrophobic imidazolium-based ILs such as [BMIM]NTf₂. In a first set of experiments, the authors have investigated the transesterification of ethyl sorbitate with 1-propanol

Table 12 Activity and selectivity of Novozym® 435 in the transesterification of ethylsorbate with 1-propanol

		
Solvent	Activity/ $\mu\text{mol min}^{-1} \text{g}^{-1}$	Selectivity (%)
<i>t</i> -Butanol	0.57	>99
1-Propanol	0.10	>99
Glycerol	0.71	38
ChCl/urea (1 : 2)	1.00	>99
ChCl/glycerol (1 : 2)	1.12	45
ChOAc/glycerol (1 : 2)	0.21	40
ChOAc/EG (1 : 2) ^a	0.07	12 ^b
ChOAc/glycerol (1 : 2)	1.02	99

^a EG = ethylene glycol. ^b EG is reactive explaining the lower selectivity.

catalyzed by Novozym® 435 (*Candida antarctica* lipase B immobilized on acrylic resin) in various DESs. Among tested DESs, the highest initial rate ($\sim 1 \mu\text{mol min}^{-1} \text{g}^{-1}$) and selectivity (>99%) were obtained in ChCl/urea and ChOAc/glycerol DESs. When the reaction was performed in neat glycerol, *t*-butanol or 1-propanol, the activity of enzyme was lower, indicating the superior performances of the ChOAc/glycerol DES (Table 12).

A decrease of the ChCl/glycerol mass ratio from 1 : 2 to 1 : 1 resulted in a decrease of the lipase activity. This phenomenon was ascribed by the authors to the higher concentration of the chloride anion in the melt resulting in the destabilization of lipase. Remarkably, in a ChOAc/glycerol (1 : 1.5) DES, the lipase was highly stable since Novozym® 435 maintained 92% and 50% of its activity after 48 h and 168 h of pre-incubation, respectively, showing the potential offered by this cheap and biodegradable medium for biotransformations. Note that no side transesterification reaction with the glycerol or cholinium cation was observed in agreement with the work of Kazlauskas and co-workers, who have showed that, in a ChCl/glycerol DES, the reactivity of glycerol was 600 times lower than that of 1-butanol.⁶⁶

In continuation of their efforts, the same group next investigated the methanolysis of Miglyol® oil 812, a mixture of triglycerides of caprylic acid and capric acid. After 1 h of reaction at 50 °C, 82% conversion was achieved in a ChOAc/glycerol (1 : 1.5) DES containing 1.0 vol% of water and 20 vol% of methanol. Nearly complete conversion was observed after 3 h of reaction whereas 24 to 96 h were required with traditionally used imidazolium-based ILs, showing the highest compatibility of ChOAc/glycerol DES for lipase.

Later, Zhao *et al.* reported that proteases, known to be less stable in non-aqueous medium than lipases can also be successfully used in choline acetate (ChOAc)/glycerol and ChCl/glycerol DESs.⁶⁹ Such DESs have been preferred to ChCl/urea owing to their lower viscosity and because glycerol is less denaturant than urea for proteases. In order to highlight the potential of the choline–glycerol eutectic mixtures for biotransformations, the protease-catalyzed transesterification of *N*-acetyl-L-phenylalanine ethyl ester with 1-propanol has been chosen as a representative model reaction. This reaction involves two stages: (1) formation of an acyl-enzyme intermediate

Table 13 Activities of subtilisin and α -chymotrypsin in glycerol-derived DESs

Solvent	Protease ^a	Water content (v/v)%	Activity/ $\mu\text{mol min}^{-1} \text{g}^{-1}$	Sel. (%)
<i>t</i> -Butanol	S/Chit	2	0.50	29
ChOAc/glycerol (1 : 1.5)	S/Chit	2	0.42	99
ChOAc/glycerol (1 : 1.5)	S/Chit	3	0.40	99
ChOAc/glycerol (1 : 1.5)	S/Chit	4	0.90	99
ChCl/glycerol (1 : 2)	Free α -C	2	0.028	99
ChCl/glycerol (1 : 2)	α -C/Chit	2	0.031	99
ChCl/glycerol (1 : 2)	α -C/Chit	3	0.75	99
ChCl/glycerol (1 : 2)	S/Chit	3	2.90	98

^a 50 °C, S = subtilisin, α -C = α -chymotrypsin, Chit = chitosan.

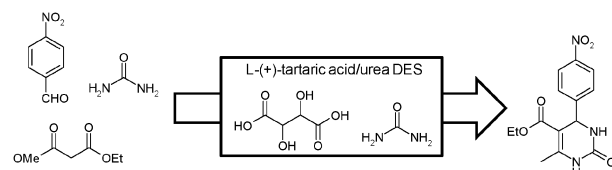
followed by (2) a competition between transesterification and hydrolysis. All reactions were performed at 50 °C either in ChOAc/glycerol or ChCl/glycerol DESs in the presence of cross-linked proteases (subtilisin and α -chymotrypsin), immobilized on chitosan. As shown in Table 13, the best results were obtained in ChCl/glycerol (1 : 2) with 3 vol% of water using subtilisin on chitosan. Under such conditions, activity of the protease reached 2.9 $\mu\text{mol min}^{-1} \text{g}^{-1}$ along with the formation of the desired propyl ester with 98% selectivity, indicating that glycerol-derived DESs were very attractive for biocatalytic reactions involving more sensitive enzyme than lipase. As compared to *t*-butanol used as a reference solvent, ChCl/glycerol DES provided much better results in terms of activity and selectivity. Interestingly, as observed above, glycerol seems to be chemically inert. Although protease can be denatured by an anion such as chloride or acetate, their effect is dramatically lowered in a DES due to the presence of glycerol which tends to form strong hydrogen bonds with these anions.

It is noteworthy that in 2010, Gutierrez *et al.* have reported the use of a freeze-drying process for the efficient incorporation of enzymes in ChCl/glycerol (1 : 2) DES without altering their integrity and viability.⁷⁰ It is our opinion that this work definitely opens a promising route to widen the scope of DESs for biotransformations.

The remarkable stability of enzymes in DESs has been recently highlighted by Verpoorte and co-workers in a scientific correspondence. In particular, the authors have hypothesized that the formation of natural DESs from chemicals that are present at high concentration in living cells may contribute to explain (1) mechanisms and phenomena that are nowadays difficult to understand and (2) the resistance of living organisms under extreme conditions.⁷¹

6. Organic synthesis in DESs

In the field of organic synthesis, the search for a green solvent is also of great interest and aims at reducing the use of toxic chemicals.



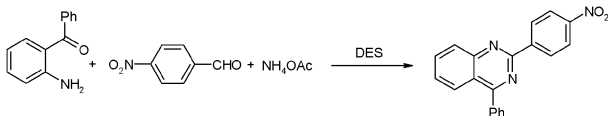
Scheme 18 Example of Biginelli reaction performed in acid L-(+)-tartaric acid/DMU (3 : 7) DES. (Adapted from ref. 72.)

In this context, Gore *et al.* reported the multicomponent synthesis of valuable biologically active dihydropyrimidinone (DHPM) in acidic DESs.⁷² This work aims at by-passing the traditional use of Brönsted and Lewis acids which dramatically impact the economical and ecological footprint of this reaction. DHPM was synthesized from urea, aldehyde and β -ketoesters (Biginelli reaction, Scheme 18). Hence, urea was used in this example not only as a reactant but also as a component of the DES. For instance, in a citric acid/DMU (2 : 3) DES, *p*-4-nitrobenzaldehyde, ethylacetacetate and DMU were selectively assembled at 65 °C to the desired DHPM which was obtained with 90% yield. An even higher yield (96%) was reported in a L-(+)-tartaric acid/DMU (3 : 7) DES.

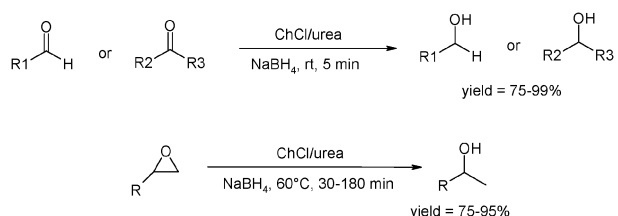
This methodology exhibits a very broad substrate scope and many aldehydes and β -ketoesters were successfully assembled in L-(+)-tartaric acid/DMU (3 : 7), affording DHPM with good to excellent yields. Note that in L-(+)-tartaric acid/ChCl (1 : 1), thiourea and 3-hydroxybenzaldehyde smoothly reacted with ethylacetacetate to produce an anticancer drug named monastrol with 86% yield. Finally, the authors highlighted that masked aldehydes can also be used in the L-(+)-tartaric acid/DMU melt for the production of DHPM.

Multicomponent reaction can also take place in other carbohydrate-derived melts. In this context, Zhang *et al.* reported the synthesis of quinazoline derivatives *via* a one-pot three component reaction of 2-aminoaryl ketones, aldehydes and ammonium acetate in various carbohydrate-derived melts.⁷³ The best results were obtained in a maltose/DMU/NH₄Cl DES and the desired quinazoline was obtained with 92% yield (Table 14). This work exhibited a broad substrate scope and products of the reaction were conveniently isolated from the DES either by crystallization or by extraction with ethyl acetate, allowing the DES to be recycled.

Table 14 Three component reactions of 2-amino-benzophenone, 4-nitrobenzaldehyde and ammonium acetate in various DESs



Melt	T/°C	Yield (%)
Citric acid/DMU (4 : 6)	65	85
Fructose/DMU (7 : 3)	71	75
Tartaric acid/DMU (3 : 7)	70	82
Tartaric acid/ChCl (5 : 5)	90	89
Mannose/DMU/NH ₄ Cl (5 : 4 : 1)	89	82
Lactose/DMU/NH ₄ Cl (5 : 4 : 1)	88	86
Maltose/DMU/NH ₄ Cl (5 : 4 : 1)	84	92



Scheme 19 Reduction of aldehydes and epoxides by NaBH₄ in ChCl/urea. (Adapted from ref. 75.)

Very recently, Zhang *et al.* extended this work and have reported that synthesis of quinoline derivatives (from aniline and ketones derivatives) can also be conveniently performed *via* the Friedländer reaction in low melting tartaric acid–urea mixtures.⁷⁴ This reaction exhibits a broad substrate scope in such DES and the targeted quinoline derivatives were obtained with fair to excellent yields.

Azizi and co-workers reported the chemoselective reduction of functionalized carbonyl derivatives and epoxides in ChCl/urea in the presence of sodium borohydride (NaBH₄).⁷⁵ At room temperature and with 2 eq. of NaBH₄, a wide range of aldehydes and ketones were reduced in less than 5 min in ChCl/urea, affording the corresponding alcohol with a yield in the range of 75–99% (Scheme 19). Additionally, a broad range of epoxides were also reduced in the presence of NaBH₄ in ChCl/urea, affording the desired alcohols with 75–95% yield.

7. Electrochemistry in DESs

The earliest research studies on ionic fluids started with the purpose of electrochemical application, *viz.* Humphrey Davy's pioneering works on the electrodeposition of simple molten salts. Due to their unique properties, ILs found a wide range of applications in various electrochemical devices including for instance lithium ion batteries, fuel cells, super capacitors, dye sensitized solar cells, *etc.* Similar to ILs, DESs were also used in electrochemistry as electrolytes for electrodeposition of metal, as solvents for electrochemistry reaction and for electropolishing (metal dissolution), *etc.*

7.1 Electrodeposition

Electrodeposition is a process leading to the formation of solid materials by electrochemical reactions in a liquid phase. The setup is composed of a three-electrode electrochemical cell (a reference electrode, a specially designed cathode, and an anode or counter electrode). In a very simple way, the metal (cationic form) contained in the electrolyte is reduced at the cathode and deposited as metal as shown in Fig. 6.

Electrodeposition of metals is widely used to functionalize surfaces for corrosion-resistance, electrocatalysis, magnetic applications, photoactive semiconductors (photovoltaics) electrolytes in the printing industry and hardening of steel for engineered components or in electronic industries for the production of printed circuit boards.⁷⁶ Electrodeposition of metals can be performed in the presence of various solvents but this process is obviously limited by the redox potential windows of the considered solvent. Electrolytes should indeed have a high resistance against electrochemical reduction and

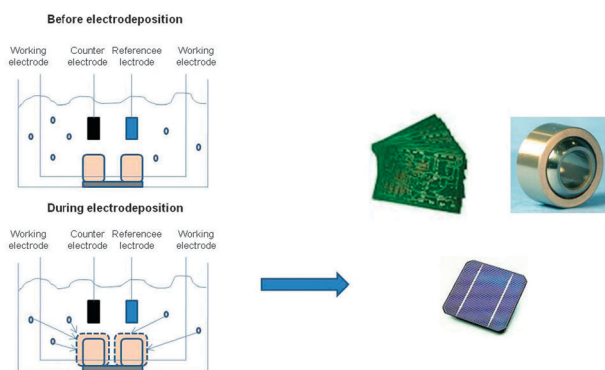


Fig. 6 Schematic view of the electrodeposition process.

oxidation. In aqueous solutions, electrodeposition of metals is generally restricted to those exhibiting a redox potential higher than that of water. Organic solvents are also attractive for electrodeposition mainly because some of them exhibit a potential window that is 1.5–2.5 times wider than that of common aqueous acid electrolytes. In this context, DMF, DMSO, THF, methylene chloride and propylene carbonate are of particular interest for electrodeposition processes.⁷⁷

In the past two decades ILs have received considerable interest for electrodeposition.⁷⁸ In particular, electrodeposition of metals and alloys, which is carried out with difficulties in aqueous solvents, was successfully achieved in ILs.⁷⁹ Although promising results have been reported, syntheses of ILs, their sensitivity to water and their possible degradation under oxygen represent some major drawbacks. Thanks to their similar properties with those of ILs, DESs have received growing interest for their use as electrolytes. In particular, their tolerance to water together with their low price and biodegradability represent three major advantages over ILs. In this section, we will describe the contribution of DESs for electrodeposition of metals. In this field of research, DESs made of ChCl and either urea or ethylene glycol or glycerol have been mostly investigated.

7.1.1 Electrodeposition in a ChCl/urea DES. Electrodeposition of SmCo has been successfully performed in a ChCl/urea (1 : 2) DES by Gomez *et al.* using a cylindrical three electrode cell of one single compartment.⁸⁰ The working electrode was a vitreous carbon and the counter electrode was a platinum spiral. The reference electrode was an Ag/AgCl/NaCl 3 M fixed in a Luggin Capillary containing the DES. The redox window of the DES (−2.4 to 0.4 V) is compatible with the use of vitreous carbon electrodes. The electrodeposition was performed at 70 °C in order to decrease the viscosity of the DES and to overcome the mass transfer problem. In a first set of experiments, cobalt alone was deposited on vitreous carbon in the ChCl/urea (1 : 2) DES. These experiments have shown that the nucleation and growth of metallic cobalt readily takes place in ChCl/urea. When samarium was deposited instead of cobalt, an unusual deposition process was observed. Two reduction regions were indeed identified with Sm. At low overpotential, the deposit of Sm formed was less conductive than the vitreous carbon used as substrate. When the potential becomes higher (*i.e.* −1.6 V), the deposition of samarium is

more efficient. Note that at this high potential, the current density increases with the stirring. Concomitant deposition of cobalt and samarium can also be achieved in this DES. Starting from a Sm^{III}/Co^{II} molar ratio of 4 : 1, SmCo was deposited. The deposit contained up to 70 wt% of Sm when the potential applied to vitreous carbon was sufficiently negative (−1.6 V) or when anodic metallic substrate (Ni/Cu/Au) was used instead of vitreous carbon. Note that composition of the Sm/Co deposit may be changed when the deposition process was achieved at a potential higher than −0.85 V. Using such a process, deposition of SmCo formed either films or nanowires, depending on the temperature.⁸¹

The electrodeposition of Cu–Ga can also be performed in ChCl/urea DES, yielding cheap thin film with interesting applications in solar cells. Shivagan *et al.* have shown that electrodeposition of (Cu–In–5Ga)–Se can be performed in ChCl/urea DES, leading to 6–8% of incorporation of Ga into Cu–In–Se film even when the concentration of GaCl₃ was very high (40–80 mM).⁸² Later, Dale *et al.* have shown that, in a ChCl/urea DES, Gd can also be deposited over a Mo electrode in a reversible process without any interference of the solvent.⁸³ In particular, an increase in the temperature induced an increase in the redox window of the DES, owing to a decrease in the DES viscosity.

Nickel was also successfully electrodeposited in a ChCl/urea DES using a copper microelectrode. The potential window of the ChCl/urea DES is between −1.35 and 0.24 V.⁸⁴ Morphology, microstructure and redox behaviour of Ni(II) deposited on Cu was affected by the addition of nicotinic acid in the DES. In particular, addition of nicotinic acid to the DES led to an inhibition of the nickel deposition current explained by the adsorption of nicotinic acid in the DES and the formation of a Ni(II) complex with nicotinic acid. By controlling the amount of nicotinic acid in DES, it was possible to control the nature of the deposit. In a similar way, Abbott *et al.* have reported that addition of ethylenediamine to the DES containing 0.2 M NiCl₂·6H₂O led to the formation of a deposit with smaller particles size mainly due to the formation of a [Ni(ethylenediamine)₃]²⁺ complex.⁸⁵ Effect of nicotinic acid and ethylenediamine on the electrodeposition of Ni was attributed to (i) the formation of a Ni complex and (ii) its absorption on the electrode surface, which block the nucleation and the particle growth. Compact nickel-multiwalled carbon nanotube composites were also deposited on a copper substrate.⁸⁶ Success of this reaction relied on the homogeneous dispersion of microwall carbon nanotubes (MWCNTs) which is a pre-requisite step for an efficient electrodeposition with the nickel matrix. Remarkably, in ChCl/urea DES, the dispersion of MWCNTs was very good (high stability of the suspension). Addition of anhydrous nickel chloride to the suspension of MWCNTs in DES did not drastically affect the dispersion of MWCNTs. Morphology, roughness and crystallinity of deposited Ni were obviously affected by the presence of MWCNTs in the DES. Ni was also deposited on a Pt electrode in a ChCl/EG DES.⁸⁷ The deposition is quasi-reversible. Two different morphologies of metal deposits, nanodeposits and bulk metal, were observed.

Ethylenediamine (en) and sodium acetylacetone (acac) were also used as additives (brighteners) during the nickel

deposition process. This experiment aimed at (i) producing more stable Ni complex (ii) suppressing underpotential deposition and (iii) decreasing the ability of the metal to nucleate. In the cathodic part, three moles of additives were necessary to reduce free ethylenediamine and to form $[\text{Ni}(\text{en})_3]^{2+}$. In the anodic part only 1 mol equivalent is necessary to oxidize nickel. Birbilis *et al.* have studied the electrodeposition of Ni-Zn alloys in a ChCl/urea DES using a copper electrode.⁸⁸ Electrodeposition was carried out at 70 °C in the presence of anhydrous nickel and zinc chlorides. Composition, surface morphology and phase structure of the Ni-Zn alloys are dependent on the current density and the working potential. Although Ni was incorporated in a higher amount than Zn in the Ni-Zn alloy, the Ni content decreased when (i) the deposition potential became more negative (decrease from -0.6 to -1.2 V) and (ii) the current density increased. Similar alloy was obtained using a platinum electrode.⁸⁹ The Ni-Zn alloy formed in this last case was made of cubic crystallites. The electrochemical depositions were rather slow in ChCl/urea DES due to its high viscosity that induces low diffusion coefficients. Note that electrodeposition of neat zinc was also possible by this method and led to the formation of small crystallites.

Dale *et al.* have reported that CdS, CdSe and ZnS can be electrodeposited in a ChCl/urea DES.⁹⁰ In this study, the working electrode was a glassy carbon or fluorine doped with tin oxide (FTO). In a first set of experiments, the authors have studied the stability of both electrodes and they have observed that in the case of glassy carbon, the DES was partly contaminated by carbon residues. In the presence of FTO, the reversible reduction of SnO_2 to metallic Sn occurred. The deposition of a film of CdS on fluorine doped tin oxide was performed in a potential range of -0.6 to -0.8 V. During the electrodeposition, a change of the CdS film colour from pale transparent yellow (-0.6 V) to dark brown (-0.8 V) was observed due to the accumulation of Cd in the film. The recovered CdS film exhibited a thickness lower than 50 nm.

Magnesium is a water-sensitive substrate (from the electrodeposition point of view), making technically difficult its electrodeposition in aqueous solution. Hence, the ChCl/urea DES was also investigated for the electrodeposition of Zn onto several Mg alloys.⁹¹ The authors have compared the efficiency of several DESs such as ChCl/ethylene glycol (2/1), ChCl/malonic acid (1/1), ChCl/glycerol (1/2) and ChCl/ZnCl₂ (1/2). From this study it appears that ChCl/urea and ChCl/glycerol were the most efficient systems leading to the lowest corrosion of magnesium. The use of ChCl/glycerol DES, however, resulted in the pitting of the magnesium surface. Hence, the ChCl-urea mixture was found to be the most appropriate DES for the electrodeposition of Zn on Mg.

Ying *et al.* have studied the stability of the ChCl/urea DES during the electrodeposition process. In particular, the authors have observed the formation of gaseous chemicals at the cathode (trimethylamine) and anode (chlorine) during the nucleation of metal (Co-Cr) suggesting a partial degradation of the DES during the electrodeposition process.⁹²

7.1.2 Electrodeposition in a ChCl/ethylene glycol DES.

Electrodeposition of Zn, Sn and Zn-Sn alloy has been carried

out in ChCl/ethylene glycol by Abbott *et al.*⁹³ They have studied the deposition of Zn on a polished gold-coated quartz crystal, by atomic force microscopy and quartz crystal microbalance. Zinc was deposited with a mean current of 92%. A gradual formation and growth of crystallites, suggesting a progressive nucleation mechanism, was observed. Later, the same group has studied the effect of additives such as acetonitrile, ethylene diamine and ammonia on the zinc electrodeposition.⁹⁴ Although viscosity of the DES was not modified, the electrodeposition was affected by the presence of these additives. Ammonia and ethylene diamine inhibited the adsorption of chloride on the electrode surface. The presence of these additives, however, acts as a brightener for zinc deposition. It should be noted that, like in water, the presence of these additives to the DES led to the formation of macro-crystalline deposits. Conversely to the ChCl/urea DES, the same group has also shown that the concentration of ZnCl₂ has no effect on the conductivity of the ChCl/ethylene glycol DES.⁹⁵ In ChCl/ethylene glycol DES, the mechanism is different to what is observed in ChCl/urea DES. This difference might be due to the specific adsorption of chloride on the electrode surface, blocking the growth of few crystal faces (Fig. 7). Another group has studied the electrodeposition of Zn-Sn on carbon nanotubes.⁹⁶ They have successfully performed the deposition with a high density and well distributed Zn-Sn spherical NPs with an average diameter of 120 nm.

Electrodeposition of Cu is more difficult in such DES. Abbott *et al.* have observed a progressive nucleation of Cu that led to a bright nano-structured deposit. When the concentration of Cu in DES was lowered (less than 0.01 M), a spontaneous nucleation of Cu was observed, leading to the formation of a black deposit. For a copper concentration from 0.01 M and 0.1 M a bright deposit was obtained. The authors have next demonstrated that composites of Cu and Al₂O₃ or SiC can also be produced in such DES.⁹⁷ Addition of Al₂O₃ or SiC particles in the DES did not modify the morphology and size of Cu particles. The composition of the composite material was dependent on the amount of Al₂O₃ or SiC particles. They have shown that the use of 5 wt% of Al₂O₃ yielded a composite with 3.5 wt% of Al (1 μm particle) whereas from 10 wt% of Al₂O₃, the composite contained 23 wt% of Al (1 μm particle). Llyod *et al.* have studied the kinetics of electron transfer of the Cu(i)/Cu(ii) redox couple at a platinum electrode in a ChCl/ethylene glycol DES.⁹⁸ They have shown that the reaction was reversible and that a large amount of free chloride was present in the DES due to the dissociation of ChCl.

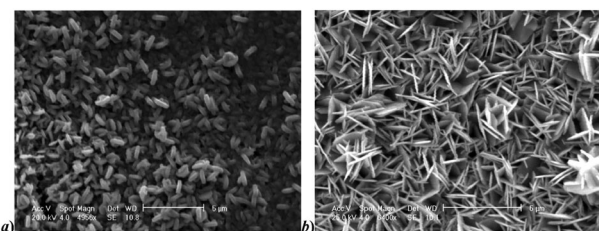


Fig. 7 SEM images of Zn deposits obtained from 0.3 M ZnCl₂ in (a) 1 : 2 ChCl:U (b) 1 : 2 ChCl:EG at 50 °C, on mild steel at $I = 3 \text{ mA cm}^{-2}$. (Reproduced with permission from ref. 95. Copyright (2011) Royal Society of Chemistry.)

This leads to the formation of copper chloride-based complexes. The authors have demonstrated that in this system the energy efficiency of electrodeposition can be double because (i) the cathodic efficiency is very high and (ii) the low oxidation state of metal complexes is stable.

Ag was also successfully electrodeposited on a Cu electrode in ChCl/ethylene glycol DES.⁹⁹ It was shown that silver can not only oxidize copper but can also be deposited on the copper surface at the same time. The deposit of silver was nano-crystalline and gave a smooth shiny coating. Later, the same team has studied the electrodeposition of silver using a platinum working electrode.¹⁰⁰ As mentioned earlier, AgCl was found to be highly soluble in this DES (0.2 mol kg^{-1}). When SiC was added to the solution of AgCl in ChCl/ethylene glycol, the viscosity decreased due to microstirring effects. Morphology of the Ag deposit was not affected by the presence of SiC. A similar trend was observed in the case of Al₂O₃. Note that the Ag particle size is however smaller in the presence of SiC microparticles. The authors have also shown that upon incorporation of SiC, the hardness of recovered Ag in DES is higher than in aqueous solution. Note that the hardness of metallic Ag did not depend on the SiC particles size (from 50 nm to 2 μm). Incorporation of SiC or Al₂O₃ has, however, an effect on the friction coefficient and wear volume of the Ag-based deposit. In particular, in the presence of Al₂O₃, Ag particles are less abrasive. Since lithium salts are known to modify the mechanism of metal nucleation and the mechanical properties of the deposited films, the addition of LiF during the deposition of Ag was also investigated. The hardness was greatly improved, but the structure of the Ag/SiC film was unchanged with the addition of 1 wt% of LiF. Later, Tu *et al.* have performed the deposition of Ag on copper alloys.¹⁰¹ They have shown that at 0 °C or at 50 °C a self-assembled nanoporous network of Ag films with ligament or channel structure was obtained.

Saravanan and co-workers have shown that electrodeposition of a Cr–Co alloy is also feasible in ChCl/ethylene glycol DES, opening an interesting route for the replacement of common noble metal alloys in dentistry.¹⁰² The authors have used an anode made of graphite and a cathode composed of a brass and mild-steel plates. Two electrodeposition methods were developed (i) direct current deposition (DCD) and (ii) pulsed electrodeposition (PED). In the DCD method, an alloy composed of 80.04% of Co and 19.95% of Cr was obtained with a nodular grain shape with sizes ranging from 2–4 μm . From the PED method, the recovered alloy was composed of 65.44% of Co and 34.56% of Cr with particle sizes ranging from 1–2.5 μm .

The electrodeposition of nickel was also performed at 90 °C in ChCl/ethylene glycol on polished brass foil (Cu_{0.64}Zn_{0.36} alloy).¹⁰³ A highly rough surface was obtained at 90 °C while it is not the case at room temperature. Nickel is randomly distributed on the film. Nanosheets with a thickness of 10–20 nm and grains with 10–50 nm size were obtained. Clearly, the authors have highlighted an increase in the Ni deposit roughness with the temperature. This was explained by a decrease of the DES viscosity, leading to an increase of ion species mobility, favouring the nucleation and deposition process of nickel. Moreover, the authors have shown that

the nickel films present a low corrosion potential. Abbott *et al.* have also studied the deposition of nickel in ChCl/ethylene glycol DES.⁸⁷ A dark grey deposit was obtained and the underpotential deposition of Ni was suppressed by the addition of ethylenediamine and acetylacetamide in the DES.

Polymers such as polypyrrole films can also be electrodeposited in ChCl/ethylene glycol.¹⁰⁴ As observed above for the ChCl/urea DES, the ChCl/ethylene glycol DES was unfortunately partly decomposed during the electrodeposition process even in the presence of sacrificial agents such as oxalic, phthalic, formic or acetic acids.¹⁰⁵

7.1.3 Electrodeposition in a ChCl/glycerol DES.

Silva and coworkers have investigated the interface properties between ChCl/glycerol and either Au or Pt or glassy electrode.¹⁰⁶ The authors have shown that Au has the highest effect on the capacitance–potential curves. Except for gold, an increase in temperature led to an improvement of the capacitance in the presence of Pt and glassy carbon electrodes.

This DES was also studied by Mason *et al.* In particular, the authors have shown that mass transfer and cathodic current increased in the presence of ultrasound during the electrodeposition of copper chloride on Pt electrodes.¹⁰⁷ This property resulted in an increase in the limited current density. Under ultrasound, the anodic potential peak in cyclic voltammetry was also increased 10 times and shifted to a more positive value as compared to silent conditions. This phenomenon can be ascribed to (i) an increase of mass transfer, (ii) a local increase in temperature, (iii) a decrease in concentration over potential, (iv) a cleaning effect by ultrasound, (v) a decrease in overpotential and (vi) formation of a hydroxyl radical. It should be noted that after 30 seconds of ultrasound, the solution containing copper chloride and glycerol turned from bright yellow to a turbid pale colour due to cavitation events occurring in such highly viscous mixture. This change of colour can be due to the decomposition of ChCl/glycerol under sonication.

7.1.4 Electrodeposition in others ChCl-derived DES.

Lesuer *et al.* have demonstrated that a ChCl/TFA (2,2,2-trifluoracetamide) (1 : 2) DES can dissolve ferrocene.¹⁰⁸ In particular, they have studied electron-transfer reaction mechanisms in this DES. It appears from this study that this DES behaved as a non-Newtonian fluid.

Abbott *et al.* have reported that a ChCl/chromium chloride DES with similar properties to ILs can be produced.¹⁰⁹ In this DES, electrodeposition of thick and adherent chromium films was achieved, offering an alternative to acid solutions commonly used for chromium electrodeposition.

In conclusion, the above-described results clearly show that electrodeposition of metals can be conveniently performed in various DESs with similar efficiency than methods based on ILs (Fig. 8).¹⁰⁹

However, instability of DESs during the electrodeposition process still remains a major problem that needs to be solved prior to a possible industrial transfer.

7.2 Other applications of DES in electrochemistry

DESs were also used in electrochemistry as electrolytes for dye-sensitized solar cells.¹¹⁰ In this case, 3.88% of the sunlight

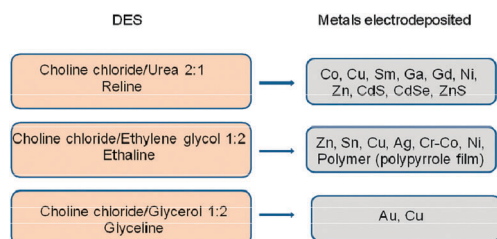


Fig. 8 Metals electrodeposited in the three main DES used in this process.

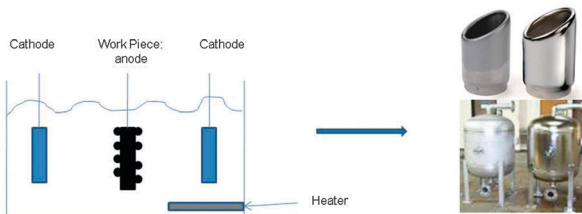


Fig. 9 Electropolishing process.

energy was converted in a ChCl/glycerol based electrolyte which is comparable to most of IL-based electrolytes. The photoanodes used were a double layer of TiO₂ mesoporous films. The electrolyte was made by adding 0.2 M of I₂ and 0.5 M of *N*-methylbenzimidazole to a mixture of 1-propyl-3-methylimidazolium iodide and ChCl/Gly (v/v 13 : 7). This study has shown that ChCl/glycerol is a promising candidate for future electrolytes for dye-sensitized solar cells.

Electropolishing of metal (surface treatment that aims at removing oxidized metal on surface) which corresponds to the metal corrosion was also investigated in DES (Fig. 9).

A ChCl/ethylene glycol DES has been used for the electro-polishing (anodic dissolution) of stainless steel, affording an alternative to phosphoric and sulfuric acid solution commonly used for such treatment. This electropolishing process was not corrosive and tolerant to the presence of air and moisture. Additionally, it is anisotropic and has micro roughness.¹¹¹ The authors have also shown that the metal surface oxidation was rapid under aerobic conditions. Moreover, the anodic dissolution of metal ions was faster when the oxide layer was continuously removed.¹¹²

Metal separation was also studied in DESs. The idea is to use the ability of the chloride anion of DES electrolytes to stabilize metal ions. In the process, chemical oxidation of metals by I₂ led to iodide and soluble metal species. The iodide formed was oxidized at the anode, regenerating iodine. Conversely, at the cathode, purified metal was obtained by reduction reaction.¹¹³

DESs were also used to obtain natural polymer-based electrolytes such as cellulose acetate¹¹⁴ or corn starch based polymers,^{115,116} or p-doped polypyrrole¹¹⁶ with high conductivities.

8. Preparation of materials in DESs

Conventional preparation of inorganic materials often takes place in water or organic solvents, using in many cases the thermal step for crystallization and structure formation. The

“solvothermal synthesis” then consists in growing single crystals from a non-aqueous solution, by thermal treatment under pressure. Recently, the ionothermal synthesis, a new synthetic strategy involving predominantly ILs or deep-eutectic solvents (DESs) as solvent, has been developed. In these syntheses, ILs or DESs can be used as both solvent and template (also called structure-directing agents). In solvothermal reactions where solvents are predominantly volatile molecules, the high temperature required for crystallization or pore structure formation needs the use of autoclaves. Contrarily, ionothermal synthesis can be readily conducted in a low-pressure environment (*e.g.* under ambient pressure) due to the low volatility of ILs or DESs. The use of such solvents thereby reduces all security risks arising from the use of low boiling point solvents and simplifies the synthesis process. More importantly, the possibility to tune the ionic nature of DESs provides modulating reaction environments under which novel materials with useful structures (surface properties and porosity) may be produced.

Nowadays, the ionothermal synthesis is gaining considerable attention. In this context, a newly emerging trend of this field consists in the replacement of ILs by cheap and safe DESs. For example, DESs based on ChCl/urea or ChCl/renewable carboxylic acids have been used as an alternative medium to ILs in the ionothermal strategy. As mentioned above, compared to ILs, DESs have notable advantages including low toxicity, biodegradability and low cost. Additionally, the presence of neutral components with high boiling point such as urea, carbohydrates or carboxylic acids also provide new and complementary environments to ILs that are completely ionic. In addition, DESs can play multiple roles during synthesis, including the classical role of solvent, templating agent, reactant, *etc.* Thanks to these properties, DESs are now receiving considerable attentions for the ionothermal synthesis of materials and the design of novel structures.

Up to now, many inorganic materials with valuable properties and structures, including zeolite-type materials, metal–organic frameworks (MOFs), metal oxides, nano-materials, carbon materials, among others, have been synthesized using the ionothermal synthesis strategy. Although a few reviews focusing on the preparation of inorganic materials using ILs can be found in the recent literature,^{117,118} a comprehensive review dedicated to the use of DESs in the ionothermal synthesis of materials has not been covered yet in the current literature. In this section we describe the promising materials prepared in DESs for various applications including gas separation, hydrogen storage, catalysis, *etc.* This review also highlights the versatile role played by DESs during the material synthesis.

8.1 Metal phosphates and phosphites with open-framework structures

8.1.1 Aluminophosphates.

Zeolites or zeolite-like materials are of great importance owing to their applications in different areas of modern science. These zeolite-analogous framework materials are often synthesized in water or organic solvents by a traditional solvothermal approach and using structure directing agents. In 2004, the DES-mediated ionothermal procedure was firstly introduced for the preparation of

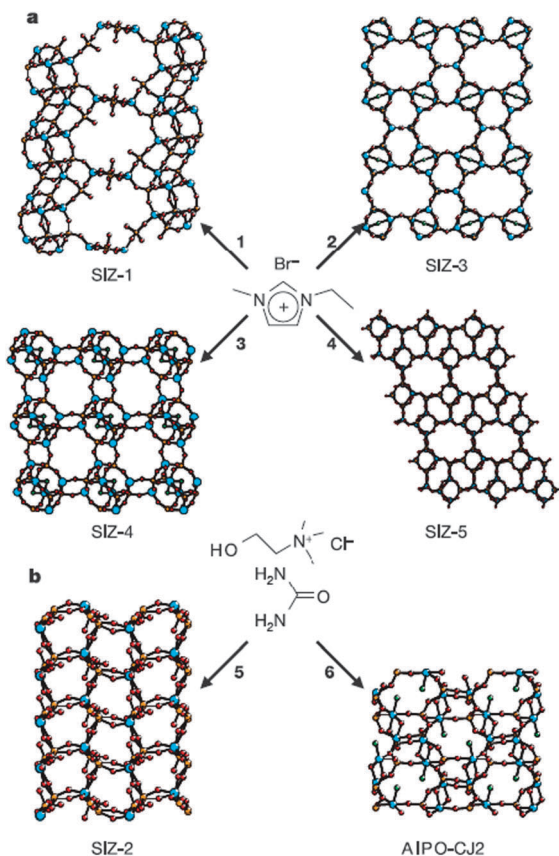


Fig. 10 The synthesis of zeotypes by using ionic liquids and eutectic mixtures. (a) Ball-and-stick diagrams of aluminophosphate materials SIZ-1, SIZ-3, SIZ-4, and SIZ-5 synthesized ionothermally using [EMIm]Br; (b) SIZ-2 and AlPO-CJ2 synthesized using a ChCl-urea mixture. The structure-directing agents have been omitted for clarity. Orange, cyan and red spheres correspond to phosphorus, aluminium and oxygen atoms respectively.¹¹⁹ (Reproduced with permission from ref. 119. Copyright (2004) Nature Publishing Group.)

microporous crystalline zeolite analogues by Morris and co-workers.¹¹⁹ DESs based on ChCl/urea or IL ([EMIm]Br) were used as alternative solvents for the synthesis of zeotypes. In the presence of [EMIm]Br, four different aluminophosphate zeotypes, SIZ-1, SIZ-3, SIZ-4, and SIZ-5 (Fig. 10), were prepared under different experimental conditions, in which the imidazolium-based IL acted as both the solvent and template. For example, at 150 °C, SIZ-1, with a framework structure composed of hexagonal prismatic units joined together to form a three-dimensional framework, was obtained. The framework is however interrupted by an unusual hydrogen bond. Fully condensed structures can also be achieved using a mineralizing agent (fluoride) to promote oxygen bond formation. Different from IL, the use of ChCl/urea led to another type of framework, *viz.* SIZ-2. The Al–O–P alternation is maintained and the chemical formula (NH₄)₃[Al₂(PO₄)₃] shows that SIZ-2 is also an interrupted structure. Compared to the synthesis in IL, the addition of fluoride to the ChCl-urea eutectic mixture led to the formation of a non-zeolitic aluminophosphate known as AlPO-CJ2 (Fig. 10). During the ionothermal synthesis in DES, ammonium ions released by partial decomposition of urea play an

important role in the formation of the inorganic framework by templating and balancing charges generated by the terminal P–O bonds in the framework. The pore architecture consists in three intersecting channels of small size. Even with this size limitation, the authors succeeded in the subsequent and partial exchange of ammonium by copper cation. Due to the low volatility of ILs or DESs, the synthesis takes place at ambient pressure.

Similarly, other SIZ-n type materials with zeolitic frameworks, *i.e.* SIZ-6, SIZ-7, SIZ-8, SIZ-9, have been synthesized by means of ionothermal synthesis using [EMIm]Br.^{120,121} However, these syntheses without the involvement of DESs fall out the scope of this section and therefore will not be particularly discussed here.

As compared to traditional solvents (*e.g.* water), use of ILs or DESs can also modify the way how material precursors are assembled. Novel types of inorganic materials can then be synthesized. The absence of competition between template-framework and solvent-framework interactions encountered in classical hydrothermal preparations is then completely depressed when using DES. As rightly notified by Copper *et al.*, this is an important specificity of these syntheses.¹¹⁹ Based on the successful preparation of SIZ-n type materials, Morris and co-workers reported the ionothermal synthesis of materials using various unstable DESs as template-delivery agents.¹²² 1,3-Dimethyl urea (DMU), 2-imidazolindone (ethylene urea or e-urea) and tetrahydro-2-pyrimidione (THP, N,N'-trimethylene urea) derivatives were investigated as eutectic mixtures in combination with quaternary ammonium halides (choline chloride or tetraethylammonium bromide). Aluminophosphate-based materials with new structures have been prepared using this strategy. For example, the use of ChCl/e-urea led to the formation of two similar related aluminophosphate materials (Fig. 11, materials 4 and 5). In this case, materials were templated by ethylene diammonium cations plus some ammonium issued from DES decomposition when temperature exceeded 200 °C. The use of ChCl/DMP, which decomposes into propylene diammonium or ammonium (conditions: high temperature and large excess of water), induced the crystallization of four other types of solids (Fig. 11). The obtained structures support the mechanistic pathways previously proposed for the crystallization of aluminophosphates (through hydrolytic assembly of the parent chain).¹²³ Indeed, the mild hydrolytic conditions of the ionothermal synthesis (as compared to the classical hydrothermal/solvothermal routes) allowed the isolation of an aluminophosphate structure close to the parent chain structure (suggested to form before condensation in classical synthesis). Some mechanistic studies also suggested that the nucleation and crystallization of the structures take place at relatively low levels of DES degradation, when concentration of the template (propylene diammonium or ammonium) remains low.

Although the ionothermal synthesis was thought to take place in a relatively “dry” and predominantly “ionic” environment, the presence of water cannot be ruled out. Interestingly, when present in trace amounts, water did not have a detrimental effect on the DES-mediated ionothermal synthesis of some materials.¹²⁴ The low reactivity of water (in trace amounts) was attributed to its strong interaction with the

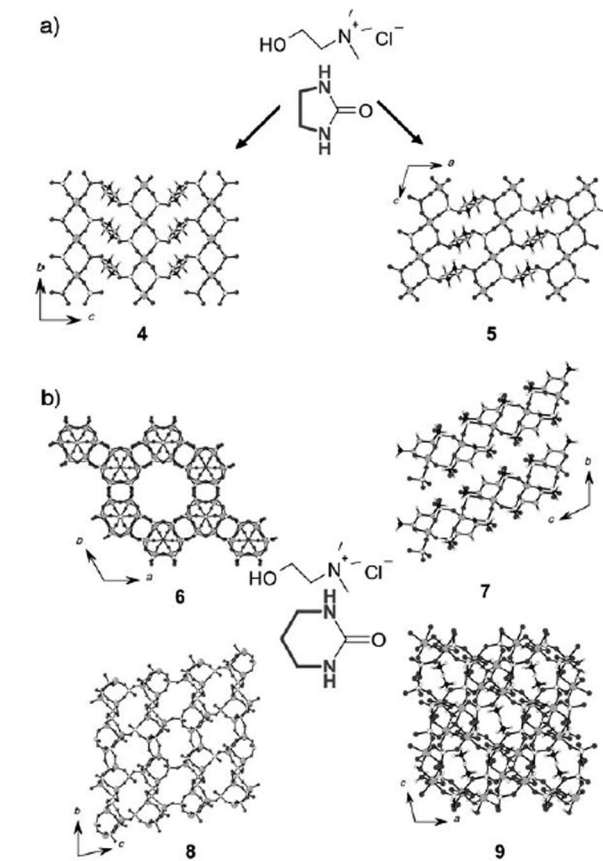


Fig. 11 The synthesis of aluminophosphate materials from DESs. (a) Materials 4–5 prepared from ChCl/IMI. (b) Four materials prepared from ChCl/DMP. In compounds 6–8 the template is a propylene diammonium cation while in compound 9, prepared at higher temperature, the template is ammonium. For clarity the location of the templates in 6 and 8 is not shown.¹²² (Reproduced with permission from ref. 122. Copyright (2006) Wiley-VCH.)

anion of the DES that drastically limits its reactivity.¹²⁵ In other words, it means that new inorganic materials that are sensitive to water can be theoretically prepared by the ionothermal synthesis in DESs. In this context, three different ChCl/carboxylic acid-derived DESs were recently used for the synthesis of unusual aluminophosphate layered materials with chemical compositions that are unlikely to be accessible using traditional hydrothermal methods. The possibility to achieve new structures was then clearly exemplified by Morris *et al.*¹²⁶ The use of ChCl/carboxylic acid (succinic, glutaric or citric acid) DESs allowed the production of dense aluminophosphate phases. When bases are used to control solvent properties (cyclam or pyridine), new CoAlPO structures, SIZ-13, are obtained, independently of the base used. The structure of SIZ-13 consists in $[Al_3CoClP_4O_{16}]^{2-}$ layers templated by choline cations filling the interlayer (Fig. 12). The specificity of the structure is that cobalt ions are located in only one crystallographic position, at the corner of the building unit. Note that formation of Co–Cl bonds present in the SIZ-13 structure is not possible using traditional routes due to their high sensitivity to hydrolysis. As mentioned previously, the strong interaction of water with the anion of the DESs (at low content of water) provides media with very

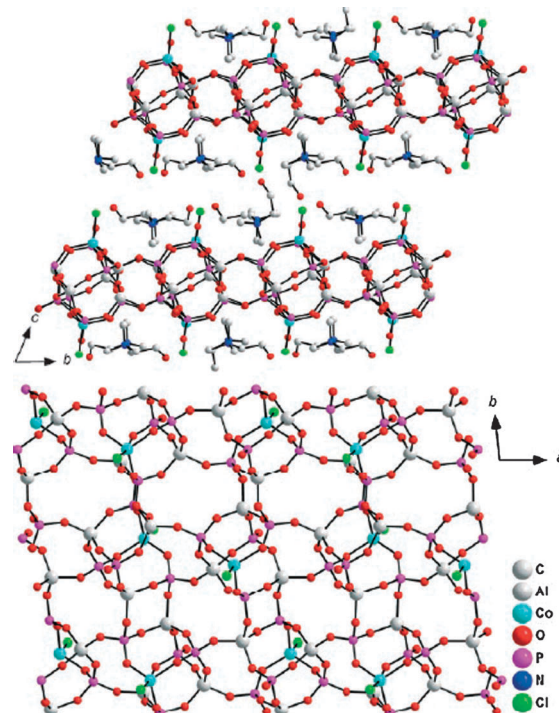


Fig. 12 The layered structure of SIZ-13 viewed parallel to the *a* axis (top; hydrogen atoms are omitted), and a single $[Al_3CoClP_4O_{16}]^{2-}$ layer viewed parallel to the *c* axis (bottom; choline template molecules are omitted).¹²⁶ (Reproduced with permission from ref. 126. Copyright (2007) Wiley-VCH.)

limited hydrolyzing properties.¹²⁵ Like mentioned above in the biocatalysis part, inhibition of the water reactivity in DES is then proposed as the reason for the Co–Cl stabilization in SIZ-13. Raising the temperature of the synthesis increases the reactivity of water contained in DES, and thereby promotes the formation of a fully connected zeolite framework, SIZ-14. The authors highlighted that the presence of accessible relatively large cages in the structure of SIZ-14 ($3.6 \times 4.8 \text{ \AA}^2$) is of great importance, especially for catalytic and adsorption applications.

8.1.2 Zinc phosphates. The above described results clearly show that the material structure obtained by ionothermal synthesis is influenced by the chemical composition of the DES (*e.g.* template species, mineralizers, charge balance, *etc.*). DESs can play a multiple role such as template and solvent.

Zinc phosphates are an important subset of the large phosphate family. More than 20 zinc phosphate structures, exhibiting 1D, 2D or 3D framework structures have already been synthesized, with the possibility to obtain large pore structures.¹²⁷ Inspired by the methodology reported for the preparation of aluminophosphate-based materials, Liao and co-workers reported in 2005 the ionothermal synthesis of a $[Zn(O_3PCH_2CO_2)]\cdot NH_4$ structure using a ChCl–urea eutectic mixture as the reaction medium.¹²⁸ Deep investigations showed that NH_4^+ , generated *in situ* from the partial decomposition of urea at high temperature, played a pivotal role in the formation of the targeted material. Ammonium acted as a structure-directing agent which filled the voids of the structure, and interacted with the C=O groups present on the surface of

the helix-like tunnels through a hydrogen bond (3D framework). Similarly, Harrison also obtained zincophosphate type structure [with Zn^{2+} cation, HPO_3^{2-} anion, and chloride ion incorporated into the structure by a Zn–Cl covalent bond]. In this system, choline from the DES was incorporated into the hybrid structure. Cholinium cations interacted with $[ZnCl(HPO_3)]^-$ macroanionic layers by means of O–H···O hydrogen bonds.¹²⁹ Later, Dong and co-workers have described the synthesis of a three-dimensional zinc phosphate material (designated $ZnPO_4$ -EU1). *In situ* generation of the structure directing agent (from imidazolidone) using an unstable $ChCl$ /imidazolidone DES (in a molar ratio of 1 : 2) as the reaction medium at 150–200 °C allows the material formation.¹³⁰ The obtained zinc phosphate material belongs to the DFT topology framework structure, which is similar to that of the previously reported $(ZnPO_4)_2(NH_3CH_2CH_2NH_3)$ material (DAF-3).¹³¹ Then, the expected decomposition product of the DES based on choline chloride and imidazolidone is ethylenediamine, which is progressively delivered in the reaction media at a temperature higher than 150 °C. The progressive ethylenediamine delivery allows the crystallization of the 3D $ZnPO_4$ -EU1 structure.

In the synthesis of metal phosphate-based materials, quaternary ammonium salts, such as TMABr, TEABr, TPABr, and $ChCl$, have been extensively used. Quaternary ammonium cations are capable of templating a wide variety of frameworks. Thus, addition of these quaternary ammonium salts to oxalic acid leads to DESs that are able to template such zincophosphate structures. Lin and co-workers reported a new 2D crystalline layered zinc phosphate, $[N_2C_6H_{12}]_2[Zn_7H_3(HPO_4-x)_5(PO_4)_3]\cdot H_2O$ (denoted $ZnPO$ -DES1).¹³² Structure of this material consists in 10-membered-ring ellipsoidal channels perpendicular to the ladder-shaped layers. This material was prepared by ionothermal synthesis from a TPABr/oxalic acid DES, zinc acetate, H_3PO_4 , and triethanolamine (TEA) at 150–180 °C for 3 days. During the reaction, 1,4-diazabicyclo[2.2.2]octane (DABCO) is supposed to be generated by TEA conversion and is suggested to template the $ZnPO$ -DES1 structure. Indeed, DABCO is classically used to template zincophosphate structure. Next, two new zincophosphate materials, *i.e.* $ZnPO_4$ -EU2 (Thomsonite-type framework) and $ZnPO_4$ -EU3 (JBW zeolite-type structure), have been ionothermally synthesized by Dong *et al.*¹³³ In this example, two DESs composed of 1,3-dimethylurea (DMU) mixed with either tetraethylammonium bromide (TEABr) or *N,N*-dimethyl piperidinium chloride have been used. The thermal decomposition of the DMU/TEABr DES produced intermediates that exhibited strong structure-directing abilities for zincophosphate framework formations, yielding the $ZnPO_4$ -EU2 material. The negative charge of the framework is compensated by protonated methylamine (from DMU decomposition) and water. Protonated methylamine molecules are then located in the 8-rings pore channels of the structure. The presence of H_3O^+ in the channels also confirms the necessity to have a small amount of residual water in the DES in order to successfully perform this synthesis. SEM analysis shows that crystallites have a brick-like morphology with a maximum edge length of about 100 μm. However, crystal structure determination showed some small

differences from the classical Thomsonite structure, *e.g.* unit cell and space group. $ZnPO_4$ -EU3 is templated by methylammonium cations issued from the DMU decomposition, with Na^+ added for the phase formation. As mentioned by the authors, this is the first DES mediated synthesis of a metal phosphate analogue of Na-J JBW-type zeolitic material. Morphology slightly differs from that of $ZnPO_4$ -EU2 (rod-like structure).

Although decomposition of urea derivatives from the DES has been widely used to produce ionic templates, the same strategy was employed using the cationic component of DES. Very recently, Wang and co-workers have synthesized the first metal-activator-free orange phosphorus material NTHU-9 by using a $ChCl$ –oxalic acid dihydrate (1 : 1) eutectic mixture as a synthesis medium. The material exhibits a layered structure of zinc chlorophosphate with occluded organic templates (Fig. 13).¹³⁴ This zincophosphate material is the first metal phosphate exhibiting dual properties of photoluminescence and photochromism. During the ionothermal synthesis, the authors proposed that the hydrolysis of the choline cation (the water content of the DES originates from oxalic acid dihydrate) led to ethylene glycol (EG) and trimethylamine which can react with CH_3^+ (from demethylation of choline) to form tetramethylammonium ions (TMA). CH_3^+ is also proposed to react with amines derivatives to form *N,N'*-dimethylamine derivatives. All these intermediates play an important role in the formation of the layered structure of NTHU-9. The particular properties of the obtained materials are attributed to these two concurrent reaction pathways:

(1) methylenium cations and *N,N'*-dimethylamine derivatives entrapped in the structure are responsible for the photochromism;

(2) EG in the layered structure is at the origin of the photoluminescence properties.

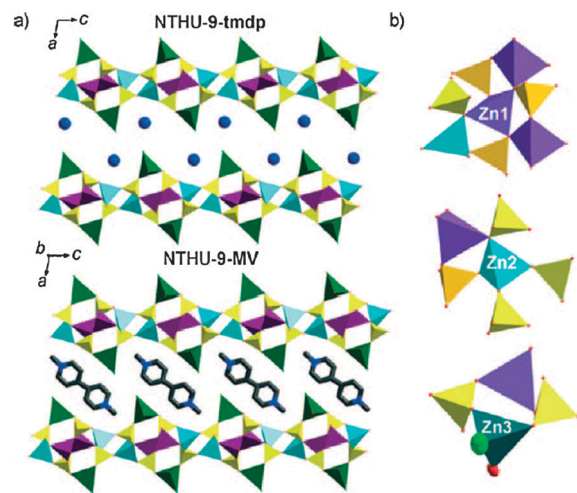


Fig. 13 Polyhedral plots of the inorganic layers in NTHU-9. (a) Layers with disordered sites for choline ions (only N atom found) in 9-tmdp (top) and dimethylated bpy molecules in 9-MV (bottom). (b) Three types of tetrahedral Zn centers with different connectivity. Blue, green, and red balls represent N, Cl, and water O atoms, respectively.¹³⁴ (Reproduced with permission from ref. 134. Copyright (2010) Wiley-VCH.)

8.1.3 Zirconium phosphates. As previously observed, the use of DESs with different ionic compositions provides notable advantages not only in terms of green solvent but also for the rational design of new materials with open structures. Like the aluminophosphate and zincophosphate, zirconium phosphates with one-, two-, and three-dimensional connectivities are usually prepared using a solvothermal approach in water or organic solvents. Recently, Dong and co-workers¹³⁵ reported the synthesis of three different zirconium phosphate frameworks using zirconium(IV) oxychloride, H_3PO_4 and HF in DESs composed of tetramethylammonium chloride (TMA)/urea and TMA/oxalic acid hydrate. Among the reported materials, two are new and exhibit chain or layered framework structures which are unfortunately unstable upon calcination (elimination step of the template). Using the TMA/urea DES, $ZrPO_4$ -DES1 $[(NH_4)_4[Zr(PO_4)_2F_2]$, at an F/Zr ratio of 2.8] and $ZrPO_4$ -DES2 $[(NH_4)_3[Zr(PO_4)_2F]$, at an F/Zr ratio of 0.61] were obtained. $ZrPO_4$ -DES1 is a chain framework structure composed of $\{ZrO_4F_2\}$ octahedra linked each to four $\{PO_4\}$ tetrahedra to form infinite macroanionic $[ZrP_2O_8F_2]^{4n-}$ chains. The NH_4^+ cations originating from the DES decomposition are located along the chains and act as template and balance of the framework charge. $ZrPO_4$ -DES2 is a 2D layered structure in which $\{ZrO_5F\}$ octahedra are linked to $\{PO_4\}$ tetrahedra. The inorganic sheet consists in the alternation of $\{ZrO_5F\}$ octahedra and $\{PO_4\}$ tetrahedra to form 8- and 4-membered rings. Another material, $ZrPO_4$ -DES3, has also been obtained when urea was replaced by oxalic acid. This substitution aimed at avoiding the templating competition between NH_4^+ (from urea decomposition – evidenced to template the two previous structures) and TMA⁺. $ZrPO_4$ -DES3 exhibits a tridimensional framework with 10-ring and 8-ring channels. Structural characteristics are close to the known structure $[Zr_{12}P_{16}O_{60}(OH)_4F_8]$ (C_5H_6N)₄ (H_2O)₂ ($ZrPOF$ -pyr).¹³⁶ However, in this example, the material composition slightly differed since only the TMA cation templated the structure. Thermal stability was also evaluated, and logically the 3D structure ($ZrPO_4$ -DES3) presented satisfying stability up to 450 °C while the two other 1D and 2D structures collapsed. Catalytic properties of these newly prepared materials were evaluated in the selective oxidation of cyclohexane, an industrially relevant reaction. Results showed that tridimensional $ZrPO_4$ -DES3 exhibited good catalytic performance, with a cyclohexane conversion of 32% and up to 83% of selectivity to cyclohexanone. In contrast, the chain and layered materials are relatively poor catalysts for this catalytic reaction. The difference of catalytic performances between these catalysts was attributed to their different framework structures that affected the adsorption of reactants.

To further investigate the effects of the quaternary ammonium cation in ionothermal syntheses, a TPABr/oxalic acid DES was used for the preparation of novel zirconium phosphate materials. Dong and co-workers described the possibility to form the known zirconium phosphate layered structure α -Zr(HPO_4)₂·3H₂O (α -ZrP) in pure TPABr/urea. In this case, contrary to what was observed above with the TMA cation,¹³⁵ the TPA cation cannot template the framework structure.¹³⁷ However, when 1,4-dimethylpiperazine (DMP) was added to the eutectic mixture, a new layered zirconium phosphate

$[C_6H_{16}N_2]_{0.5}Zr(H_{0.5}PO_4)_2 \cdot H_2O$ denoted $ZrPO_4$ -DES8 was successfully obtained. The layered structure of this material is similar to that found in α -ZrP and can be regarded as a DMP pillared α -ZrP structure. The DMP molecules are in chair conformation and form an organic monolayer. However, the direct DMP intercalation in classical α -ZrP structure does not provide material with $ZrPO_4$ -DS8 structural properties. Monitoring the *in situ* crystallization by XRD analyses showed that, before crystallization of $ZrPO_4$ -DS8, an unknown phase was formed after a short period of time. It should be noted that layered zirconium phosphate materials, α -ZrP and $ZrPO_4$ -DES8, are used as additives in a liquid lubricant. Excellent friction behaviors with higher load-carrying and antiwear capacities are obtained.

Very recently, Dong and co-workers¹³⁸ also synthesized a novel open-framework zirconium phosphate with small 7- and 8-ring channels. $ZrPOF$ -EA, $[(C_2H_7NH)_8(H_2O)_8] \cdot [Zr_{32}P_{48}O_{176}F_8(OH)_{16}]$ formulae by ionothermal synthesis in ethylammonium chloride–oxalic acid eutectic mixture. The structure of $ZrPOF$ -EA consists in units arranged in a rectangular array connected by ZrO_6 , ZrO_5F , and PO_4 linkages (Fig. 14a–c). One-dimensional channels parallel to the *c* (7-ring) and *a* (8-ring) axes form due to the 3-, 4-, 5-, 6-, 7-, and 8-ring units present in the structure.

Trapped water and organic species in the structure can be removed by calcination to produce a material with permanent channel-like porosity. Elimination can be done under relatively mild conditions (410 °C for 9 h). SEM images have showed that crystallites had a flat needle-like morphology with

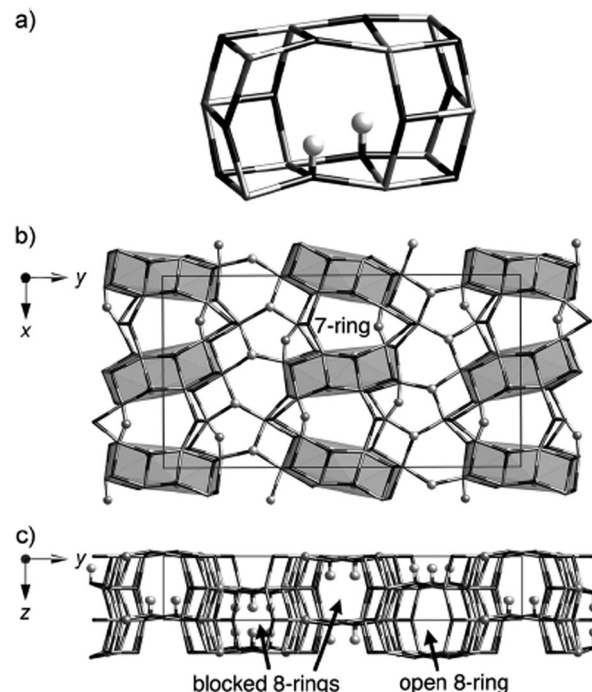


Fig. 14 $ZrPOF$ -EA framework structure showing (a) the characteristic [41482] unit, (b) the projection along the *c*-axis with the [41482] units highlighted, and (c) the projection along the *a* axis. Bridging O atoms have been omitted for clarity. Terminal O atoms and bridging F atoms are shown as balls, Zr gray, and P black.¹³⁸ (Reproduced with permission from ref. 138. Copyright (2011) Wiley-VCH.)

dimensions of about $10 \times 2 \times 0.2 \mu\text{m}^3$. More interestingly, due to the 8-ring dimensional channel, this porous material showed a CO_2 adsorption capacity largely higher than for CH_4 . CO_2 adsorption capacity is also significantly higher than that observed over conventional 8-ring pore materials [adsorption performed at 25 °C and low pressure (0–1 bar)]. The selective adsorption of CO_2 may be here the result of the pore architecture and the presence of polar hydroxyl groups located into the pore channels. Nevertheless, the selective adsorption of CO_2 vs. CH_4 decreases by increasing the adsorption pressure, due to the flexibility of the framework.

8.1.4 Borophosphates. Like aluminophosphate and zeolites, borate compounds have found a wide variety of applications, especially in the field of nonlinear optics. Synthesis of metal borate materials remains, however, difficult. The volatility of boron oxide limits the potential of solid state reaction syntheses. In addition, the presence of multiple borate species in equilibrium in solution makes the hydrothermal synthesis very complex. Recently, the use of choline chloride–1,3-dimethyl urea eutectic mixture has been reported as an efficient medium for the preparation of cobalt phosphate–borate material that incorporates the $[\text{B}_5\text{O}_6(\text{OH})_4]^-$ anion between cobalt phosphate layers.¹³⁹ The structure of this material is composed of two-dimensional cobalt phosphate layers pillared by polyborate building units, *i.e.* $[\text{B}_5\text{O}_6(\text{OH})_4]^-$. The inorganic layer is formed by corner-sharing cobalt oxide and phosphate tetrahedrons. Oxygens from $[\text{PO}_4]^{3-}$ tetrahedra are localized on the surface of the layers, and are in interaction with the polyborate unit by H-bond interaction. Unlike the vast majority of metalloborophosphates, there is no direct covalent bonding between phosphate and borate moieties. In this ionothermal synthesis, two different alkyl ammonium cations derived from the ionic media have distinct template effects on the formation of cobalt phosphate layers and hydrophobic borate channels. Indeed, the terminal NH_3^+ from methylammonium, issued from dimethyl-urea decomposition, is involved in H-bond interaction with oxygen atoms from phosphate tetrahedrons. This interaction directs the orientation of Co- and P-tetrahedrons, while the methyl groups are located on the channel surface. Space between the methyl groups as well as their hydrophobic nature allows the incorporation of the tetramethyl ammonium ions derived from the choline cation to compensate the framework charge structure.

8.1.5 Iron oxalatophosphates. Although the ionothermal synthesis in DESs has been widely used for the synthesis of phosphates with open-framework structures, preparation of metal oxalatophosphates in DESs has been reported only once to our knowledge.¹⁴⁰ Two new iron(III) oxalatophosphates, $\text{Cs}_2\text{Fe}(\text{C}_2\text{O}_4)_{0.5}(\text{HPO}_4)_2$ (**1**) and $\text{CsFe}(\text{C}_2\text{O}_4)_{0.5}(\text{H}_2\text{PO}_4)(\text{HPO}_4)$ (**2**), have been synthesized in an eutectic mixture of ChCl and malonic acid. While classical hydrothermal synthesis generally leads to the formation of bi-valence [Fe(II) and Fe(III)] oxalatophosphate, only Fe(III) was found in these novel structures. The structure of compound **1**, obtained by reaction between $\text{FeCl}_3 \cdot 6\text{H}_2\text{O}$, H_3PO_4 , $\text{H}_2\text{C}_2\text{O}_4 \cdot 2\text{H}_2\text{O}$ and 1,4-bis(3-aminopropyl)-piperazine (APPPIP) in DES, is presented in Fig. 15.

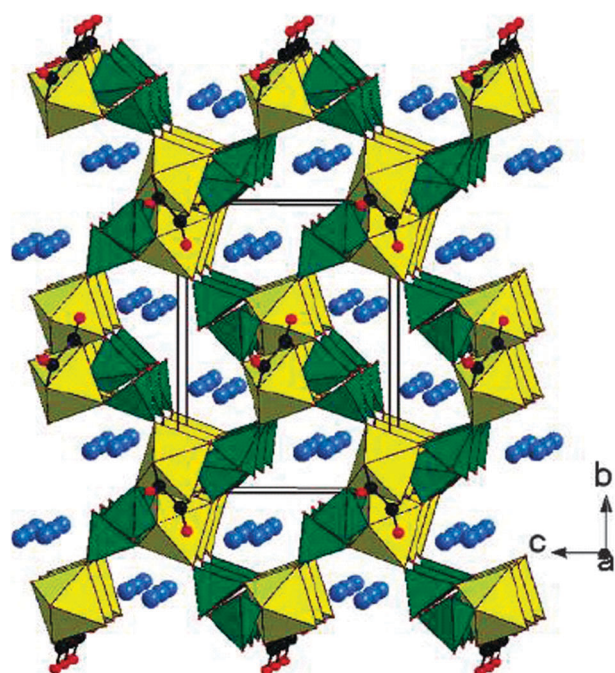


Fig. 15 Polyhedral plot of the structure of **1** along the c -axis. The yellow and green polyhedra represent FeO_6 octahedra and phosphate tetrahedra, respectively. Blue circles: Cs atoms. Black circles: C atoms. Red circles: O atoms.¹⁴⁰ (Reproduced with permission from ref. 140. Copyright (2006) American Chemical Society.)

It comprises $\text{Fe}^{\text{III}}\text{O}_6$ octahedra connected by HPO_4^{2-} tetrahedra and bisbidentate oxalate ($\text{C}_2\text{O}_4^{2-}$) anions to form a 3D framework. Fig. 15 shows that the tunnels parallel to the [100] direction have a window formed by six FeO_6 octahedra and six phosphate tetrahedra. The second kind of tunnel is formed by six octahedra, four tetrahedra and two oxalate units. The intersecting 12-ring channels form the 3D open structure, with the framework charge-compensating Cs^+ cations being located at the intersections of these channels (Fig. 15). Another structure (not shown), is obtained from the same reactants but without 1,4-bis(3-aminopropyl)piperazine (APPPIP), resulting in a higher pH of the solution during the preparation of the material. This material $\text{Fe}^{\text{III}}\text{O}_6$ octahedra coordinate to $\text{C}_2\text{O}_4^{2-}$, H_2PO_4^- and HPO_4^{2-} anions to form macroanionic layers, with Cs^+ cations located between the layers. Four FeO_6 octahedra, connected to three HPO_4^{2-} tetrahedra and one oxalate unit form eight-membered windows in the layers. The H_2PO_4^- tetrahedra, positioned between the chains, stabilize the 2D-layer structure.

For information, these materials cannot be prepared by a hydrothermal method under similar reaction conditions pushing forward the contribution of DESs for the ionothermal synthesis of new materials (even if no template effect is evidenced in this study).

8.1.6 Metal oxalatophosphates. In line with their previous research on photoluminescence properties of open framework metallophosphate, *i.e.* NTHU-4 and NTHU-6,¹⁴¹ Wang *et al.* demonstrated the successful synthesis of another luminescent gallium oxalatophosphate in ChCl /oxalic acid dihydrate DES (NTHU-7) (Fig. 16). The nanosized channel structure emits

intense yellow light under excitation in near-ultraviolet (NUV) and blue light.¹⁴² This material was prepared by reaction between 4,4'-trimethylenedipiperidine (TMDPP), GaO, H₃PO₄, and residual water contained in DES. Similar structures were prepared by substituting the TMDPP by either 4,4'-trimethylenedipyridine (TMDP) or KOH, NaOH, RbOH, CsOH. The NTHU-7 structure exhibits an organic–inorganic hybrid nanotubular structure composed of GaO₆ octahedra, bis(bidentate oxalate) groups and HPO₃ tetrahedra. Chemical composition of the hybrid structure is [Ga₂(HPO₃)₂(C₂O₄)(OH)(H₂O)]⁻, where the negative charge can be balanced by different cations depending on the base used during the synthesis. However, the counter cation always contains the choline ion, base and lattice water molecule. The oxalate group incorporation into the structure highlights that the tubular structure assembles with DES contribution. Then all DES components, including residual water, participated in the structure formation. The role of DES is then multiple with a contribution as a solvent, template, reactant, charge balancer and space filler. As described in Fig. 16b, [Ga₂(HPO₃)₂] units and oxalate groups form a 16-ring aperture window at the tubule opening.

Five analogues of NTHU-7 (not presented) were also prepared in the same water-containing DES by changing the base used during the synthesis.¹⁴² However, only 4,4'-trimethylenedipiperidine containing NTHU-7 nanotubules are able to luminesce brightly under exposure to long-wavelength UV light (365 nm). This indicates that they could be potentially used as a yellow-green phosphor for blue LEDs as well as a green phosphor for UV LEDs. Then, the photoluminescence properties are not only related to the defect sites in the structure, but also to the template occluded in the structure (as a sensitizer) and to the host properties (nanoporous structure).

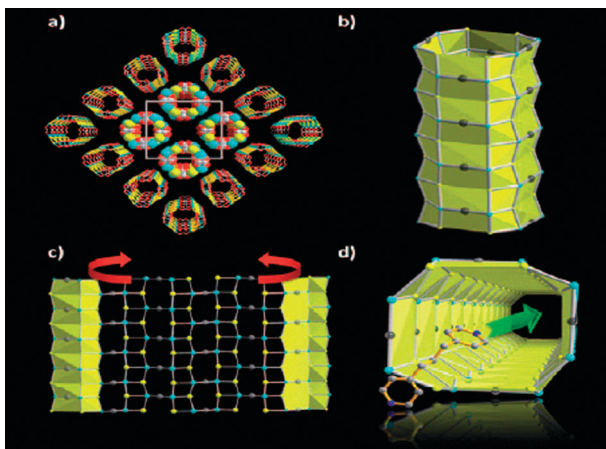


Fig. 16 Structure plots of NTHU-7. (a) A perspective view of the square-packing nanotubes. Ga centers cyan, P yellow, oxalate groups white and red; (b) topological representation of one nanotube showing the 16-ring aperture window surrounded by four strips of [Ga₂(HPO₃)₂] ribbons and four oxalate groups (gray balls); (c) section of the single layer sheet of the layer polymorph NTHU-7L, which may be viewed as the two-dimensional counterpart of NTHU-7. The red arrows indicate folding to form a nanotube and (d) a NTHU-7 nanotube with template tmdp. The green arrow indicates that emission can occur as the sensitizer is encapsulated.¹⁴² (Reproduced with permission from ref. 142. Copyright (2009) Wiley-VCH.)

8.2 Metal–organic frameworks (MOFs)

Recently, the synthesis of metal–organic frameworks (MOFs) has received great interest due to their potential applications in many fields such as hydrogen storage, gas separation, etc.^{143,144} Through the rational assembly of organic ligands and metals or metal clusters, a huge variety of MOFs have been obtained by means of solvothermal synthesis using organic solvents such as *N,N*-dimethylformamide (DMF). Taking advantage of the physico-chemical, economical and ecological advantages of DESs in the ionothermal synthesis of materials, eutectic mixtures are now regarded as promising and particularly attractive media for large-scale synthesis of new MOF structures. Different from ILs (two-component systems with anions and cations), which were also used for the MOF synthesis, DESs also contain neutral ligands such as urea that can induce structure-directing effects making DES a solvent of choice for the preparation of MOFs. To date, efforts have been made toward the ionothermal synthesis of new porous MOFs in DESs, due to the multiple roles that they can play in such synthesis (Fig. 17).¹⁴⁵

Bu and co-workers synthesized new MOF structures in different urea-derived solvents (urothermal synthesis).¹⁴⁶ More than 40 structures were obtained by assembly between:

- a nitrate precursor of trivalent lanthanide or transition metal or alkali and alkaline-earth metals (amongst In, Y, Nd, Sm, Gd, Dy, Ho, Yb, Ce, Pr, Er, Cd, Mg, Cu, Co, Zn and Li)
- 1,4-benzenedicarboxylic acid (ligand bdc), 1,2,4-benzenetricarboxylic acid (ligand btc), naphthalene-1,4-dicarboxylic acid (ligand ndc), thiophene-1,4-dicarboxylic acid, 1,3,5-benzene-tribenzoic acid
- ethylene urea hemihydrate (e-urea), propyleneurea (p-urea), 1,3-dimethyl-propyleneurea (p-murea), tetramethylurea (tm-urea)
- diethylformamide (DEF), dimethylformamide (DMF), 2-pyrrolidinone (pyrol) (amide as solvent)

In these syntheses, urea derivatives (e-urea and others) can act as a template for the formation of porous frameworks, but also as a ligand and mixed pendant ligand. This is the case for the URO-44 material, [Co₃(bdc)₃] (tm-urea)_x, assembled from H₂bdc, cobalt nitrate and tm-urea, in which tm-urea

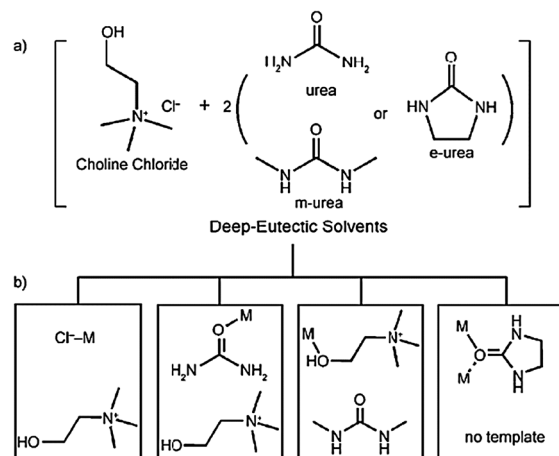


Fig. 17 (a) The structures of different DESs and (b) their multiple roles in the ionothermal synthesis of MOFs (M = metal).¹⁴⁵ (Reproduced with permission from ref. 145. Copyright (2009) Wiley-VCH.)

acts as a template. In opposition, in $[Y_2(bdc)_3(e\text{-}urea)]_4$, assembled from H_2bdc , yttrium nitrate and e-urea hemihydrate, e-urea acts as a pendant ligand. Sometimes, urea-derivative is also found to play a dual role [case of URO-162, $[Cd(thb)(en)_{1/2}(e\text{-}urea)]\cdot(e\text{-}urea)$] or can be the reactant for *in situ* ligand formation. However, these syntheses are beyond the scope of DESs and therefore will not be particularly discussed here. Some of these materials have a microporous structure and thus exhibit promising gas-storage capabilities for CO_2 and H_2 ($[Sm(bdc)_{3/2}(e\text{-}urea)]$, *viz.* the CO_2 adsorption is $26.8\text{ cm}^3\text{ g}^{-1}$ at approximately 1 atm and an H_2 uptake of $74.9\text{ cm}^3\text{ g}^{-1}$ (0.66 wt%) at 77 K and 1 atm).

In 2009, Bu's research group highlighted the versatile role of the DES in the generation of porosity and open metal sites in MOF structures for gas storage application.¹⁴⁵ They then first reported the synthesis of a series of MOFs in DES, composed of trivalent metal (In, Y, Nd, Sm), 1,4-benzenedicarboxylate (bdc) and one or two components from the DES. Six different topologies were obtained, and DES, in addition to its role of solvent, acted as a structure directing agent. In the In-containing structure, the extraframework choline ion was retained with Cl^- bounded to the polymeric layers. In addition to the external choline ion, neutral urea molecules can also be bonded to the framework (example of the material (choline)- $[Sm(bdc)_2(urea)]$). Choline can also be bounded to the MOF framework through its OH groups, and neutral urea molecules can serve as an external structure directing agent (the case of $[Nd(bdc)_2(choline)]\cdot(m\text{-}urea)$). The last role of DES highlighted by the authors consists in the direct bonding of neutral m-urea and e-urea to the polymeric framework (the case of $[Yb_2(bdc)_3(e\text{-}urea)]_4$ material). All the novel structures have clearly evidenced that DES not only acts as a solvent but also as template and/or ligand supplier. Summary of the main characteristics of the structures are given below:

- 2D anionic layer-type structure $\{[InCl(bdc)_{3/2}(H_2O)]_n\}^{n-}$. Charge is compensated by guest extraframework choline cations.
- 3D anionic framework (three isostructural compounds, $[M^{III}_2(bdc)_2(urea)]$ with $M = Y, Yb, Sm$), filled with guest choline cations.
- Structures having neutral framework (when urea is substituted by larger urea derivatives, *i.e.* e-urea and m-urea). In $[Nd(bdc)_2(choline)]\cdot(m\text{-}urea)$, choline ion acts as a ligand bound to the metal sites while m-urea acts as an extraframework template. In the other structures ($[Gd_2(bdc)_3(m\text{-}urea)]_4$, $[M^{III}_2(bdc)_3(e\text{-}urea)]_4$ with $M = Yb, Dy, Ho$, and $[Sm(bdc)_{3/2}(e\text{-}urea)]$), urea-derived molecules act as bounded ligands to the framework.

$[Sm(bdc)_{3/2}(e\text{-}urea)]$, which displays an excellent thermal stability, was used to exemplify the potential of such structures for gas storage application. After elimination of the neutral e-urea ligand from the structure, a porosity was generated in the obtained structure: $[Sm(bdc)_{3/2}]_n$, as confirmed by XRD.

In a similar way, the authors next prepared a series of porous anionic C_3N_4 -type ($[In_3(btc)]_n^{3n-}$, btc = 1,3,5-benzenetricarboxylate) MOFs that contain size-tunable and ion-exchangeable extraframework organic charge-compensating cations. Synthesis was performed in different solvent including molecular solvents, ILs and DESs.¹⁴⁷ In $ChCl/e\text{-}urea$ media, a

C_3N_4 -type ($[In_3(btc)]_n^{3n-}$) framework was formed. The choline cation compensated the framework charge, while e-urea was also incorporated into the structure. The ionic nature of DES may be particularly helpful in the formation of the anionic $[In_3(btc)]_n^{3n-}$ framework. While similar framework compositions and topologies were obtained in DESs, six different organic charge-compensating cations, having different sizes, were entrapped in the structure. These new MOFs exhibited different gas sorption capacity (N_2, H_2, CO_2) due to the different degrees of pore blockage by entrapment occluded organic cations having different sizes. When pores are filled with choline cation, high CO_2 uptake capacity is obtained. The authors suggest that strong interaction between the hydroxyl group of the choline cation and CO_2 is at the origin of the high uptake capacity in this DES mediated structure.

Morris and co-workers¹⁴⁸ also reported the ionothermal synthesis of three new lanthanide/organic-derived MOFs in a $ChCl/dimethylurea$ DES. The use of hydrated mineral lanthanide precursors unavoidably leads to the contamination of DES with water. As observed above, the strong binding of isolated molecules of water in DES through the hydrogen bond network drastically limited its reactivity, affording a direct access to materials that are hardly obtained with common methods. The three obtained MOF structures are isostructural materials of $Ln(TMA)(DMU)_2$, with Ln among La-Nd-Eu, TMA is trimesate ($C_9O_6H_3$) and DMU is dimethylurea [$(CH_3NH)_2CO$]. The ionothermal synthesis is performed by reaction between the lanthanide salt (nitrate hydrate or chloride hydrate) and trimesic acid in a $ChCl/dimethylurea$ DES. For the Nd-structure, HF in water was also used as a mineralizing agent. Structures crystallized in the triclinic space group $P\bar{1}$ ($Z = 2$). The asymmetric unit of $Ln(TMA)(DMU)_2$ was composed of the trivalent lanthanide atom, TMA and DMU molecules, with eight-coordination of the lanthanide. In the structure, TMA (through the COO^- group) acts as a linking agent between neighboring lanthanide atoms to form dimers. The 3D framework formation is ensured by H-bond interaction between DMU and the carboxyl groups of Lanthanide dimers. In opposition to the classical decomposition of DESs during ionothermal synthesis, DMU was not degraded and was recovered in its initial form in the structure. This shows that DMU acts as a ligand for the structure assembly.

Very recently, eight unique three dimensional lanthanide-thiophene-2,5-dicarboxylate (TCD) materials were synthesized in $ChCl/e\text{-}urea$ DESs.¹⁴⁹ Among them, six compounds are isostructural, crystallizing in the $P2_1/c$ space group of monoclinic symmetry, *i.e.* $[Ln(TDC)_2](choline)$ with $Ln = Gd, Nd, Eu, Er, Tb, Dy$. In these structures, choline cation compensates the charge of the anionic frameworks. A similar material was already obtained using 1-methyl-3-ethylimidazolium bromide IL, showing that the guest cation (choline in the case of the DES) did not play a template role. In the structure, four carboxylate groups bridge two Gd^{3+} ions to generate dinuclear units. These latter are bridged by TCD ligands to form layers which thereafter interconnect with TCD ligands to generate the 3D framework. The Yb-containing compound, prepared under similar conditions, displays a different structure. In $[Yb(TCD)_2(e\text{-}urea)]\cdot(choline)(H_2O)$, Yb^{3+} has an additional coordination with a second ligand, e-urea.

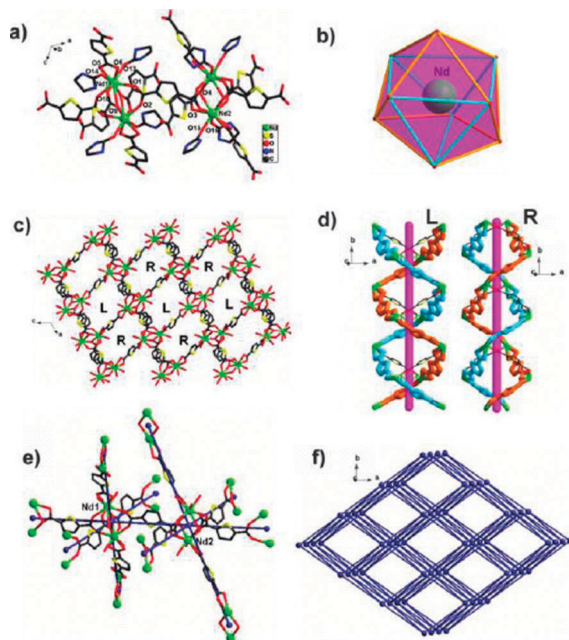


Fig. 18 (a) Coordination environment in $[\text{Nd}_2(\text{TCD})_3(\text{e-urea})_4] \cdot 3(\text{e-urea})$; (b) distorted dicapped trigonal prism coordination polyhedron of the Nd(III) ion; (c) view of the framework along the *b* axis; (d) two left- and two right-handed helices alternatively along the *b* axis; (e) uninodal 6-connected nodes represented by $\{\text{Nd}_2\}$ units; (f) the rob topology of $[\text{Nd}_2(\text{TCD})_3(\text{e-urea})_4] \cdot 3(\text{e-urea})$.¹⁴⁹ (Reproduced with permission from ref. 149. Copyright (2012) American Chemical Society.)

Two Yb³⁺ are bridged by two carboxyl groups to give a dinuclear unit. TCD ligands bridge these dinuclear units to form layers, which thereafter interconnect together to generate the 3D framework. Finally, the $[\text{Nd}_2(\text{TCD})_3(\text{e-urea})_4] \cdot 3(\text{e-urea})$ material presents a neutral framework with neutral e-urea guest molecules. The structure characteristics are presented in Fig. 18. A neutral 6-connected rob-type framework (Fig. 18e–f) with neutral guest e-urea molecules was obtained. In this last structure, the dinuclear units are composed of two Nd³⁺ ions, three TCD ligands, four terminal e-urea ligands and the three guest e-urea molecules.

These materials are characterized by the presence of helical substructures, as observed for $[\text{Yb}(\text{TCD})_2(\text{e-urea})] \cdot (\text{choline})(\text{H}_2\text{O})$ material, due to the different coordination modes of the TCD ligands (Fig. 18d).

Interestingly, with this material, single-crystal-to-single-crystal guest exchange between e-urea (the guest molecule) and ethanol can be achieved.

Bu *et al.*¹⁵⁰ also reported the synthesis of zinc(II)-boron(III)-imidazole framework with unusual pentagonal channels by synthesis in ChCl/m-urea media. In $\text{Zn}_2(\text{im})\text{Cl}_2[\text{B}(\text{im})_4]$, neither cation nor neutral ligand incorporates the material structure, but DES helps to stabilize the metal–halogen bonds. Then, the DES media allow the synthesis of a material which integrates two distinct imidazolate frameworks, with Zn-im linkage and $\text{B}(\text{im})_4^-$ complex.

8.3 Organic–inorganic hybrids

The recent literature on crystalline porous materials such as zeotypes has highlighted the great potential of DESs for the

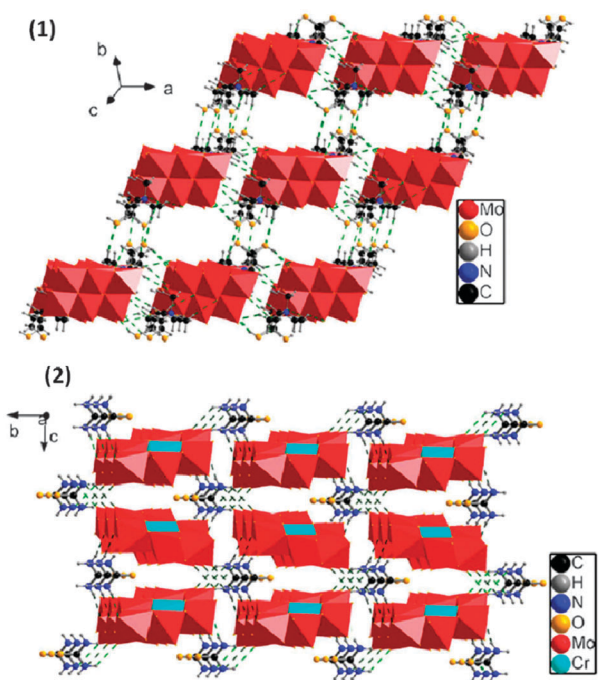


Fig. 19 The three-dimensional hydrogen-bonded supramolecular framework of (1) material 1, and (2) material 2.¹⁵¹ (Reproduced with permission from ref. 151. Copyright (2010) Elsevier.)

ionothermal synthesis of new materials. Besides metal phosphates with open-framework structures and MOFs, hybrid polyoxometalate materials were also successfully synthesized in DESs. Wang and co-workers¹⁵¹ first reported the use of DESs to prepare polyoxometalate (POM)-based hybrids. By using the ChCl/urea DES as the reaction solvent, two new compounds, $\{[(\text{CH}_3)_3\text{N}(\text{CH}_2)_2\text{OH}]_4[\beta\text{-Mo}_8\text{O}_{26}]\}$ (1) and $\{(\text{N}_2\text{H}_5\text{CO})[(\text{CH}_3)_3\text{N}(\text{CH}_2)_2\text{OH}]_2\}[\text{Cr-Mo}_6\text{O}_{24}\text{H}_6] \cdot 4\text{H}_2\text{O}$ (2), were successfully obtained at 30 °C starting from $\text{Na}_2\text{MoO}_4 \cdot 2\text{H}_2\text{O}$ and $\text{Cr}(\text{NO}_3)_3 \cdot 9\text{H}_2\text{O}$ as precursors for materials 1 and 2, respectively. Owing to an important hydrogen bond network between organic cations and polyoxoanions, both compounds exhibit a 3D supramolecular framework (Fig. 19).

For material 1, β-octamolybdate isopolyanion $[\beta\text{-Mo}_8\text{O}_{26}]^{4-}$ and four choline cations constitute the structural unit. The polyoxoanion consists in eight $\{\text{MoO}_6\}$ edge-shared. The structural unit of material 2 is composed of one $[\text{CrMo}_6\text{O}_{24}\text{H}_6]^{3-}$ Anderson-type anion, two choline cations, one protonated urea molecule and four molecules of water. Subsequently, three new polyoxometalate (POM)-based hybrids were successfully synthesized in the DES ChCl/urea by the same group.¹⁵² During the material syntheses, the decomposition of urea was avoided thanks to the mild reaction conditions (*e.g.* room temperature).

Consequently, the urea molecule was preserved in two POM-based hybrid materials. The choline cations not only act as the counter cation, but can also enter into the final structure of the material. In the basic structural unit of the first material, the $[\text{IMo}_6\text{O}_{24}]^{5-}$ Anderson type anion links with one $[\text{Na}_2(\text{H}_2\text{O})_6]^{2+}$ cation, two choline cations, one protonated water molecule and one lattice water molecule: $\{[(\text{CH}_3)_3\text{N}(\text{CH}_2)_2\text{OH}]_2(\text{H}_3\text{O})\}[\text{Na}_2(\text{H}_2\text{O})_6][\text{IMo}_6\text{O}_{24}] \cdot \text{H}_2\text{O}$.

For the second structure, $\{Na_2[(CH_3)(N(CH_2)_2OH]_4\} \cdot [Al(OH)_6Mo_6O_{18}]_2 \cdot 8NH_2CONH_2 \cdot 4H_2O$, two Anderson anions are present. The two Anderson anions link with Na^+ , four choline cations, eight urea molecules, and four water molecules to form the basic structural unit. Finally, in the last structure, $\{Na_6(H_2O)_{18}[(CH_3)_3N(CH_2)_2OH]_2(Con_2H_5)_2\} \cdot [NaMo_7O_{24}]_2 \cdot 4NH_2CONH_2 \cdot H_2O$, two heptamolybdate cations $[Na_2Mo_7O_{24}]^{4-}$ are linked to $\{Na_6(H_2O)_{18}[(CH_3)_3N(CH_2)_2OH]_2(Con_2H_5)_2\}$, four dissociated urea molecules, and lattice water to form the structural unit. Some of these Mo-based POM structures present interesting photocatalytic activity for the rhodamine B elimination.

In line with their pioneer works on the use of DESs and ILs for the synthesis of novel structures, Morris's research group¹⁵³ studied the synthesis of vanadium (oxy)fluoride materials by an ionothermal procedure in DESs or ILs media. Among the 10 presented materials, six are new materials. From a ChCl/1,3-dimethylurea DES, V_2O_5 (or VOF_3) and HF, three novel structures were obtained:

- the monomeric $(HNH_2CH_3)_2VOF_4(H_2O)$
- the dimer $(HNH_2CH_3)_4V_2O_2F_8(H_2O)$
- the 1D chain $(HNH_2CH_3)_2VF_5(V_3)$

Using the ChCl/2-imidazolidinone DES, V_2O_5 (or VOF_3) and HF, two novel structures are reported:

- $\alpha-(H_2NH_2(CH_2)_2 NH_2)VOF_4$
- $\beta-(H_2NH_2(CH_2)_2 NH_2)VOF_4$

Due to the mild reaction temperature (110–150 °C), DESs have been proved to play a template role in the formation of the final structure. In ChCl/1,3-dimethylurea, dimethylurea decomposed and provided a methylammonium cation to produce the monomeric structure after only 2 days of reaction. After ageing for 3 days, the dimeric structure is formed by removal of one molecule of water.

8.4 Nanoparticles

Compared to their bulk counterparts, nano-materials have unique properties including magnetic, electrochemical, and photonic properties. Hence, nano-materials found a wide variety of applications in different fields such as catalysis, electronics, optical devices, magnetism, life science, etc.¹⁵⁴ It is well established that the control of the morphology of these nanoparticles (NPs) is of considerable interest since it leads to materials with different physicochemical properties and functions. Therefore, the large-scale manufacture of nanoparticles with well-defined size and functionality is a great challenge in contemporary nanoscopic research.

In 2008, Sun and co-workers¹⁵⁵ reported a simple route for the shape-controlled synthesis of gold NPs. ChCl/urea DES was used in replacement of the traditional surfactants, $HAuCl_4 \cdot 4H_2O$ as the gold precursor, and L-ascorbic acid as an anisotropic growth promoter. Synthesis was performed at 30 °C, with different water contents to orientate particle shape. At intermediate water content (5000 ppm), star-shaped Au nanoparticles with (331) and vicinal high-index facets were successfully synthesized (Fig. 20(1)). More than 40% of the Au NPs present a regular pentagonal symmetry (Fig. 20(2b)), even if NPs with three, four and multiple branches were also observed (also observed in Fig. 20(1)). The size of these flat

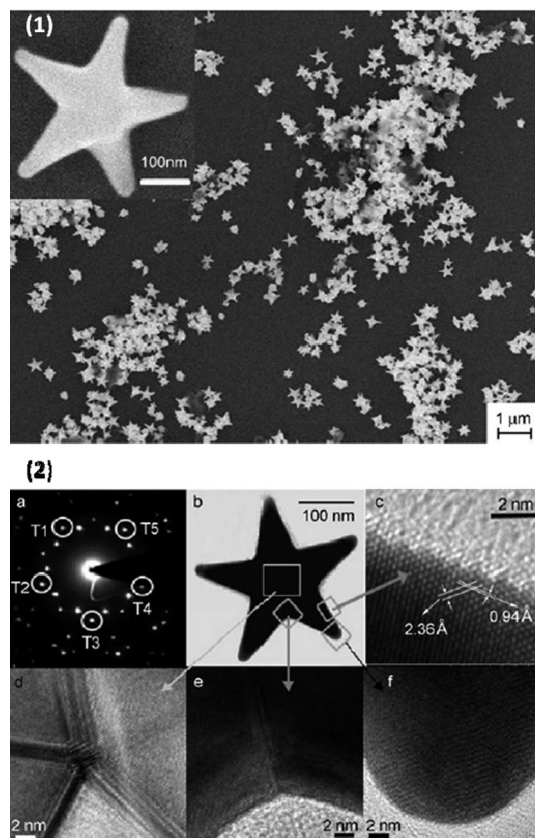


Fig. 20 (1) SEM images of the star-shaped Au nanoparticles; (2) HRTEM images of Au nanoparticles recorded along [110] (b–f) and the SAED pattern (a).¹⁵⁵ (Reproduced with permission from ref. 155. Copyright (2008) Wiley-VCH.)

nano-particles is about 300 nm. Au nanoparticles with different shapes and surface structures including snowflake-like (without water) and nanothorns (with 10 000 ppm of water) can be obtained simply by adjusting the water content in the DES.

DES also presumably played the role of a stabilizer since the NPs did not evolve with time in DES media. The obtained star-shaped Au nanoparticles are reported to exhibit high catalytic activity towards H_2O_2 electrocatalytic reduction, due to the high density of step atoms on high index facets. Lower catalytic activities were measured for the snowflake-like and nanothorns type NPs. However, for all the morphologies, measured activities are higher than over the polycrystalline Au electrode.

Very recently, another simple and efficient method was developed by Chirea *et al.* for the synthesis of gold nanowire from direct reduction of $HAuCl_4$ by $NaBH_4$ in DES.¹⁵⁶ In these syntheses, two different DESs, *i.e.* ChCl/ethylene glycol (1 : 2) or ChCl/urea (1 : 2), were employed in the absence of a surfactant. The length and average width of the nanowires formed are affected by the nature of the DES and by the $NaBH_4/HAuCl_4$ molar ratio. In particular, thinner and longer nanowire networks (NWNs) were obtained in ChCl/ethylene glycol. Different morphologies of NPs (from large plate, spherical, tripods, tetrapods) can be obtained by only changing the $NaBH_4/HAuCl_4$ ratio. FT-IR characterization of the

AuNWNs evidenced the stabilizing role of the DES. Urea acts as a stabilizing ligand on the AuNWN surface when synthesis was performed in ChCl/urea DES while ethylene glycol stabilized the AuNWN synthesized in ChCl/ethylene glycol. The obtained nanowire networks were used as catalysts for the chemical reduction of *p*-nitroaniline (4-NA) with sodium borohydride in aqueous solution. Catalytic investigations showed that gold nanowires synthesized in ChCl/urea (AuNWN2) were more active than those prepared in ChCl/ethylene glycol (AuNWN1). For instance, under similar conditions, AuNWN2 led to a complete reduction of *p*-nitroaniline, whereas AuNWN1 led to only 81% conversion. This difference in the catalytic activity is mainly attributed to the increased number of low coordinated gold atoms on the surface of AuNWN2.

Besides metal nanoparticles, nanostructured metal oxides with controllable morphology have also been prepared in DESs. Wong and co-workers developed an environmentally friendly “antisolvent approach”, which involved the use of DESs for the dissolution of metal oxides with the aim of synthesizing various ZnO nanostructures including twin-cones and nanorods with controllable dimensions.¹⁵⁷ In the synthesis, commercially available ZnO powders were first dissolved in a ChCl/urea DES. Then, various ZnO nanostructures were obtained by precipitation after introduction of an antisolvent (water/ethanol) into the DES. By closely controlling the different reaction parameters, ZnO nanostructures, including twin cones and nanorods, with controllable dimensions can be readily prepared (Fig. 21). The ratio between water and ethanol used for the precipitation of ZnO nanoparticles strongly affects their size and morphology. While rice-grain like micrometric particles are obtained when pure water is used as antisolvent (Fig. 21(1a)), an increase of the ethanol content in the antisolvent led to a decrease in ZnO crystal size.

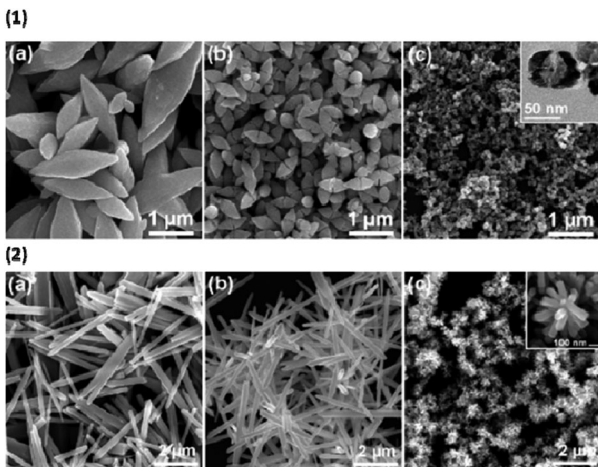


Fig. 21 (1) SEM images of ZnO twin-cone nanostructures prepared with the antisolvent of (a) pure water, (b) 50% ethanol and 50% water, and (c) 90% ethanol and 10% water (injection time = 5 s). The inset of (c) is a TEM image of a single twin-cone particle; (2) SEM images of ZnO nanorods prepared with the antisolvent of (a) pure water, (b) 50% ethanol and 50% water, and (c) 90% ethanol and 10% water (injection time = 5 h).¹⁵⁷ (Reproduced with permission from ref. 157. Copyright (2010) American Chemical Society.)

The injection rate of the ZnO-containing DES in the anti-solvent solution also has a strong impact on the final morphology (compare Fig. 21 (1) injection time = 5 s and (2) injection time = 5 h). Under slow injection conditions, nanorods and flower-assembled nanorods of different sizes can be obtained.

Additionally, monoclinic structured spindly bismuth vanadate microtubes were prepared on a large scale by a simple ionothermal treatment in a ChCl–urea eutectic mixture, starting from ammonium metavanadate, bismuth nitrate hydrate and water.¹⁵⁸ The obtained BiVO₄ microtubes exhibited spindle shape and saw-toothed structure. The authors studied the time-dependant structure growth. For the spindle shaped BiVO₄, the growth mechanism was ascribed to a reaction-crystallization process controlled by the BiOCl concentration and to a nucleation-growth process of nanosheets induced by adsorbed solvent molecules on the microtube surfaces.

The obtained spindly microtubes exhibited much higher visible-light photocatalytic activity for the rhodamine B decolorization than that of bulk BiVO₄ prepared by classical solid-state reaction (thermal crystallization at 700 °C between Bi(NO₃)₃·5H₂O and NH₄VO₃). Difference is attributed to the larger surface and improved crystallinity of the DES-derived mixed oxide.

8.5 Carbon materials

Porous carbon materials are extensively used for various applications, including catalyst supports, electrochemical devices, gas storage and separation, etc. Ionothermal synthesis has been proven to be an efficient route for the preparation of crystalline porous materials. Within this context, ILs have also been recently demonstrated to be versatile precursors for the preparation of porous carbon materials.^{159,160} In a similar way, synthesis of porous carbon materials can be achieved in DESs as reported by the group of del Monte. For example, the resorcinol-formaldehyde (RF) polycondensation in DESs for the preparation of carbons and carbon–carbon nanotube composites has been recently documented.¹⁶¹ During the polycondensation of resorcinol and formaldehyde, hydroxymethyl species are formed. These hydroxymethyl species react to form methylene and methylene ether bridged compounds. A well-documented study is then given by these authors where effects of water, catalyst, and the role of the DES (by comparison with classical aqueous conditions) was systematically investigated. During the material preparation, the RF polycondensation firstly occurred in a ChCl/ethylene glycol DES. Then, the resulting RF gels were carbonized to form monolithic carbons. Conversely to the use of water, all RF gels prepared in DESs exhibit similar textures, which is an interesting property of DESs. Conversion rate and carbon content in the final material are similar to those obtained using the classical route. After the thermal treatment of these gels, surface areas of carbon materials were largely improved. Another interesting point concerns the ability of DES to disperse carbon nanotubes, resulting in the formation of homogeneous carbon–carbon nanotube RF gels. Such a high composite homogeneity cannot be obtained in water due to the poor dispersibility of nanotubes in such a medium.

Next, the same group reported the synthesis of hierarchical porous (bimodal, with micropores and mesopores) carbon monoliths *via* formaldehyde polycondensation and subsequent carbonization in DES.¹⁶² In these syntheses, both the bimolecular RC-DES (made from resorcinol and ChCl by varying the ratio ChCl/resorcinol) and the ternary RUC-DES (made from resorcinol, urea and ChCl, also by varying the resorcinol concentration) were employed both as carbonaceous precursors and structure directing agents. Synthesis was only performed in basic media, since the authors previously evidenced that these conditions led to higher RF polycondensation. In these RU-DES and RUC-DES derived materials, the ChCl molecule was evidenced to play a template role. When the ternary RUC-DES was used, urea also participated in the condensation reactions, and was incorporated into the RF network. Carbonization of the obtained gels leads to the production of high surface area carbons ($455\text{--}612\text{ m}^2\text{ g}^{-1}$), with an important part of the surface developed in the generated microporosity. In addition, narrow mesopores, with size mainly depending on the nature of the DES, were formed. As a consequence, larger mesopores were formed when ternary RUC-DES is used, due to the incorporation of urea in the RF gel (*ca.* 23 nm for urea-derived DES vs. 10 nm for urea-free DES).

Finally, Monte and co-workers¹⁶³ reported the use of ternary DESs composed of resorcinol, 3-hydroxypyridine and ChCl (RHC-DES) as both precursors and structure-directing agents in the synthesis of nitrogen-doped hierarchical carbon monoliths. Like in their previous works, aqueous solution of formaldehyde is added to the RHC-DES for the condensation step in the presence of Na_2CO_3 , prior to calcination. The morphology of the resulting carbons always consists

in a bicontinuous porous network made of highly cross-linked clusters aggregated and assembled into interconnected structure, as observed in Fig. 22.

The DES is then described to play different roles:

- a solvent that ensures reactants homogeneity,
- the delivery of a structure-directing agent which governs the formation of the hierarchical pore structure,
- the source of carbon and nitrogen (retained in the final structure after carbonization).

While the increase in the carbonization temperature results in a decrease in *N*-content, all carbonaceous materials always retain a high nitrogen content showing the crucial participation of 3-hydroxypyridine during condensation reactions. These nitrogen doped carbon materials are found to exhibit high microporous surface area, in the range $\sim 540\text{ m}^2\text{ g}^{-1}$ (carbonized at $600\text{ }^\circ\text{C}$) to $\sim 680\text{ m}^2\text{ g}^{-1}$ (carbonized at $800\text{ }^\circ\text{C}$) and narrow micropore size centered at $\sim 0.5\text{ nm}$. The combination in these materials of a microporosity at size below 0.6 nm together with the presence of nitrogen makes these carbon materials very promising for CO_2 capture (CO_2 adsorption capacities up to 3.3 mmol g^{-1} were measured). Although other microporous carbons are also known to exhibit even higher adsorption capacities, carbon materials prepared in DES were found to be highly stable, allowing their recycling.

Finally, the group of del Monte also demonstrated that efficient synthesis of hierarchical porous multiwalled carbon nanotube (MWCNT) composites can be achieved in DESs.¹⁶⁴ Synthesis was performed through furfuryl alcohol (FA) condensation using a *p*-toluene sulfonic acid (*p*TsOH)/ChCl DES. Again, the DES is an ideal medium to achieve a homogeneous dispersion of the carbon nanotubes. Analysis of the porosity of the carbon–MWCNT composites obtained shows that high surface areas are achieved ($400\text{--}550\text{ m}^2\text{ g}^{-1}$). Microporosity and macroporosity are evidenced, with more of 60% of the surface developed in the micropores. Large differences in porosity are induced upon addition of MWCNT in the DES. Then, the morphology is progressively going to a bicontinuous porous network, which resembles a skeleton of interconnected MWCNTs, on the surface of which a carbon porous shell is formed. This particular morphology, a carbon shell that is entirely coating the MWCNT surface, leads to a high conductivity, which is suitable for a use as an electrode for supercapacitors. Finally, the authors rightly highlighted the remarkable green character of the proposed process since all the DES can be reused, due to its full recovery after condensation reaction.

9. Conclusions and outlook

From the above described results, it clearly appears that DESs exhibit close physico-chemical properties (viscosity, density, conductivity, among others) to those of traditional ILs. Additionally, like ILs, the physico-chemical properties of DESs can be tuned almost infinitely by changing the nature of the quaternary ammonium salt and the hydrogen-bond donor, making possible the preparation of task-specific DESs. As compared to ILs, DESs have however notable advantages stemming from (1) their convenient synthesis (100% atom economy), (2) their very low price since most of DESs can be

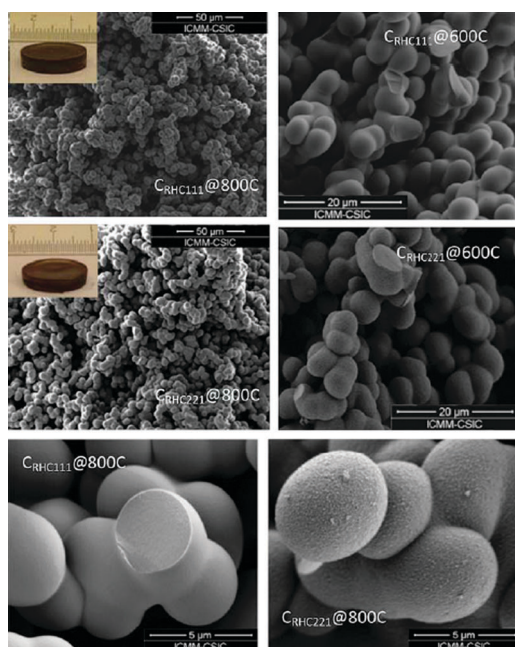


Fig. 22 SEM micrographs of $\text{C}_{\text{RHC}221}\text{-DES}$ and $\text{C}_{\text{RHC}111}\text{-DES}$ obtained after thermal treatments at 600 and $800\text{ }^\circ\text{C}$. Insets show pictures of the $\text{C}_{\text{RHC}221}\text{-DES}$ and $\text{C}_{\text{RHC}111}\text{-DES}$ monoliths after thermal treatment at $800\text{ }^\circ\text{C}$.¹⁶³ (Reproduced with permission from ref. 163. Copyright (2011) Royal Society of Chemistry.)

prepared from readily accessible chemicals and (3) their low toxicity, especially DESs derived from ChCl and renewable chemicals. Clearly, these notable ecological and economical advantages of DESs now open alternative routes for the emergence of ionic fluids at a larger scale. It should also be noted that although components of DESs are potentially reactive chemicals, their auto-association by a hydrogen bond drastically limits their reactivity, allowing their use in many fields of research.

In the field of catalysis and organic synthesis, it is clear that DESs will definitely contribute to the design of eco-efficient processes. In particular, the possibility to (1) selectively and conveniently extract products of the reaction from the DESs phase, (2) adjust the pH of DESs, (3) dissolve not only organic and inorganic salts but also transition metal-derived complexes or nanoparticles and (4) recycle these media is among the most promising advantages of DESs. It is our opinion that development of DESs in the field of catalysis will also be drastically boosted by the need to urgently design innovative processes for the catalytic conversion of biomass. Indeed, imidazolium-based ILs have the unique ability to dissolve large amounts of cellulose and more largely lignocelluloses opening promising routes for the saccharification of biomass. However, it is also clear that the price and toxicity of ILs represent two serious drawbacks that hamper the scale-up of these processes. We are fully convinced that the recent progress made in the field of DESs for the catalytic conversion of carbohydrates will definitely open soon new methodologies for converting lignocellulosic biomass in a more rational way.

In the field of material chemistry, it is also apparent that ILs can be advantageously replaced by cheap and safe DESs for the ionothermal synthesis of a wide range of inorganic materials with different textures and structures. Although a proper selection of the exactly required DESs still remains a big challenge, the above described works have clearly demonstrated that very important materials, from microporous zeotypes to carbon materials, can be synthesized in DESs. The very recent use of DESs for material synthesis demonstrates the exceptional potential of these media for the generation of novel structures and engineered materials. In these syntheses DESs may play different roles such as solvent, structure-directing agent, water inhibitor, reactant for structure crystallization, etc.

Besides excellent dissolution properties for CO₂, inorganic salts, and organic molecules, many DESs can also selectively dissolve different metal oxides, which thus provide great potential for the selective recovery of pure metals, especially in electrochemistry. In the particular field of metal electrodeposition, similar results to those reported in conventional ILs were obtained in DESs.

Despite all these promising applications, much effort is still needed in order to widen the utilization of DESs in chemistry. For instance, the instability of DESs during electrochemical processes still represents an important issue that needs to be addressed in the future. Viscosity of DESs can also be regarded as a serious problem, especially for heterogeneously-catalyzed processes. In this context, it makes no doubt that future research will particularly focus on DESs with low viscosity. Finally, a particular attention should also be given to the

reactivity of DESs that can, in some cases, lead to formation of undesirable side-products.

More than a green medium, DESs can also be regarded as a poorly toxic and biocompatible lipotropic agent, thus opening a new strategy for the vectorisation of pharmaceutical ingredients in the human body. This is motivated by the fact that many DESs are suspected to be formed in living cells and responsible for unexpected mechanisms.

Clearly, although DESs cannot replace ILs in all fields of chemistry, we are fully convinced that their low ecological footprint and attractive price will definitely contribute to the industrial emergence of this new medium in a close future.

The authors are grateful to the French Ministry of Research and the CNRS for their financial support. The authors would also like to thank Prof. A. P. Abbott and his co-workers for their pioneering works in this field of research and their significant contribution to the emergence of DESs in chemistry and biology.

Notes and references

- (a) J. P. Hallett and T. Welton, *Chem. Rev.*, 2011, **111**, 3508–3576; P. Wasserscheid and W. Keim, *Angew. Chem., Int. Ed.*, 2000, **39**, 3772–3789; (b) H. Wang, G. Gurau and R. D. Rogers, *Chem. Soc. Rev.*, 2012, **41**, 1519–1537.
- D. A. Walsh, K. R. J. Lovelock and P. Licence, *Chem. Soc. Rev.*, 2010, **39**, 4185–4194; *Electrodeposition from Ionic Liquids*, ed. F. Endres, D. MacFarlane and A. Abbott, Wiley-VCH, 2008.
- (a) J. Dupont and J. D. Scholten, *Chem. Soc. Rev.*, 2010, **39**, 1780–1804; (b) J. L. Bideau, L. Viau and A. Vioux, *Chem. Soc. Rev.*, 2011, **40**, 907–925.
- Green Industrial Applications of Ionic Liquids*, ed. R. Rogers, K. Seddon and S. Volkov, Springer, 2003.
- (a) M. J. Earle, S. P. Katdare and K. R. Seddon, *Org. Lett.*, 2004, **6**, 707–710; (b) Q. Zhang, S. Zhang and Y. Deng, *Green Chem.*, 2011, **13**, 2619–2637.
- M. Deetlefs and K. R. Seddon, *Green Chem.*, 2010, **12**, 17–30.
- (a) A. Romero, A. Santos, J. Tojo and A. Rodríguez, *J. Hazard. Mater.*, 2008, **151**, 268–273; (b) N. V. Plechkova and K. R. Seddon, *Chem. Soc. Rev.*, 2008, **37**, 123–150.
- Y. Yu, X. Lu, Q. Zhou, K. Dong, H. Yao and S. Zhang, *Chem.–Eur. J.*, 2008, **14**, 11174–11182.
- K. D. Weaver, H. J. Kim, J. Sun, D. R. MacFarlane and G. D. Elliott, *Green Chem.*, 2010, **12**, 507–513.
- F. Ilgen, D. Ott, D. Kralish, C. Reil, A. Palmberger and B. König, *Green Chem.*, 2009, **11**, 1948–1954.
- D. Reinhardt, F. Ilgen, D. Kralisch, B. König and G. Kreisel, *Green Chem.*, 2008, **10**, 1170–1181.
- A. P. Abbott, J. C. Barron, K. S. Ryder and D. Wilson, *Chem.–Eur. J.*, 2007, **13**, 6495–6501.
- S. Tang, A. Gary, Baker and H. Zhao, *Chem. Soc. Rev.*, 2012, **41**, 4030–4066.
- A. P. Abbott, D. Boothby, G. Capper, D. L. Davies and R. K. Rasheed, *J. Am. Chem. Soc.*, 2004, **126**, 9142–9147.
- A. P. Abbott, G. Capper, D. L. Davies, R. K. Rasheed and V. Tambayrahah, *Chem. Commun.*, 2003, 70–71.
- K. A. Shahbaz, F. S. Mjalli, M. A. Hashim and I. M. AlNashef, *J. Appl. Sci.*, 2010, **10**, 3349–3354.
- M. Hayyan, F. S. Mjalli, M. A. Hashim and I. M. AlNashef, *Fuel Process. Technol.*, 2010, **91**, 116–120.
- Y. Hou, Y. Gu, S. Zhang, F. Yang, H. Ding and Y. Shan, *J. Mol. Liq.*, 2008, **143**, 154–159.
- Z. Maugeri and P. Domínguez de María, *RSC Adv.*, 2012, **2**, 421–425.
- D. Carriazo, M. C. Gutiérrez, M. Luisa Ferrer and F. del Monte, *Chem. Mater.*, 2010, **22**, 6146–6152.
- K. Shahbaz, F. S. Mjalli, M. A. Hashim and I. M. AlNashef, *Energy Fuels*, 2011, **25**, 2671–2678.

- Published on 17 July 2012. Downloaded by Centro Federal de Educacão Tecnológica do Rio de Janeiro on 12/10/2018 12:18:23 PM.
- 22 M. A. Kareem, F. S. Mjalli, M. A. Hashim and I. M. AlNashef, *J. Chem. Eng. Data*, 2010, **55**, 4632–4637.
- 23 A. P. Abbott, G. Capper and S. Gray, *ChemPhysChem*, 2006, **7**, 803–806.
- 24 C. D'Agostino, R. C. Harris, A. P. Abbott, L. F. Gladden and M. D. Mantle, *Phys. Chem. Chem. Phys.*, 2011, **13**, 21383–21391.
- 25 A. P. Abbott, R. C. Harris and K. S. Ryder, *J. Phys. Chem. B*, 2007, **111**, 4910–4913.
- 26 K. Shahbaz, S. Baroutian, F. S. Mjalli, M. A. Hashim and I. M. AlNashef, *Thermochim. Acta*, 2012, **527**, 59–66.
- 27 A. P. Abbott, R. C. Harris, k. S. Ryder, C. D'Agostino, L. F. Gladden and M. D. Mantle, *Green Chem.*, 2011, **13**, 82–90.
- 28 K. Shahbaz, F. S. Mjalli, M. A. Hashim and I. M. AlNashef, *Thermochim. Acta*, 2011, **515**, 67–72.
- 29 A. P. Abbott, G. Capper, D. L. Davies and R. Rasheed, *Inorg. Chem.*, 2004, **43**, 3447–3452.
- 30 M. G. D. Pópolo, J. Kohanoff and R. M. Lynden-Bell, *J. Phys. Chem. B*, 2006, **110**, 8798–8803.
- 31 W. Li, Z. Zhang, B. Han, S. Hu, J. Song, Y. Xie and X. Zhou, *Green Chem.*, 2008, **10**, 1142–1145.
- 32 X. Li, M. Hou, B. Han, X. Wang and L. Zou, *J. Chem. Eng. Data*, 2008, **53**, 548–550.
- 33 W. C. Su, D. S. H. Wong and M. H. Li, *J. Chem. Eng. Data*, 2009, **54**, 1951–1955.
- 34 A. P. Abbott, G. Frisch, J. Hartley and K. S. Ryder, *Green Chem.*, 2011, **13**, 471–481.
- 35 A. P. Abbott, G. Capper and P. Shikotra, *Trans. Inst. Min. Metall., Sect. C*, 2006, **115**, 15–18.
- 36 A. P. Abbott, G. Capper, D. L. Davies, K. J. McKenzie and Stephen U. Obi, *J. Chem. Eng. Data*, 2006, **51**, 1280–1282.
- 37 J. M. Rimsza and L. R. Corrales, *Comput. Theor. Chem.*, 2012, **987**(1), 57–61.
- 38 H. G. Morrison, C. C. Sun and S. Neervannan, *Int. J. Pharm.*, 2009, **378**, 136–139.
- 39 I. Mamajanov, A. E. Engelhart, H. D. Bean and N. V. Hud, *Angew. Chem., Int. Ed.*, 2010, **49**, 6310–6314.
- 40 A. P. Abbott, P. M. Cullis, M. J. Gibson, R. C. Harris and E. Raven, *Green Chem.*, 2007, **9**, 868–872.
- 41 (a) F. Jutz, J. Andanson and A. Baiker, *Chem. Rev.*, 2011, **111**, 322–353; (b) V. I. Părvulescu and C. Hardacre, *Chem. Rev.*, 2007, **107**, 2615–2665; (c) F. Rantwijk and R. A. Sheldon, *Chem. Rev.*, 2007, **107**, 2757–2785.
- 42 S. B. Phadtare and G. S. Shankarling, *Green Chem.*, 2010, **12**, 458–462.
- 43 (a) Y. Jung and R. A. Marcus, *J. Am. Chem. Soc.*, 2007, **129**, 5492–5502; (b) R. Breslow, *Acc. Chem. Res.*, 1991, **24**, 159–164; (c) A. Lubineau, J. Augé and Y. Queneau, *Synthesis*, 1994, 741–760.
- 44 P. M. Pawar, K. J. Jarag and G. S. Shankarling, *Green Chem.*, 2011, **13**, 2130–2134.
- 45 Y. A. Sonawane, S. B. Phadtare, B. N. Borse, A. R. Jagtap and G. S. Shankarling, *Org. Lett.*, 2010, **12**, 1456–1459.
- 46 F. Ilgen and B. König, *Green Chem.*, 2009, **11**, 848–854.
- 47 O. Coulembier, V. Lemaur, T. Josse, A. Minoia, J. Cornil and P. Dubois, *Chem. Sci.*, 2012, **3**, 723–726.
- 48 B. Singh, H. Lobo and G. Shankarling, *Catal. Lett.*, 2011, **141**, 178–182.
- 49 (a) E. Zakrzewska Malgorzata, E. Bogel-Lukasik and R. Bogel-Lukasik, *Chem. Rev.*, 2011, **111**(2), 397–417; (b) R. Karinen, K. Vilonen and M. Niemela, *ChemSusChem*, 2011, **4**(8), 1002–1016.
- 50 S. Hu, Z. Zhang, Y. Zhou, B. Han, H. Fan, W. Li, J. Song and Y. Xie, *Green Chem.*, 2008, **10**, 1280–1283.
- 51 H. Zhao, J. E. Holladay, H. Brown and Z. C. Zhang, *Science*, 2007, **316**, 1597–1600.
- 52 S. Hu, Z. Zhang, Y. Zhou, J. Song, H. Fan and B. Han, *Green Chem.*, 2009, **11**, 873–877.
- 53 K. de Oliveira Vigier, A. Benguerba, J. Barrault and F. Jérôme, *Green Chem.*, 2012, **14**, 285–289.
- 54 (a) A. Biswas, R. L. Shogren, D. G. Stevenson, J. L. Willett and P. K. Bhowmik, *Carbohydr. Polym.*, 2006, **66**, 546–550; (b) A. P. Abbott, T. J. Bell, S. Handa and B. Stoddart, *Green Chem.*, 2005, **7**, 705–707.
- 55 As a recent example please see A. P. Abbott, A. D. Ballantyne, J. Palenzuela Conde, K. S. Ryder and W. R. Wise, *Green Chem.*, 2012, **14**, 1302–1037.
- 56 Z. Chen, B. Zhou, H. Cai and X. Zou, *Green Chem.*, 2009, **11**, 275–278.
- 57 A. P. Abbott, G. Capper, D. L. Davies, R. K. Rasheed and V. Tambyrajah, *Green Chem.*, 2002, **4**, 24–26.
- 58 N. Azizi and Z. Manocheri, *Res. Chem. Intermed.*, 2012, DOI: 10.1007/s11164-011-0479-4.
- 59 G. Imperato, E. Eibler, J. Niedermaier and B. König, *Chem. Commun.*, 2005, 1170–1172.
- 60 J. D. mota-Morales, M. C. Gutierrez, I. C. Sanchez, G. Luna-Barcenas and F. del monte, *Chem. Commun.*, 2011, **47**, 5328–5330.
- 61 M. C. Serrano, M. C. Gutierrez, R. Jimenez, M. L. Ferrer and F. del Monte, *Chem. Commun.*, 2012, **48**, 579–581.
- 62 G. Imperato, S. Höger, D. Lenoir and B. König, *Green Chem.*, 2006, **8**, 1051–1055.
- 63 G. Imperato, R. Vasold and B. König, *Adv. Synth. Catal.*, 2006, **348**, 2243–2247.
- 64 H. Zhang, Q. Cai and D. Ma, *J. Org. Chem.*, 2005, **70**, 5164–5173.
- 65 (a) P. Dominguez de Maria and Z. Mauger, *Curr. Opin. Chem. Biol.*, 2011, **15**, 220–225; (b) J. Gorke, F. Srienc and R. Kazlauskas, *Biotechnol. Bioprocess Eng.*, 2010, **15**, 40–53.
- 66 J. T. Gorke, F. Srienc and R. J. Kazlauskas, *Chem. Commun.*, 2008, 1235–1237.
- 67 D. Linberg, M. de la Fuente Revenga and M. Widersten, *J. Biotechnol.*, 2010, **147**, 169–171.
- 68 H. Zhao, G. A. Baker and S. Holmes, *Org. Bio. Chem.*, 2011, **9**, 1908–1916.
- 69 H. Zhao, G. A. baker and S. Holmes, *J. Mol. Cat. B: Enzymatic*, 2011, **72**, 163–167.
- 70 M. C. Gutierrez, M. L. Ferrer, L. Yuste, F. Rojo and F. del Monte, *Angew. Chem., Int. Ed.*, 2010, **49**, 2158–2162.
- 71 Y. H. Choi, J. van Spronsen, Y. Dai, M. Verbene, F. hollmann, I. W. C. E. Arends, G. J. Witkamp and R. Verpoorte, *Plant Physiol.*, 2011, **156**, 1701–1705.
- 72 S. Gore, S. Baskaran and B. König, *Green Chem.*, 2011, **13**, 1009–1013.
- 73 Z.-H. Zhang, X.-N. Zhang, L.-P. Mo, Y.-X. Li and F. P. Ma, *Green Chem.*, 2012, **14**, 1502–1506.
- 74 F.-P. Ma, G.-T. Cheng, Z.-G. He and Z.-H. Zhang, *Aust. J. Chem.*, 2012, **65**(4), 409–416.
- 75 N. Azizi, E. Batebi, S. Bagherpour and H. Ghafuri, *RSC Adv.*, 2012, **2**, 2289–2293.
- 76 (a) P. C. Andricacos, C. Uzoh, J. O. Dukovic, J. Horkans and H. Deligianni, *Electrochim. Microfabr.*, 1998, **42**, 5; (b) P. C. Andricacos, *Interface*, 1998, **7**, 23; (c) G. Pattanaik, D. M. Kirkwood, X. Xu and G. Zangari, *Electrochim. Acta*, 2007, **52**, 2755–2764; (d) R. Hasegawa, *Physica B*, 2001, **299**, 199.
- 77 (a) D. Wei and M. Okido, *Curr. Top. Electrochem.*, 1997, **5**, 21–26; (b) A. Etenko, T. McKechine, A. Shchetkovskiy and A. Smirnov, *ECS Trans.*, 2007, **3**, 151–157; (c) M. Gibilaro, L. Massot, P. Chamelot and P. Taxil, *Electrochim. Acta*, 2009, **54**, 5300–5306; (d) D. J. Fray and G. Z. Chen, *Master. Sci. Technol.*, 2004, **20**, 295.
- 78 (a) T. Welton, *Chem. Rev.*, 1999, **99**, 2071; (b) P. Wassershied and T. Welton, *Ionic liquids in Synthesis*, Wiley-VCH Verlag, Weinheim, Germany 2003; (c) R. Wang, T. Okajima, F. kitamura and T. Oshaka, *Electroanalysis*, 2004, **16**, 66–72; (d) R. T. Carlin, H. C. De Long, J. Fuller and P. C. Truelove, *J. Electrochem. Soc.*, 1994, **141**, L73; (e) A. B. Mc Ewen, S. F. McDevitt and V. Koch, *J. Electrochem. Soc.*, 1997, **144**, L84; (f) M. C. Buzzeo, R. G. Evans and R. G. Compton, *ChemPhysChem.*, 2004, **5**, 1106; (g) F. Endres, *Z. Phys. Chem.* 2004, **218**, 255; (h) M. Galinski, A. Lewandowski and I. Stepienak, *Electrochim. Acta*, 2006, **51**, 5567; (i) A. P. Abbott and K. J. McKenzie, *Phys. Chem. Chem. Phys.*, 2006, **8**, 4265–4279.
- 79 (a) J. S. Wilkes and M. J. awototko, *Chem. Commun.*, 1992, 965; (b) J. Fuller, R. T. Carli and R. A. Osteryoung, *J. Electrochem. Soc.*, 1999, **144**, 3881; (c) A. P. Abbott, G. Capper, D. L. Davies, H. Munro and R. Rashreed, *Inorg. Chem.*, 2004, **43**, 3447; (d) J. Z. Yang, W. G. Xu, P. Tian and L. L. He, *Fluid Phase Equilib.*, 2003, **204**, 295.
- 80 E. Gomez, P. Cojocaru, L. Magagnin and E. Valles, *J. Electroanalytical Chem.*, 2011, **658**, 18–24.
- 81 P. Cojocaru, L. Magagnin, E. Gomez and E. Vallés, *Mater. Lett.*, 2011, **65**, 3597–3600.
- 82 D. D. Shivagan, P. J. Dale, A. P. Samantilleke and L. M. Peter, *Thin Solid Films*, 2007, **515**, 5899–5903.

- 83 M. Steichen, M. Thomassey, S. Siebentritt and P. J. Dale, *Phys. Chem. Chem. Phys.*, 2011, **13**, 4292.
- 84 H. Yang, X. Guo, N. Birbilis, G. Wu and W. Ding, *Appl. Surf. Sci.*, 2011, **257**, 9094–9102.
- 85 A. P. Abbott, G. Capper, D. L. Davies, K. J. McKenzie and S. U. Obi, *J. Chem. Eng. Data*, 2006, **51**, 1280–1282.
- 86 P. Martis, V. S. Dilimon, J. Delhalle and Z. Mekhalif, *Electrochim. Acta*, 2010, **55**, 5407–5410.
- 87 A. P. Abbott, K. El Ttaib, K. S. Ryder and E. L. Smith, *Trans. Inst. Met. Finish.*, 2008, **86**, 234–240.
- 88 H. Y. Yang, W. Guo, X. B. Chen, S. H. Wang, G. H. Wu, W. J. Ding and N. Birbilis, *Electrochim. Acta*, 2012, **63**, 131–138.
- 89 A. P. Abbott, G. Capper, K. J. McKenzie and K. S. Ryder, *J. Electroanal. Chem.*, 2007, **599**, 288–294.
- 90 P. Dale, A. P. Samantilleke, D. D. Shivagan and L. M. Peter, *Thin Solid Films*, 2007, **515**, 5751–5754.
- 91 A. Bakkar and V. Neubert, *Electrochim. Commun.*, 2007, **9**, 2428–2435.
- 92 D. Yue, Y. Jia, Y. Yao, J. Sun and Y. Jing, *Electrochim. Acta*, 2012, **65**, 30–36.
- 93 E. L. Smith, J. C. Barron, A. P. Abbott and K. S. Ryder, *Anal. Chem.*, 2009, **81**, 8466–8471.
- 94 A. P. Abbott, J. C. Barron, G. Frisch, K. S. Ryder and A. Fernando Silva, *Electrochim. Acta*, 2011, **56**, 5272–5279.
- 95 A. P. Abbott, J. C. Barron, G. Frisch, S. Gurman, K. S. Ryder and A. Fernando Silva, *Phys. Chem. Chem. Phys.*, 2011, **13**, 10224–10231.
- 96 A. Sun, H. Zhao and J. Zheng, *Talanta*, 2012, **88**, 259–264.
- 97 A. P. Abbott, K. El Ttaib, G. Frisch and K. J. McKenzie, *Phys. Chem. Chem. Phys.*, 2009, **11**, 4269–4277.
- 98 D. Lloyd, T. Vainikka, L. Murtomäki, K. Kontturi and E. Ahlberg, *Electrochim. Acta*, 2011, **56**, 4942–4948.
- 99 A. P. Abbott, S. Nandhra, S. Postlethwark, E. Smith and K. S. Ryder, *Phys. Chem. Chem. Phys.*, 2007, **9**, 3735–3743.
- 100 A. P. Abbott, K. El Ttaib, G. Frisch, K. S. Ryder and D. Weston, *Phys. Chem. Chem. Phys.*, 2012, **14**, 2443–2449.
- 101 C. D. Gu, X. J. Xu and J. P. Tu, *J. Phys. Chem.*, 2010, **114**, 13614–13619.
- 102 G. Saravanan and S. Mohan, *J. Alloys Compounds*, 2012, **522**, 162–166.
- 103 C. Gu and J. Tu, *Langmuir*, 2011, **27**, 10132–10140.
- 104 M. A. Skopek, M. A. Mohamoud, K. S. Ryder and A. R. Hillman, *Chem. Commun.*, 2009, 935–937.
- 105 K. Haerens, E. Matthijs, K. Binnemans and B. Ven Der Bruggen, *Green Chem.*, 2009, **11**, 1357–1365.
- 106 M. Figueiredo, C. Gomes, E. Costa, A. Martins, C. M. Pereira and F. Silva, *Electrochim. Acta*, 2009, **54**, 2630–2634.
- 107 B. G. Pollet, J. Y. Hihn and T. J. Mason, *Electrochim. Acta*, 2008, **53**, 4248–4256.
- 108 C. A. Nkuku and R. J. LeSuer, *J. Phys. Chem. B*, 2007, **111**, 13271–13277.
- 109 A. P. Abbott, G. Capper, D. L. Davies and R. K. Rasheed, *Chem.–Eur. J.*, 2004, **10**, 3769–3774.
- 110 H.-R. Jhong, D. Shan-Hill Wog, C.-C. Wan, Y.-Y. Wang and T.-C. Wei, *Electrochim. Commun.*, 2009, **11**, 209–211.
- 111 A. P. Abbott, G. Capper, K. J. McKenzie and K. S. Ryder, *Electrochim. Acta*, 2006, **51**, 4420–4425.
- 112 A. P. Abbott, G. Capper, K. J. McKenzie, A. Glidle and K. S. Ryder, *Phys. Chem. Chem. Phys.*, 2006, **8**, 4214–4221.
- 113 A. P. Abbott, G. Frisch, S. J. Gurman, A. R. Hillman, J. Hartley, F. Holyoak and K. S. Ryder, *Chem. Commun.*, 2011, **47**, 10031–10033.
- 114 S. Ramesh, R. Shanti and E. Morris, *J. Mater. Sci.*, 2012, **47**, 1787–1793.
- 115 S. Ramesh, R. Shanti and E. Morris, *Carbohydr. Polym.*, 2012, **87**, 701–706.
- 116 S. Ramesh, R. Shanti and E. Morris, *J. Mol. Liq.*, 2012, **166**, 40–43.
- 117 (a) D. Freudenmann, S. Wolf, M. Wolff and C. Feldmann, *Angew. Chem., Int. Ed.*, 2011, **50**, 11050–11060; (b) Z. Ma, J. Yu and S. Dai, *Adv. Mater.*, 2010, **22**, 261–285.
- 118 (a) E. R. Parnham and R. E. Morris, *Acc. Chem. Res.*, 2007, **40**, 1005–1013; (b) R. E. Morris, *Chem. Commun.*, 2009, 2990–2998; A. Taubert, *Acta Chim. Slov.*, 2005, **52**, 183–186.
- 119 E. R. Cooper, C. D. Andrews, P. S. Wheatley, P. B. Webb, P. Wormald and R. E. Morris, *Nature*, 2004, **430**, 1012–1016.
- 120 E. R. Parnham, P. S. Wheatley and R. E. Morris, *Chem. Commun.*, 2006, 380–382.
- 121 (a) E. R. Parnham and R. E. Morris, *J. Am. Chem. Soc.*, 2006, **128**, 2204–2205; (b) E. R. Parnham and R. E. Morris, *Chem. Mater.*, 2006, **18**, 4882–4887.
- 122 E. R. Parnham, E. A. Drylie, P. S. Wheatley, A. M. Z. Slawin and R. E. Morris, *Angew. Chem., Int. Ed.*, 2006, **45**, 4962–4966.
- 123 L. Vidal, C. Marichal, V. Gramlich, J. Patarin and Z. Gabelica, *Chem. Mater.*, 1999, **11**, 2728–2736.
- 124 H. J. Ma, Z. J. Tian, R. S. Xu, B. C. Wang, Y. Wei, L. Wang, Y. P. Xu, W. P. Zhang and L. W. Lin, *J. Am. Chem. Soc.*, 2008, **130**, 8120–8120.
- 125 (a) L. Cammarata, S. G. Kazarian, P. A. Salter and T. Welton, *Phys. Chem. Chem. Phys.*, 2001, **3**, 5192–5200; (b) C. G. Hanke and R. M. Lynden-Bell, *J. Phys. Chem. B*, 2003, **107**, 10873–10878.
- 126 E. A. Drylie, D. S. Wragg, E. R. Parnham, P. S. Wheatley, A. M. Z. Slawin, J. E. Warren and R. E. Morris, *Angew. Chem., Int. Ed.*, 2007, **46**, 7839–7843.
- 127 G. Y. Yang and S. C. Sevov, *J. Am. Chem. Soc.*, 1999, **121**, 8389–8390.
- 128 J. H. Liao, P. C. Wu and Y. H. Bai, *Inorg. Chem. Commun.*, 2005, **8**, 390–392.
- 129 W. T. A. Harrison, *Inorg. Chem. Commun.*, 2007, **10**, 833–838.
- 130 L. Liu, Y. Kong, H. Xu, J. P. Li, J. X. Dong and Z. Lin, *Microporous Mesoporous Mater.*, 2008, **115**, 624–628.
- 131 R. H. Jones, J. Chen, G. Sankar and J. M. Thomas, *Stud. Surf. Sci. Catal.*, 1994, **84**, 2229–2236.
- 132 L. Liu, S. Ferdov, C. Coelho, Y. Kong, L. Mafra, J. P. Li, J. X. Dong, U. Kolitsch, R. A. S. Ferreira, E. Tillmanns, J. Rocha and Z. Lin, *Inorg. Chem.*, 2009, **48**, 4598–4600.
- 133 L. Liu, D. S. Wragg, H. Zhang, Y. Kong, P. J. Byrne, T. J. Prior, J. E. Warren, Z. Lin, J. Dong and R. E. Morris, *Dalton Trans.*, 2009, 6715–6718.
- 134 P. Jhang, N. Chuang and S. Wang, *Angew. Chem., Int. Ed.*, 2010, **49**, 4200–4204.
- 135 L. Liu, Y. Li, H. Wei, M. Dong, J. Wang, A. M. Z. Slawin, J. Li, J. Dong and R. E. Morris, *Angew. Chem., Int. Ed.*, 2009, **48**, 2206–2209.
- 136 J. X. Dong, L. Liu, J. Li, Y. Li, C. Baerlocher and L. B. McCusker, *Microporous Mesoporous Mater.*, 2007, **104**, 185–191.
- 137 L. Liu, Z. F. Chen, H. B. Wei, Y. Li, Y. C. Fu, H. Xu, J. P. Li, A. M. Z. Slawin and J. X. Dong, *Inorg. Chem.*, 2010, **49**, 8270–8275.
- 138 L. Liu, J. Yang, J. Li, J. Dong, D. Šišák, M. Luzzatto and L. McCusker, *Angew. Chem., Int. Ed.*, 2011, **50**, 8139–8142.
- 139 Z. Lin, D. S. Wragg, P. Lightfoot and R. E. Morris, *Dalton Trans.*, 2009, 5287–5289.
- 140 C. Y. Sheu, S. F. Lee and K. H. Lii, *Inorg. Chem.*, 2006, **45**, 1891–1893.
- 141 (a) Y. C. Liao, C. H. Lin and S. L. Wang, *J. Am. Chem. Soc.*, 2005, **127**, 9986; (b) Y. C. Yang and S. L. Wang, *J. Am. Chem. Soc.*, 2008, **130**, 1146–1147.
- 142 P. C. Jhang, Y. C. Yang, Y. C. Lai, W. R. Liu and S. L. Wang, *Angew. Chem., Int. Ed.*, 2009, **48**, 742–745.
- 143 N. A. Ramsahye, G. Maurin, S. Bourrelly, P. L. Llewellyn, C. Serre, T. Loiseau, T. Devic and G. Férey, *J. Phys. Chem. C*, 2008, **112**, 514–520.
- 144 (a) T. K. Trung, P. Trens, N. Tanchoux, S. Bourrelly, P. L. Llewellyn, S. Loera-Serna, C. Serre, T. Loiseau, F. Fajula and G. Férey, *J. Am. Chem. Soc.*, 2008, **130**, 16926–16932; (b) G. Férey, *Chem. Soc. Rev.*, 2008, **37**, 191–241.
- 145 J. Zhang, T. Wu, S. Chen, P. Feng and X. Bu, *Angew. Chem., Int. Ed.*, 2009, **48**, 3486–3490.
- 146 J. Zhang, J. T. Bu, S. Chen, T. Wu, S. Zheng, Y. Chen, R. A. Nieto, P. Feng and X. Bu, *Angew. Chem., Int. Ed.*, 2010, **49**, 8876–8879.
- 147 S. Chen, J. Zhang, T. Wu, P. Feng and X. Bu, *J. Am. Chem. Soc.*, 2009, **131**, 16027–16029.
- 148 F. Himeur, I. Stein, D. S. Wragg, A. M. Z. Slawin, P. Lightfoot and R. E. Morris, *Solid State Sci.*, 2010, **12**, 418–421.
- 149 C. H. Zhan, F. Wang, Y. Kang and J. Zhang, *Inorg. Chem.*, 2012, **51**, 523–530.
- 150 S. Chen, J. Zhang, T. Wu, P. Feng and X. Bu, *Dalton Trans.*, 2010, **39**, 697–699.

- Published on 17 July 2012. Downloaded by Centro Federal de Educacão Tecnológica do Rio de Janeiro on 12/10/2018 12:18:23 PM.
-
- 151 S. M. Wang, Y. W. Li, X. J. Feng, Y. G. Li and E. B. Wang, *Inorg. Chim. Acta*, 2010, **363**, 1556–1560.
- 152 S. M. Wang, W. L. Chen, E. B. Wang, Y. G. Li, X. J. Feng and L. Liu, *Inorg. Chem. Commun.*, 2010, **13**, 972–975.
- 153 F. H. Aidoudi, P. J. Byrne, P. K. Allan, S. J. Teat, P. Lightfoot and R. E. Morris, *Dalton Trans.*, 2011, **40**, 4324–4331.
- 154 G. A. Ozin, A. C. Arsenault and L. Cademartiri, in *Nanochemistry A Chemical Approach to Nanomaterials*, The Royal Society of Chemistry, 2nd edn, 2009.
- 155 H. G. Liao, Y. X. Jiang, Z. Y. Zhou, S. P. Chen and S. G. Sun, *Angew. Chem., Int. Ed.*, 2008, **47**, 9100–9103.
- 156 M. Chirea, A. Freitas, B. S. Vasile, C. Ghitulica, C. M. Pereira and F. Silva, *Langmuir*, 2011, **27**, 3906–3913.
- 157 J. Y. Dong, Y. J. Hsu, D. S. H. Wong and S. Y. Lu, *J. Phys. Chem. C*, 2010, **114**, 8867–8872.
- 158 W. Liu, Y. Yu, L. Cao, G. Su, X. Liu, L. Zhang and Y. Wang, *J. Hazard. Mater.*, 2010, **181**, 1102–1108.
- 159 (a) J. P. Paraknowitsch, J. Zhang, D. S. Su, A. Thomas and M. Antonietti, *Adv. Mater.*, 2010, **22**, 87–92; (b) J. S. Lee, X. Q. Wang, H. M. Luo and S. Dai, *Adv. Mater.*, 2010, **22**, 1004–1007.
- 160 J. S. Lee, X. Q. Wang, H. M. Luo, G. A. Baker and S. Dai, *J. Am. Chem. Soc.*, 2009, **131**, 4596–4597.
- 161 M. C. Gutiérrez, F. Rubio and F. Monte, *Chem. Mater.*, 2010, **22**, 2711–2719.
- 162 D. Carriazo, M. C. Gutiérrez, M. L. Ferrer and F. Monte, *Chem. Mater.*, 2010, **22**, 6146–6152.
- 163 M. C. Gutiérrez, D. Carriazo, C. O. Ania, J. B. Parra, M. L. Ferrer and F. Monte, *Energy Environ. Sci.*, 2011, **4**, 3535–3544.
- 164 M. C. Gutiérrez, D. Carriazo, A. Tamayo, R. Jimenez, F. Pico, J. M. Rojo, M. L. Ferrer and F. Monte, *Chem.-Eur. J.*, 2011, **17**, 10533–10537.